

Winter 1994

Polymer substrates for use in fiber optic sensors: Suspension polymerization of Kraton G1652 modified poly(vinylbenzyl chloride)

Vicki Lynn Conway

University of New Hampshire, Durham

Follow this and additional works at: <https://scholars.unh.edu/dissertation>

Recommended Citation

Conway, Vicki Lynn, "Polymer substrates for use in fiber optic sensors: Suspension polymerization of Kraton G1652 modified poly(vinylbenzyl chloride)" (1994). *Doctoral Dissertations*. 1816.
<https://scholars.unh.edu/dissertation/1816>

This Dissertation is brought to you for free and open access by the Student Scholarship at University of New Hampshire Scholars' Repository. It has been accepted for inclusion in Doctoral Dissertations by an authorized administrator of University of New Hampshire Scholars' Repository. For more information, please contact nicole.hentz@unh.edu.

INFORMATION TO USERS

This manuscript has been reproduced from the microfilm master. UMI films the text directly from the original or copy submitted. Thus, some thesis and dissertation copies are in typewriter face, while others may be from any type of computer printer.

The quality of this reproduction is dependent upon the quality of the copy submitted. Broken or indistinct print, colored or poor quality illustrations and photographs, print bleedthrough, substandard margins, and improper alignment can adversely affect reproduction.

In the unlikely event that the author did not send UMI a complete manuscript and there are missing pages, these will be noted. Also, if unauthorized copyright material had to be removed, a note will indicate the deletion.

Oversize materials (e.g., maps, drawings, charts) are reproduced by sectioning the original, beginning at the upper left-hand corner and continuing from left to right in equal sections with small overlaps. Each original is also photographed in one exposure and is included in reduced form at the back of the book.

Photographs included in the original manuscript have been reproduced xerographically in this copy. Higher quality 6" x 9" black and white photographic prints are available for any photographs or illustrations appearing in this copy for an additional charge. Contact UMI directly to order.

UMI

University Microfilms International
A Bell & Howell Information Company
300 North Zeeb Road, Ann Arbor, MI 48106-1346 USA
313/761-4700 800/521-0600

Order Number 9518481

Polymer substrates for use in fiber optic sensors: Suspension polymerization of Kraton G1652 modified poly(vinylbenzyl chloride)

Conway, Vicki Lynn, Ph.D.

University of New Hampshire, 1994

U·M·I

300 N. Zeeb Rd.
Ann Arbor, MI 48106

**POLYMER SUBSTRATES FOR USE IN FIBER OPTIC SENSORS:
SUSPENSION POLYMERIZATION OF KRATON G1652 MODIFIED
POLY(VINYLBENZYL CHLORIDE)**

BY

**VICKI LYNN CONWAY
BS, Juniata College, 1989**

DISSERTATION

**Submitted to the University of New Hampshire
in Partial Fulfillment of
the Requirements for the Degree of**

Doctor of Philosophy

in

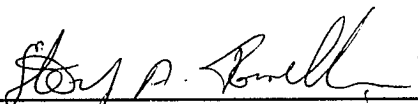
Chemistry

December, 1994

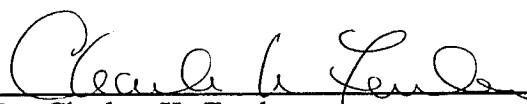
This dissertation has been examined and approved.



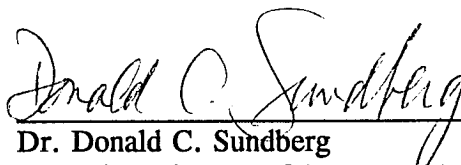
Dissertation Director, Dr. W. Rudolf Seitz
Professor of Chemistry



Dr. Sterling A. Tomelini
Associate Professor of Chemistry



Dr. Charles K. Zercher
Assistant Professor of Chemistry



Dr. Donald C. Sundberg
Executive Director of Sponsored Research



Dr. Todd W. Gross
Associate Professor of Mechanical Engineering

12/8/94

Date

DEDICATION

To my parents, Robert and Judith Conway

Sometimes I wonder how I ever got so lucky.

ACKNOWLEDGMENTS

I would first like to thank my advisor, W. Rudolf Seitz, for his support and encouragement throughout my years at UNH. If it weren't for your timely words of advice, and your ability to make me believe that I could actually obtain a doctorate, who knows where I would be? I truly enjoyed working for you, and I hope that you enjoy your chair for years to come!

Thanks to my family for dealing with all my stress-induced phone calls. Your love and support has always been a steady part of my life. Thanks for believing in me even when I didn't.

Thanks to all the faculty and staff of the Chemistry Department. I moved in and set up camp: nobody seemed to mind...

Thanks to Nancy Cherim, UNH Instrumentation Center, for all her help with Scanning Electron Microscopy and CHN. I enjoyed every one of our early morning chat sessions in the "dungeon".

Thank you to Dr. Richard Hall, Dow Chemical Corp., for all our technical discussions regarding the suspension polymerization of poly(vinylbenzyl chloride).

Thank you to Shell Chemical Company, for supplying Kraton G1652, and to Dow Chemical Corporation for supplying vinylbenzyl chloride.

Thanks to all my labmates, past and present. It was great being a part of the "Seitz research group". Over the years we were not only great scientists(!) but we also managed to make Club 150 what it is today. Thanks for making it fun.

Finally, thanks to my friends in New Hampshire. I honestly never thought that I would find it hard to leave graduate school, but it was. You will always be a large part of my life. Thanks for making my stay at UNH unforgettable, and thanks for making New Hampshire home for me.

TABLE OF CONTENTS

DEDICATION	iii
ACKNOWLEDGEMENTS	iv
LIST OF TABLES	vii
LIST OF FIGURES	ix
ABSTRACT	xiii
CHAPTER	Page
I. INTRODUCTION	1
Fiber Optic Sensors Based on Polymer Swelling	4
Polymer for Use as the Sensing Element	9
Thesis Research	12
II. THEORY	16
Mechanical Properties of Polymers	16
Suspension Polymerization	18
Nonionic Polymer Swelling	20
Ionic Polymer Equilibrium Swelling	21
III. EXPERIMENTAL	24
Suspension Polymerization of Modified Poly(vinylbenzyl chloride)	24
Reagents	24
Apparatus	25
Procedure	25
Dissolution of Suspension System (aqueous medium)	25
Monomer System (organic medium)	27
Suspension Polymerization	32
Characterization	33
Diameter Ratio and Swell Time	33
Scanning Electron Microscopy	33

Amination of Modified Poly(vinylbenzyl chloride) Beads	34
Reagents	34
Procedure	35
Characterization	35
CHN Analysis	35
Diameter Ratio and Swell Time	36
Penetration Modulus	36
Procedure	36
Mercury Porosimetry	37
IV. MORPHOLOGY	
SEM MICROGRAPHS/ MERCURY POROSIMETRY	40
V. SWELLING IN TOLUENE/ DIAMETER RATIOS AND SWELL TIMES	67
Diameter Ratio in Toluene	69
Swelling Times in Toluene	83
VI. SWELLING IN ACID/ DIAMETER RATIOS AND SWELLING TIMES	91
CHN Analyses of the Beads	91
Diameter Ratios of the Beads in Acid	101
Swelling Times of the Beads in Acid	106
VII. PENETRATION MODULUS	112
VIII. CONCLUSION	123
APPENDIX A	127
APPENDIX B	131
APPENDIX C	133
REFERENCES	134

LIST OF TABLES

	Page
Table 3-1: Factorial design for the suspension polymerization of Kraton G1652 modified poly(vinylbenzyl chloride)	29
Table 5-1: The diameter ratios and swelling times of the beads in toluene. Swelling times, in parenthesis, are reported in minutes.	69
Table 5-2: Results of an ANOVA performed on the diameter ratios of the beads in toluene, neglecting all data that includes 66% dodecane in the polymer formulation.	71
Table 5-3: Results of an ANOVA performed on the diameter ratios of the beads in toluene, neglecting all data that includes 60% total diluent in the polymer formulation.	72
Table 5-4: Results of an ANOVA performed on the swelling times of the beads in toluene, neglecting all data that includes 66% dodecane in the polymer formulation.	85
Table 5-5: Results of an ANOVA performed on the swelling times of the beads in toluene, neglecting all data that includes 60% total diluent in the polymer formulation.	86
Table 6-1: Percent nitrogen of each formulation from CHN analyses. The theoretical %N, corrected for the Kraton G1652 and divinylbenzene content.	96
Table 6-2: The diameter ratios and swelling times of the diethanolamine derivatized beads in 0.1M, pH 4 acetate buffer (IS = 0.1M).	102
Table 6-3: Results of an ANOVA performed on data obtained upon swelling the beads in acid, neglecting all data that includes 66% dodecane in the polymer formulation.	104

Table 6-4: Results of an ANOVA performed on swelling times of the beads in acid, neglecting all data that included 66% dodecane in the polymer formulation.	109
Table 7-1: Penetration moduli in MPa.	114
Table 7-2: Results of the ANOVA performed on the penetration moduli of all beads excluding those with 2% Kraton G1652 and 66% dodecane.	119

LIST OF FIGURES

	Page
Figure 1-1 Schematic of fiber optic sensor based on polymer swelling.	6
Figure 1-2 The overlap region of a two-fiber sensor arrangement (a). The increase in the overlap region as the reflector is moved further away (b).	8
Figure 2-1 Illustration of the “osmotic effect” of swelling of an ionic network.	23
Figure 3-1 Schematic of the polymerization apparatus.	26
Figure 3-2 Structures of the (a) monomer, (b) crosslinker, and (c) initiator.	28
Figure 3-3 Initiation (a) and propagation (b) of poly(vinylbenzyl chloride) polymerization.	30
Figure 3-4 Termination of poly(vinylbenzyl chloride) polymerization.	31
Figure 4-1 The pore size distribution of beads whose formulation is 0% Kraton G1652, 12% divinylbenzene, 33% dodecane and 40% total diluent.	43
Figure 4-2 The pore size distribution for beads whose formulation is 0% Kraton G1652, 6% divinylbenzene, 33% dodecane and 60% total diluent.	44
Figure 4-3 SEM micrograph of cross-section of a bead whose formulation consists of 2% Kraton G1652, 12% divinylbenzene, 33% dodecane, and 40% total diluent.	46
Figure 4-4 Pore size distribution of beads whose formulation consists of 2% Kraton G1652, 12% divinylbenzene, 33% dodecane, and 40% total diluent.	47

Figure 4-5 Cumulative volume of mercury vs. diameter for beads whose formulation consists of 2% Kraton G1652, 12% divinylbenzene, 33% dodecane, and 40% total diluent.	48
Figure 4-6 Pore size distribution for beads whose formulation is 2% Kraton G1652, 12% divinylbenzene, 40% total diluent, and 0% dodecane.	50
Figure 4-7 Pore size distribution for beads whose formulation is 2% Kraton G1652, 12% divinylbenzene, 40% total diluent, and 66% dodecane.	51
Figure 4-8 Cumulative volume of mercury vs. diameter for beads whose formulation consists of 2% Kraton G1652, 12% divinylbenzene, 0% dodecane, and 40% total diluent.	52
Figure 4-9 Cumulative volume of mercury vs. diameter for beads whose formulation consists of 2% Kraton G1652, 12% divinylbenzene, 66% dodecane, and 40% total diluent.	54
Figure 4-10 SEM micrographs of beads whose formulations are 2% Kraton G1652, 12% divinylbenzene, 40% total diluent, and (a) 0%, (b) 33% and (c) 66% dodecane.	56
Figure 4-11 SEM micrographs of beads whose formulations are 8% Kraton G1652, 12% divinylbenzene, 40% total diluent, and (a) 0%, (b) 33% and (c) 66% dodecane.	57
Figure 4-12 SEM micrographs of cross-sections of beads whose formulations are 12% divinylbenzene, 33% dodecane, 40% total diluent and (a) 2%, (b) 8%, and (c) 14% Kraton G1652.	59
Figure 4-13 SEM micrographs of beads consisting of 14% Kraton G1652, 12% divinylbenzene, 33% dodecane and 40% total diluent. Magnification (a) 40X, (b) 500X, and (c) 1000X.	61
Figure 4-14 Pore size distribution of 8% Kraton G1652 12% divinylbenzene, 33% dodecane and 40% total diluent poly(vinylbenzyl chloride) beads.	62
Figure 4-15 Pore size distribution of 14% Kraton G1652 12% divinylbenzene, 33% dodecane and 40% total diluent poly(vinylbenzyl chloride) beads.	63

Figure 4-16 Cumulative volume vs. diameter of beads whose formulation consists of 8% Kraton G1652 12% divinylbenzene, 33% dodecane and 40% total diluent.	65
Figure 4-17 Cumulative volume vs. diameter of beads whose formulation consists of 14% Kraton G1652 12% divinylbenzene, 33% dodecane and 40% total diluent.	66
Figure 5-1 Normalized Diameter vs. Time for beads whose formulations are 2% Kraton G1652, 33% dodecane, 40% total diluent and 6, 12, or 18 % divinylbenzene.	74
Figure 5-2 Normalized Diameter vs. Time for beads whose formulations are 8% Kraton G1652, 33% dodecane, 40% total diluent and 6, 12, or 18 % divinylbenzene.	75
Figure 5-3 All diameter ratios in toluene vs. % divinylbenzene.	76
Figure 5-4 Normalized diameter vs. time for beads consisting of 14% Kraton G1652, 12% divinylbenzene, 40% total diluent and 0, 33, or 66% dodecane.	78
Figure 5-5 All diameter ratios vs. percent dodecane.	80
Figure 5-6 Normalized diameter vs. swelling time of beads whose formulations are 14% Kraton G1652, 12% divinylbenzene, 33% dodecane, and 40% or 60% total diluent.	81
Figure 5-7 All diameter ratios vs. percent total diluent.	82
Figure 5-8 All data consisting of 40% total diluent vs. %Kraton G1652.	
Figure 5-9 Normalized diameter vs. time of beads whose formulations are 2% Kraton G1652, 12% divinylbenzene, 40% total diluent, and 0, 33, or 66% dodecane.	88
Figure 5-10 Swell times of all formulations vs. percent dodecane.	89
Figure 5-11 Swell times of all formulations vs. percent Kraton G1652.	92
Figure 6-1 Amination of poly(vinylbenzyl chloride) with diethanolamine.	94

Figure 6-2 All percentages of nitrogen vs. % divinylbenzene.	97
Figure 6-3 All percentages of nitrogen vs. % Kraton G1652.	98
Figure 6-4 All percentages of nitrogen vs. % dodecane.	100
Figure 6-5 All percentages of nitrogen vs. % total diluent.	101
Figure 6-6 All diameter ratios in acid vs. % divinylbenzene.	105
Figure 6-7 Normalized diameter vs. time for beads whose formulation is 2% Kraton G1652, 0% dodecane, 60% total diluent, and 6, 12, or 18% divinylbenzene.	106
Figure 6-8 All diameter ratios in acid vs. % Kraton G1652.	107
Figure 7-1 A plot of the change in displacement (Δy) vs. Force ^{2/3} for the formulation: 2% Kraton G1652, 18% divinylbenzene, 0% dodecane and 40% total diluent.	116
Figure 7-2 Force ^{2/3} vs. displacement for a bead with the formulation 2% Kraton G1652, 18% divinylbenzene, 0% dodecane and 40% total diluent.	117
Figure 7-3 Penetration moduli vs. % Kraton G1652.	120
Figure 7-4 All penetration moduli vs. % divinylbenzene.	122
Figure 7-5 All penetration moduli vs. % total diluent.	123
Figure 7-6 All penetration moduli vs. % dodecane.	124

ABSTRACT

POLYMER SUBSTRATES FOR USE IN FIBER OPTIC SENSORS: SUSPENSION POLYMERIZATION OF KRATON G1652 MODIFIED POLY(VINYLBENZYL CHLORIDE)

by

Vicki L. Conway
University of New Hampshire, December, 1994

The polymerization of Kraton G1652 modified poly(vinylbenzyl chloride) in the presence of xylene and dodecane is complex. Scanning electron micrographs and porosimetry data suggest that as polymerization proceeds, the forming poly(vinylbenzyl chloride) and the porogenic solvent separate into distinct aromatic and aliphatic phases, respectively. The Kraton G1652 acts as a surfactant between the dodecane and the forming polymer swollen in monomer, and is directly involved in stabilizing the interface. Increasing the Kraton G1652 increases the surfactant content of the monomer mixture which decreases the surface tension between the forming polymer and the dodecane during polymerization, resulting in a morphology consisting of small poly(vinylbenzyl chloride) spheres situated throughout the aliphatic matrix. Because Kraton G1652 has a stabilizing effect, the resulting morphology is due to the drive to lower energy and therefore increase the surface area between the two phases. Removal of the porogenic solvents results in a matrix that consists of microporous

poly(vinylbenzyl chloride) spheres surrounded by a “sea” of micro- and macroporous polymer.

The morphology of the matrix governs the properties of the polymer. The diameter ratio and swell time of the beads were measured in both toluene and acid. The bead formulations were further characterized by the determination of the penetration modulus, which is a measure of the mechanical strength.

The process of swelling the beads in toluene is not the same as in acid. Swelling in toluene is dependent upon the solvent’s access into the bead’s interior, whereas, swelling in acid is dependent upon the number of sites which were protonated throughout the matrix. Swelling time in toluene is dependent upon the pore structure of the polymer. It is not evident that the swell time in acid is dependent upon the same parameters, further indicating that the swelling processes are distinct. The penetration modulus is largely determined by the pore space present in the polymer matrix. As the volume of pore space increases, the penetration modulus decreases.

CHAPTER I

INTRODUCTION

The field of fiber optic chemical sensors (FOCS) has grown in recent years. The availability and technology of optical fibers provide the opportunity to break away from the traditional amperometric or potentiometric approach to chemical sensors. Incorporating optical fibers into a sensor allows for the direct measurement of an optical signal, eliminating the need for an electrochemical means of analyte detection.

There are many advantages to using optical fibers to carry the signal. Optical fibers have excellent attenuation properties. Signals can be transferred over long distances without appreciable loss, making fiber optic chemical sensors well suited for remote sensing. Another advantage is that there is no possibility for electrical interference, and if an intensity ratio is measured, no drift in the signal resulting in calibration stability. It is also possible to fabricate small sensors using one or two optical fibers. Since light (electromagnetic radiation) is the measured signal, *in situ* spectroscopic sensing of the analyte is possible, provided the analyte is spectroscopically detectable. Fiber optic chemical sensors have been developed for many applications. They generally fall into two categories: direct

secondary detection in which an immobilized indicator dye reacts with the analyte. The majority of research to date has dealt with sensors based on the measurement of color changes or luminescence.

Chemical sensors consist of a chemical recognition component coupled with a transduction element.¹ The chemical recognition component in indicator based sensors consists of a reaction which involves the analyte. This reaction produces a measurable quantity that is related to the concentration of analyte present through a calibration curve. The transduction element carries the signal from the chemical recognition component to the detector. FOCSs are unique because they use optical fibers as the transduction element to carry the light signal to the detector.

FOCSs were first almost exclusively developed to measure pH. Peterson and coworkers² were the first research group to study the measurement of pH using optical fibers. Phenol red was immobilized on polyacrylamide microspheres. A mixture of these microspheres and smaller polystyrene microspheres (added to promote light scattering) were packed in a dialysis membrane to which a pair of optical fibers was fitted. Using this sensor, it was possible to measure pH over the range of 7.0-7.4.

Seitz and Saari³ were the first to base the optical measurement on fluorescence. Fluoresceinamine was immobilized on both glass and cellulose, then

attached to the end of a bifurcated fiber optic bundle. This study verified that it was possible to use fluorescence measurements for remote chemical sensing.

It is also possible to base FOCSs on changes of optical properties other than those already mentioned. For example, a sensor was developed to monitor hydrocarbons in water based on changes in the refractive index of an immobilized reagent. Kawahara et. al⁴ removed the cladding from an optical fiber then coated it with an organophilic compound. When the coated optical fiber was placed in a solution containing hydrocarbon compounds, they were adsorbed changing the refractive index of the coating, which caused a change in fiber transmission efficiency.

Since then, fiber optic chemical sensors have been developed to measure a variety of analytes, including O₂,⁵⁻⁸ CO₂,⁹ NH₃,¹⁰ Na⁺,¹¹ as well as various metal ions^{12,13} and humidity.¹⁴ Because the potential advantages of fiber optic sensors over conventional sensors is so attractive, the field is continuing to expand, producing FOCS that are specific to individual applications.^{15,16}

Fiber optic chemical sensors based on the absorbance or luminescence of an immobilized dye have limitations. Immobilized dyes are often chemically unstable, and can usually work at specific wavelengths. The dye often leaches, and photobleaching is also a problem.

To address this problem, a new fiber optic chemical sensor has been developed based on the movement of a reflector in response to polymer swelling.

It is unique because the sensing element (a crosslinked polymer) and the transduction element (the fiber) are not in direct contact with each other. The light signal is isolated from the analyte to be measured.^{17,18} Crosslinked polymers are inherently rugged and can be derivatized for various sensing applications. They are thermally stable and mechanically strong.

In addition, these sensors are more convenient and cost-effective requiring only simple instrumentation for signal collection. The wavelength of light used in the sensor is not restricted to a particular wavelength. Therefore, near-infrared radiation can be employed allowing the use of technology and fibers developed for the telecommunications industry. This not only improves the attenuation properties, but also reduces the cost of the proposed instrumentation since LED and photodiodes can be used.

Fiber Optic Sensors Based on Polymer Swelling

Polymer molecules are crosslinked by interconnecting various polymer chains. When neutral crosslinked polymers are immersed in an compatible solvent, they try to dissolve. However, their three-dimensional network makes this impossible. Instead, they will absorb solvent, swelling to the point where the

swelling forces due to solvation are balanced by the retractive forces due to the stretching of the polymer.

Ionic polymers swell due to an osmotic effect. If the charge density inside the polymer is larger than the charge density in the surrounding solution, the system will respond to equalize that charge. Solution will enter the polymer, swelling it to the point where the retractive forces due to the stretching of the bonds balance the swelling forces.¹⁹

Seitz and McCurley²⁰ were able to build a sensor using the commercially available cation exchange resins Dowex (sulphonated polystyrene) and SP Sephadex (sulphonated dextran). The sensor responded to varying salt concentrations, i.e., the polymer bead would swell and shrink according to the concentration of salt in the solution. Thus, they were able to verify the possibility of a sensor based on polymer swelling.

The sensor design graduated²¹ from an early prototype to the more advanced and flexible design shown in Figure 1-1. A polymer bead is placed upon the diaphragm. A reflector is attached to the underside of this diaphragm. Separate optical fibers carry the light to and from the reflecting surface. As the polymer bead swells with changes in analyte concentration, it displaces the diaphragm. The amount of light reflected varies with the concentration of the analyte in the measured solution.

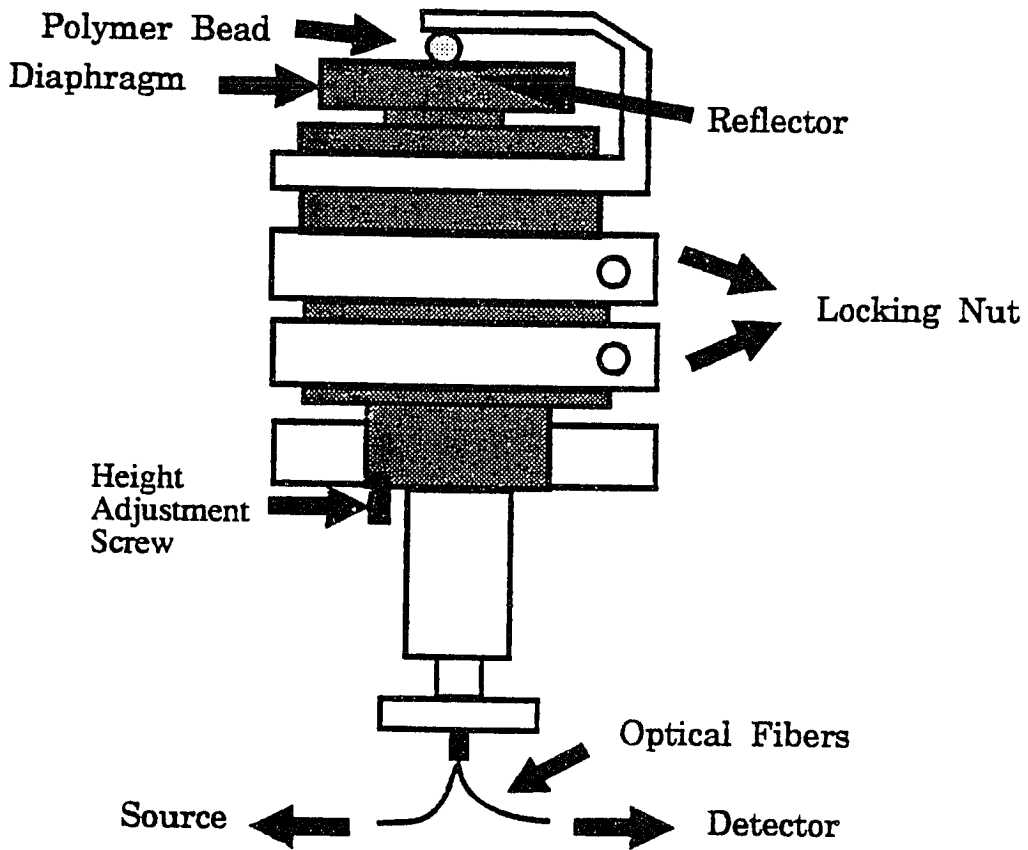


Figure 1-1 Schematic of fiber optic sensor based on polymer swelling.

The amount of light reflected is a function of the movement of the reflector. This configuration, known as an optical lever,²² is better illustrated in Figure 1-2. Each optical fiber has a specific numerical aperture, which describes the maximum angle for emitting or collecting light. When light is emitted through the fiber from the source, a cone of light of certain area will reach the reflector. Only that light within the area described by the numerical aperture of the collecting fiber will be collected and reach the detector. If the mirror is moved farther away from the two fibers, the cone of light for emitting and collecting is increased, increasing the overlap area of the two fibers and the amount of light that will reach the detector. The placement, size, and numerical aperture of the fibers have a direct effect on the amount of light reflected upon displacement.²³

Sensors based on polymer swelling have been developed for various sensing applications. Using commercially available ion exchange resins, sensors were developed to measure ionic strength²⁴ and the water content in organic solvents.²⁵ Sensors²⁶ for measuring metal ions and hydrocarbons in water have been investigated using laboratory generated beads.

While the feasibility of the proposed sensor was demonstrated with commercially available resins, these materials are unacceptable for regular use. Commercially available resins are typically designed to prevent, or, at least, minimize polymer swelling, which is an undesirable characteristic for most applications. This is accomplished using a high degree of crosslinking, which

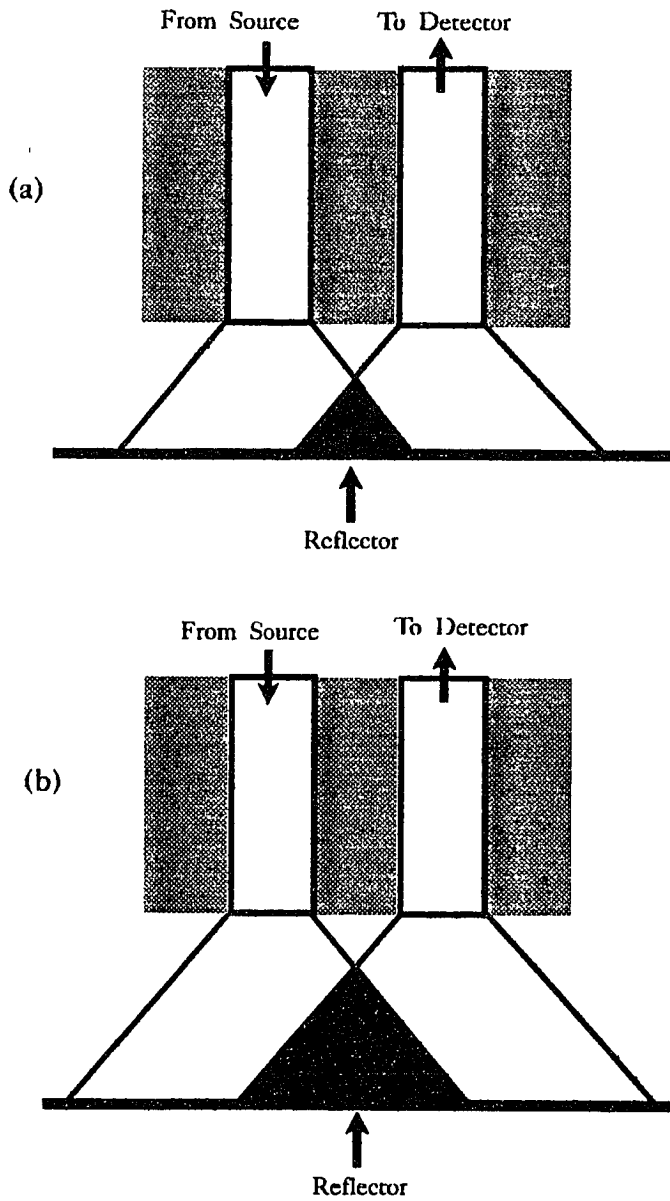


Figure 1-2: The overlap region of a two-fiber sensor arrangement (a). The increase in the overlap region as the reflector is moved further away (b).

allows only insignificant swelling. They also are not mechanically tough, breaking under repeated swelling and shrinking cycles. The resins would crack after approximately thirty cycles.²⁷

It was, therefore, necessary to synthesize beads that would swell and shrink quickly and reversibly when in contact with varying analyte concentrations, were mechanically robust with little hysteresis after repeated use, and were easily derivatized for use in various sensing applications.

Polystyrene was chosen as the substrate for use in our sensors for a variety of reasons. It has many of the optimal properties needed for a solid support. It can be easily functionalized due not only to its aromatic ring, but also because it is compatible with most organic solvents. The functional group determines the polymer's compatibility with a polar solvent like water. Polystyrene does not easily degrade under normal conditions because its aliphatic hydrocarbon backbone is resistant to attack by most reagents. The extent of crosslinking, which directly influences polystyrene's characteristics, can be easily controlled, and polystyrene is mechanically stable. Finally, porosity is easily introduced into the polystyrene matrix by including inert solvents in the polymer formulation.^{28,29}

Polymers for Use as the Sensing Element

One approach to derivatizing polystyrene involves chloromethylation, which introduces a site for attaching a variety of functional groups. However,

chloromethylation of an already formed polystyrene resin introduces further crosslinking into the polystyrene.³⁰ An alternative method to produce chloromethylated polystyrene is to use vinylbenzyl chloride as the monomer. In this way, the chloromethyl groups are included in the polymerization process, and separate chloromethylation is not necessary.³¹

Porogenic solvents, known as porogens, are used to introduce pores into the polystyrene matrix as it is forming. The size of the pores can be controlled by the type of porogen that is added to the mixture. Millar et.al³² studied the effect of adding an inert solvent compatible with the polystyrene as a diluent to the polymerization mixture. The effect of the addition of a solvent that is not compatible with the forming polymer was also studied.³³ They found that when the polymerization took place in the presence of a solvating diluent, the polymer chains were solvated at all times, leading to a polymer matrix whose chains were less entangled. If the crosslinking content was sufficient, a porous polymer resulted upon removal of the diluent. However, when the polymerization took place in the presence of a non-solvating diluent, a partial phase separation occurred between the diluent and the forming polymer. The resulting structure, upon removal of the diluent, was found to consist of regions of entangled strands connected to each other by fewer relatively untangled chains. The space occupied by the diluent became large pores (150-500 μ m) and the material was said to be macroporous.

Studies^{34,35} have also been conducted which use a mixture of both a solvating and a non-solvating diluent in the polymerization reaction. The phase separation between the non-solvating diluent is less pronounced with the added solvating diluent, resulting in more uniform pores that are smaller than those obtained with the non-solvating diluent only. Average pore size depends on the relative amounts of the two diluents, making it possible to control pore size for specific applications.

Because polystyrene has a high glass transition temperature, it is brittle at room temperature. Impact modifiers³⁶ are often formulated into plastics to improve the resistance of the polymer to stress. These additives are usually elastomeric. For example, high impact polystyrene is formed by polymerizing styrene and butadiene simultaneously with processing so that small elastic inclusions of polybutadiene are formed.³⁷ Alternatively, the polymers can be physically blended together by first dissolving them in benzene and subsequently precipitating them out.³⁸ Sardelis et.al³⁹ improved the toughness of polystyrene by polymerizing it in the presence of styrene-butadiene-styrene tri-block polymers.

Kraton G1652, produced by Shell, is a styrene/ethylene-butylene/styrene tri-block polymer.⁴⁰ As an additive, it can improve the impact toughness of a polymer and add flexibility, softness and elasticity to plastics. It is commonly used to improve the properties of adhesives, road asphalt, and roofing tiles. Kraton can also be directly injection molded into various products, including

medical/FDA regulated products. Chlanda and Cooke⁴¹ increased the mechanical stability of polystyrene sulfonated membranes by incorporating Kraton G into the membrane. Both Kraton G and polystyrene were dissolved in dichloroethane, sulphonated, then solvent cast on a glass plate to produce the membrane. The resulting membrane, after annealing, was very strong, but not brittle.

Earlier work in this group by Sizhong Pan⁴³ studied the properties of diethanolamine derivatized beads which had been modified with Kraton G1652 and the porogenic solvent toluene. He found that the aminated porous poly(vinylbenzyl chloride) beads had a larger swelling ratio when compared to aminated polystyrene and aminated, non-porous poly(vinylbenzyl chloride) beads. He also found that a small amount of Kraton G1652 incorporated into the beads significantly reduced the cracking of the beads upon swelling and shrinking, whereas, higher percentages of Kraton G1652 resulted in beads that were not mechanically stable and would crack during the first swelling cycle. The effect of Kraton G1652 on the morphology of the polymer beads was not evaluated. A further understanding of the polymerization process and morphology was necessary in order to predict the outcome of future modifications.

Thesis Research

Because commercial beads do not have the characteristics needed for use in the sensor, the synthesis of beads with optimal characteristics was necessary. The

optimal beads should: (1) be able to go through repeated swelling and shrinking cycles with little or no hysteresis; (2) be mechanically strong so that they move the diaphragm and not break under the pressure; (3) be intrinsically rugged so as not to decompose under harsh chemical conditions; (4) swell to equilibrium rapidly for fast response times; and (5) be easily derivatized for use with various analytes.

Poly(vinylbenzyl chloride), chosen as the polymer substrate, did not possess the optimal properties for sensing. The polymer matrix had to be modified to improve the physical properties of the sensing element. Kraton G1652 was added to the polymer matrix to improve the toughness of the polymer. We believed that the Kraton G1652 would create elastic inclusions within the polymer matrix. Therefore, when microcracks develop in response to swelling, they would terminate in these inclusions preventing the formation of large cracks throughout the polymer matrix.

Divinylbenzene is a monomer with two active vinyl groups. Controlling the amount of divinylbenzene essentially controls the extent of crosslinking of the polymer matrix. The crosslinking content determines the equilibrium diameter ratio, as well as having a direct effect on the rigidity of the polymer matrix.

The swelling time of the polymer is solely responsible for the response time of the sensor. If the polymer swells slowly, the response time of the sensor is undesirably high. To improve response time, a pore-forming solvent was added to the monomer mixture. The addition of pores gives the solvent better access to the

bead's interior, allowing swelling to occur more quickly, reducing the response time of the sensor. The pore-forming solvent added was actually a mixture of two solvents; dodecane and xylene.

Dodecane is a “non-solvating” pore forming solvent, commonly used to obtain macroporous polymers. It is not an efficient solvent for the forming polymer, precipitating it out of the dodecane and ultimately causing larger pores to form. Xylene is a popular microporous pore-forming solvent for styrene. It is a good solvent for the forming polymer as well as the monomer, resulting in the formation of smaller pores. Xylene was added not only as a pore-forming solvent, but also as a solvent for the Kraton G1652 elastomer. It was hypothesized that the xylene would not only keep the styrenic ends of the tri-block polymer in solution, but would help to solvate the center ethylene/butylene block. The solvent compatibility parameters⁴² for xylene, dodecane, polystyrene and polyethylene are 18.0, 16.2, 17.8, and 16.0 (MPa)^{1/2} respectively, further indicating the compatibility of the aliphatic and aromatic components of the monomer mixture.

Poly(vinylbenzyl chloride) beads were prepared by suspension polymerization, varying the four major parameters of the polymer formulation: the crosslinker, elastomer, and the two porogenic solvents. A factorially designed experiment was carried out in which the four parameters were varied systematically. A factorial design makes it possible to statistically determine the

effect and the significance of changing the four major parameters as well as interactions between the parameters on the various polymer properties.

The theoretical background of the properties of polymers, including swelling is found in Chapter II. Experimental information is presented in Chapter III. Chapter IV discusses the morphology of the modified polymer using SEM micrographs and mercury porosimetry. The rate and magnitude of swelling the underivatized beads in toluene and aminated beads in acid, are presented in Chapters V and VI, respectively. The penetration modulus, a measure of the bead's mechanical strength, is discussed in Chapter VII.

CHAPTER II

THEORY

Mechanical Properties of Polymers

Polymers are large complex molecules composed of a repeating chemical unit, called a monomer. Most polymers useful for plastics have molecular weights in the range of 10,000-1,000,000. They are prepared by two types of processes identified as step-reaction and chain-reaction polymerizations. Step-reaction polymerization is also known as condensation polymerization, and behaves similarly to a condensation reaction involving low-molecular weight compounds. Two polyfunctional molecules come together to produce one larger polyfunctional molecule typically with the elimination of a smaller molecule, such as water or HCl.

Chain reaction polymerizations are also known as radical polymerizations. A free radical is generated which reacts with a vinyl group on a monomer to produce another radical (initiation). This radical adds to the double bond, generating another radical. That chain radical then successively reacts with another vinyl monomer to form an increasingly larger polymer molecule (propagation). The reaction ends by two radicals combining and reacting

to form a bond, or by hydrogen transfer which results in the formation of two molecules with one saturated and one unsaturated end group (termination).⁴⁴

Polymers are easily crosslinked by incorporating monomers that have two reactive sites. Both sites can react essentially linking two polymer strands together so that each polymer strand is “segmented” into sections. This results in one large three-dimensional network, i.e., one large molecule whose molecular weight is essentially infinite.

Polymers are viscoelastic. When they are exposed to external forces, they respond with behavior between an elastic solid and a viscous liquid. The external force applied to the polymer is known as stress. The reaction of the polymer to that stress is defined as the strain. Measuring the relationship between stress and strain defines the polymer’s mechanical properties through moduli, which are dependent upon temperature.⁴⁵

Thermal energy is necessary to instigate movement of the polymer chains. A specific characteristic of a polymer is its glass transition temperature. It is the temperature below which there is not enough thermal energy to promote molecular movement of the polymer. Below the T_g , the polymer behaves as a glass with properties such as hardness, stiffness, brittleness and transparency.⁴⁶ As the temperature increases, the thermal energy of the polymer also increases, increasing the vibrational motion of the polymer. With a further increase in temperature, the

thermal energy will eventually be high enough for rotational and translational movement of the polymer segments.⁴⁷

Above the glass transition temperature, the polymer chains have sufficient energy to move and thereby relieve stress. The polymer is pliable and can be softened. Uncrosslinked polymers can be made to flow or melt and take on the property of a viscous liquid. Polymer melts can be easily molded to take on new shapes by various techniques.

Suspension Polymerization

A suspension polymerization is essentially a bulk polymerization that takes place in an aqueous system. The monomer is dispersed as droplets in an immiscible liquid phase, resulting in the formation of beads. It is distinguished from emulsion polymerization by the fact that the initiator is typically dissolved in the monomer phase, and the reaction follows first order kinetics.⁴⁸

The monomer soluble initiator is thermally activated, causing the radical polymerization to proceed. At the onset of gelation, usually quite early in the reaction, a tacky period is reached where the monomer swollen particles have a tendency to coalesce or stick together, forming an amorphous product. Droplet coalescence during the tacky period can be avoided by the use of suspension stabilizers and suitable stirring techniques.

The stirring process not only controls the likelihood that the beads will collide during the polymerization process, but also plays a role in determining the size distribution of the beaded polymer product. Therefore, a suitable stirring process in suspension polymerization is essential. The vortex formed around the stirring rod is avoided by using a baffled vessel along with a stirring rod whose paddles are positioned at a 90° angle to the rod. By using this type of equipment, the desired top to bottom flow is attained.⁴⁹

The suspension stabilizer helps to provide a stable dispersion of the liquid globules. Its job is primarily to reduce the surface tension between the monomer droplets and the suspension medium. It forms a “protective film” between the oil-like droplet and the aqueous medium, which reduces the tendency of the beads to collide and coalesce.

The three main categories of suspension stabilizers are soluble inorganic oxides and salts, ionic surfactants, and non-ionic surfactants. The category of non-ionic surfactants includes gums, gelatins, and synthetic polymers, which are used widely in suspension polymerizations.

Bead sizes typically range from 100µm-1mm. The droplet size is controlled by changing the surface tension that exists between the droplet and the aqueous system, the stirring rate, or the volume fraction of monomer/aqueous phase. A decrease in surface tension between the beads will result in a decrease in

bead size. The optimal monomer/aqueous phase ratio used to keep the weight ratio of stabilizer to monomer adequate was found to be about 1:10.⁵⁰

Nonionic Polymer Swelling

When crosslinked polymers are immersed in a compatible solvent, they will try to dissolve. However, their three dimensional network makes this impossible. Instead, they will absorb the solvent, swelling to the point where the forces due to swelling balance the retractive forces of the bonds. Polymer swelling in a compatible solvent behaves according to the relationship first described by Flory⁵¹ (Equation (1)):

$$(q_m)^{\frac{5}{3}} = \left(\frac{v \cdot M_c}{M} \right) \cdot \left(1 - 2 \cdot \frac{M_c}{M} \right) \cdot \frac{\left(\frac{1}{2} \right)^{-\chi_1}}{V_1}$$

where q_m = equilibrium swell ratio,
 v = specific volume of the polymer,
 M_c = molecular weight per cross-linked unit,
 M = Total molecular weight of the polymer network,
 χ_1 = interaction parameter that expresses first neighbor interaction
 free energy, divided by kT , for solvent with polymer, and
 V_1 = molecular volume of solvent.

This relationship indicates that polymer swelling in a compatible solvent is dependent upon the extent of crosslinking and the affinity of the solvent for the polymer. The extent of swelling is related to the extent of crosslinking (M_c/M), and to the solvent interaction parameter (χ_1).

Ionic Polymer Equilibrium Swelling

Swelling of an ionic polymer is inherently different than that of a neutral polymer. The swelling of a neutral polymer is mainly dependent upon crosslinking density and solvent compatibility. The swelling of an ionic polymer, while still dependent upon the effects described for the neutral polymer, is also dependent upon electrostatic repulsion.

When immersed in acid, the amine derivatized polymers become protonated. The presence of positive charges close together cause electrostatic repulsion, which, in turn, causes the polymer to swell. When the same polymer is placed in base, the aminated sites become deprotonated, and the polymer shrinks.

An equation describing the swelling relationship for charged polymers was published by Flory⁵² (Equation (2)):

$$q_m^{5/3} = [(i/2V_u S^{1/2})^2 + (1/2 - \chi_1)/V_1]/(v_e/V_0)$$

where,

i = number of electronic charges per polymer unit,

V_u = molecular volume of polymer repeating unit,

S = molar ionic strength,

ν_e = effective number of chains in a network, and

V_0 = Volume of the unswollen polymer network.

The first term of the equation deals with the ionic strength/electrostatic effects of polymer swelling, while the second term refers to the solvent/polymer compatibility. As can be seen from the equation, the swell ratio (q_m) decreases with increasing ionic strength (S). This phenomenon can be better described using the principle of osmosis.

A polymer that has been protonated has a certain charge density. If that polymer is put into a solution whose charge density (ionic strength) is lower than that of the polymer, solvent will enter that polymer in an attempt to equalize the charge density in the system. This is illustrated in Figure 2-1. As the ionic strength of the outside solution increases, the difference in charge density between the solution and the polymer decreases.

Swelling of an ionic polymer network is, therefore, mainly dependent upon three factors: 1) the degree of crosslinking, 2) the compatibility of the polymer and solvent and 3) and the electrostatic characteristics of the polymer network.

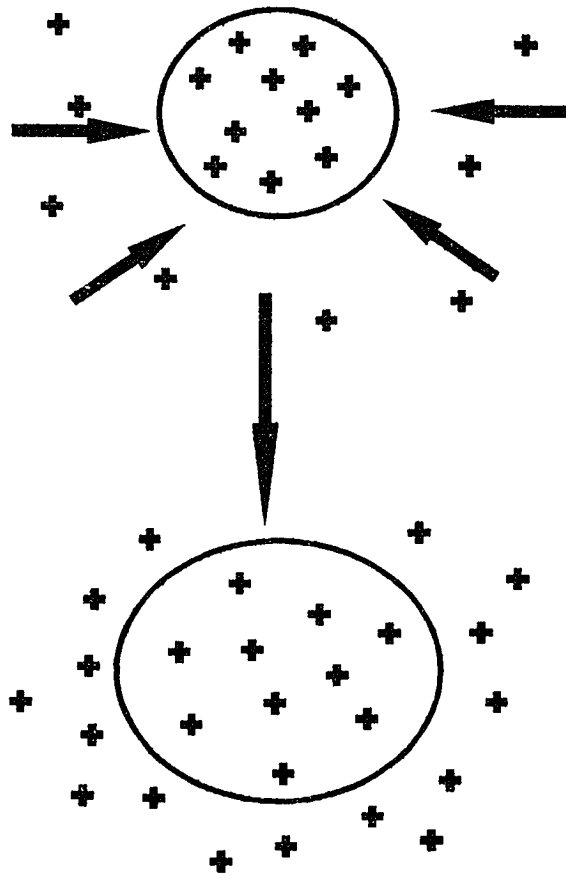


Figure 2-1 Illustration of the “osmotic effect” of swelling of an ionic network.

CHAPTER III

EXPERIMENTAL

Suspension Polymerization of Modified Poly(vinylbenzyl chloride)

Reagents

Vinyl benzyl chloride (30% para/ 70% meta) was donated by Dow Chemical Corp., Midland, MI. Divinylbenzene (45-55% active, 2:3 meta/para) and benzoyl peroxide (water wet, 77%) were both purchased from Polysciences, Inc., Warrington, PA. Kraton G1652, a styrene - ethylene/butylene - styrene triblock polymer (29% styrene, 71% ethylene/butylene), was donated by Shell Chemical Co. Dodecane, o-xylene, hydroxybutyl methyl cellulose, and xanthan gum were purchased from Aldrich Chemical Co., Inc., Milwaukee, WI. Acetone and toluene were obtained from Fisher Scientific, Fair Lawn, NJ. All chemicals were reagent grade and were used without further purification. Water was doubly deionized, then distilled in a Corning Megapure water distillation apparatus.

Apparatus

A schematic diagram of the polymerization apparatus is shown in Figure 3-

1. A 750 mL, indented cylindrical reaction flask with a 3-neck head, purchased from Chemglass, Vineland, NJ, was used as the polymerization vessel.

Polymerizations were carried out in a constant temperature water bath. A mechanical stirrer was used with a stir rod equipped with 90° paddles purchased from VWR Scientific. Diameter ratios were measured with a Fisher Scientific Stereomaster microscope, magnification 30X or 60X.

Procedure

Dissolution of Suspension System (aqueous medium)

Xanthan gum and hydroxybutyl methyl cellulose are high molecular weight molecules, and therefore, do not readily go into solution. Dissolution was most easily accomplished by allowing the solid to swell on the surface of the water before stirring. Xanthan gum (0.04g) and 0.28g hydroxybutyl methyl cellulose were dispersed on the surface of 500mL of distilled water. After approximately one hour, the mixture was vigorously stirred with minimal heat until a homogeneous solution was obtained.

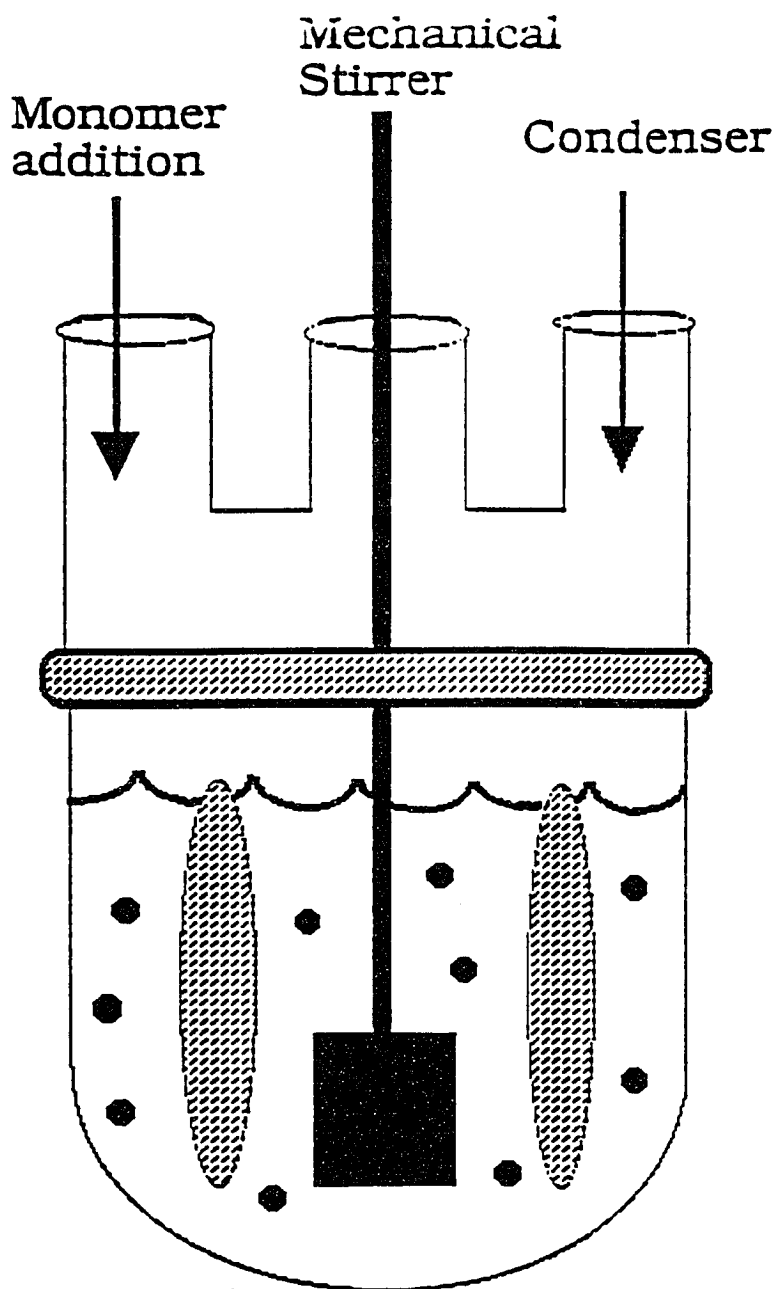
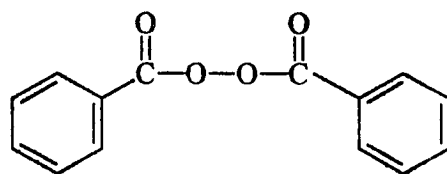
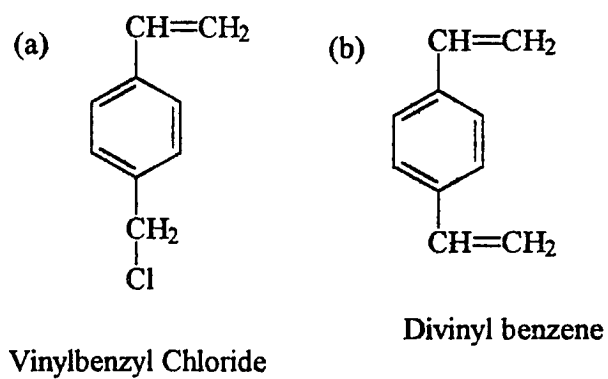


Figure 3-1 Schematic of suspension polymerization apparatus.

Monomer System (organic medium)

Vinylbenzyl chloride, divinylbenzene, benzoyl peroxide (see Figure 3-2), Kraton G1652, dodecane and o-xylene were dissolved into one solution according to the percentages in the factorial design shown in Table 1. The reaction mechanism is shown in Figure 3-3 and 3-4. All percentages are based solely upon the amount of vinylbenzyl chloride in the monomer mixture. The percentage of divinylbenzene was calculated by a mole/mole ratio. The calculated volume was then multiplied by two because the divinylbenzene purchased from Polysciences was approximately 50% active. The amount of benzoyl peroxide used was 1-2 wt% of the vinylbenzyl chloride in the monomer mixture. Kraton G1652 was also calculated by wt% of the monomer. The total diluent content refers to the percentage of the total volume of dodecane and xylene in the monomer mixture, again calculated according to the volume of vinylbenzyl chloride in the mixture. The percentage of dodecane refers to the volume of dodecane versus the volume of xylene in the total diluent content only. For example, the recipe for beads consisting of 2% Kraton G1652, 6% divinylbenzene, 33% dodecane and 60% total diluent is as follows: 0.176 moles vinylbenzyl chloride (25.0 mL), 0.021 moles divinylbenzene (3.0 mL), 0.527g Kraton G1652, 0.0242 moles dodecane (5.5 mL), 0.0929 moles xylene (11.2 mL) and 0.00165 moles of benzoyl peroxide (0.400 g).



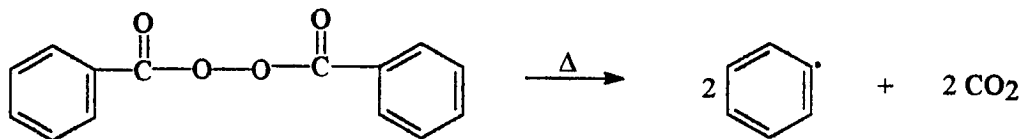
Benzoyl peroxide

Figure 3-2 Structures of the (a) monomer, (b) crosslinker, and (c) initiator.

		% Kraton G1652									
		2			8			14			
		0	33	66	v% Dodecane in Diluent			0	33	66	
% Divinylbenzene	6	40									
		60									
	12	40									
		60									
	18	40									
		60									

Table 3-1 Factorial design for the suspension polymerization of Kraton G1652 modified poly(vinylbenzyl chloride).

(a) Initiation



(b) Propagation

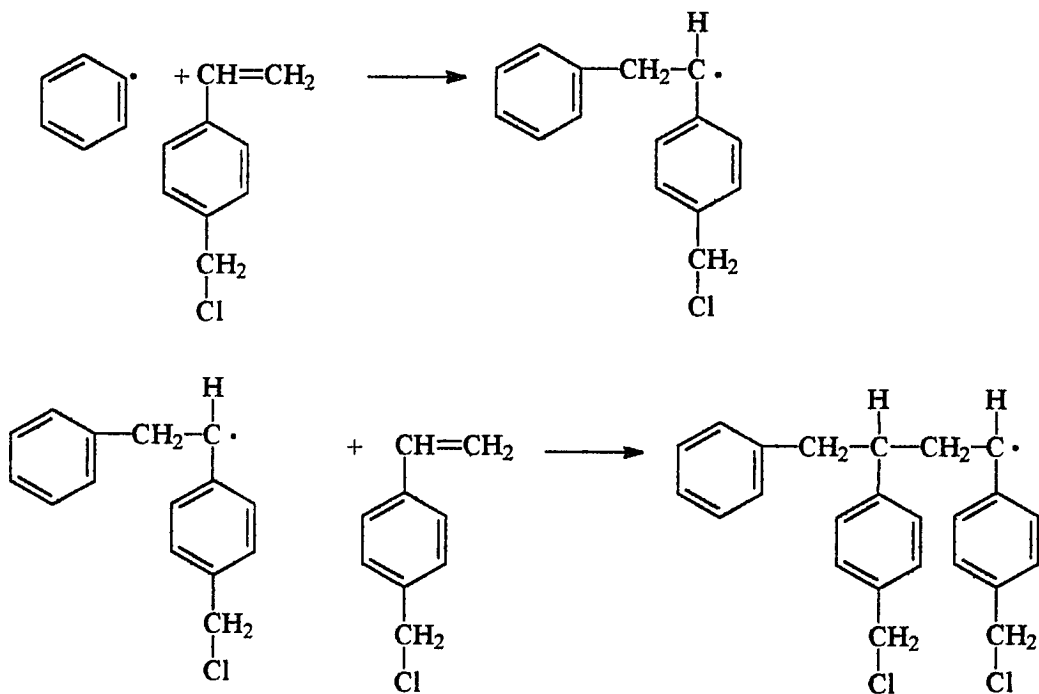


Figure 3-3 Initiation (a) and propagation (b) of poly(vinylbenzyl chloride) polymerization.

Termination

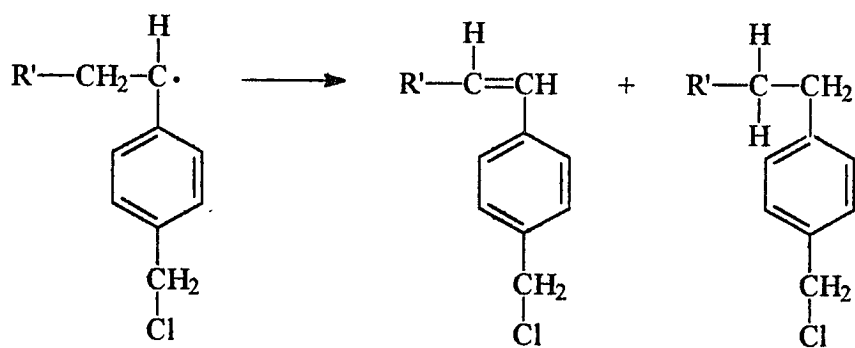
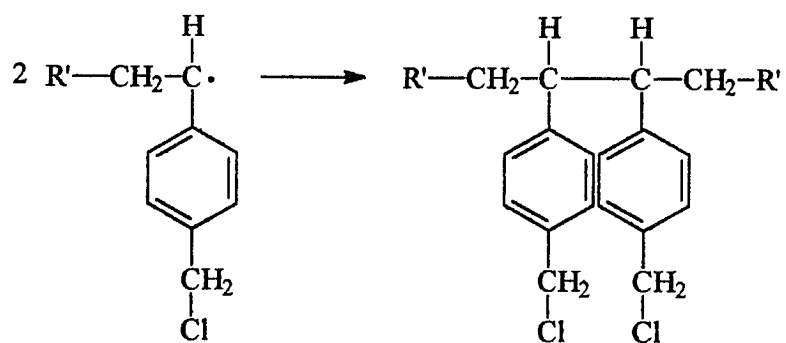


Figure 3-4 Termination of poly(vinylbenzyl chloride) polymerization.

Suspension Polymerization

The dissolved suspension system (aqueous medium) was transferred to the polymerization vessel equipped with the mechanical stirrer. The suspension system was allowed to come to temperature, with stirring, in the water bath set at 83°C. The monomer system was transferred into the suspension system, while stirring at the rate of approximately 200 rpm. The reaction was allowed to proceed for 7 hours, with careful supervision. After approximately 3 hours, the reaction reaches what is known as the “tacky stage” of the polymerization. At this time, the stir rate must be slightly increased to insure that the beads do not coalesce causing them to stick together in clumps.

After 7 hours, the beads were filtered using a Buchner funnel, and rinsed with water to remove the excess suspension system. The beads were then soaked overnight in acetone to wash and remove the excess xylene and dodecane. The washing process did not involve stirring because the prepared beads were swollen due to the inclusion of porogenic solvents in the reaction mixture. Stirring pulverized the newly formed polymer beads. After the final wash, the beads were again filtered using a Buchner funnel, and put in a 60°C oven to dry.

Characterization

Diameter Ratio and Swell Time

The beads were characterized by finding the diameter ratio and swell time in toluene. The diameter ratio was found by measuring the diameter of the beads as they swelled in toluene at various time intervals, then dividing by the original diameter of the unswollen bead. The diameter was recorded to +/- 0.025 mm. The swell time was defined as the time necessary for the bead to swell to equilibrium. The size of the measured beads were as close to 0.500mm as possible.

Scanning Electron Microscopy

Micrographs were taken of both the surface and cross-sections of the beads. For cross-sectioning, the beads were first embedded in epoxy using the Polybed 812 embedding kit purchased from Polysciences, Inc. This was accomplished by first placing approximately 6 beads into a BEEM capsule (Polysciences) then filling it completely with epoxy mixture. The filled capsule was then placed in a 60°C oven for 2 days or until the epoxy mixture had completely hardened. The capsule was removed, leaving the beads embedded in a “bullet” of hardened epoxy. A BEEM capsule is a polyethylene capsule with a pointed end. The sample is placed in the bottom of the BEEM capsule then filled with epoxy. The sample is, therefore, embedded in the pointed end of the BEEM capsule where the

minimal amount of epoxy is located. In our case, the bead samples were less dense than the embedding epoxy causing the beads to float to the top of the BEEM capsule. The hardened epoxy had to be trimmed away from around the bead using a sharp razor blade. The trimmed bullet was then sliced to obtain the cross-sections of the beads using a Reichart Ultracut E Ultramicrotome with glass knives (LKB Glass).

Slices of the beads were placed on microscope slides to be used later for further characterization using light microscopy. The bullet, now sliced to expose the cross-section of the bead, was coated with a 200 angstrom layer of gold-palladium using a Hummer V Sputter Coater. The SEM micrographs were taken using an AMR 1000. The beads were prepared for surface micrographs by directly coating the surface of the beads with gold-palladium. All scanning electron microscopy was performed by Nancy Cherim, UNH Instrumentation Center.

Amination of Modified Poly(vinylbenzyl chloride) Beads

Reagents

Purified diethanolamine was obtained from Fisher Scientific, Fair Lawn, NJ. 1,4 Dioxane(99%) was purchased from Aldrich Chemical Co., Inc., Milwaukee, WI. Sodium hydroxide, hydrochloric acid, sodium acetate, sodium chloride and ammonium chloride were also purchased from Aldrich. All water

used was doubly deionized, then distilled with a Corning Megapure distillation apparatus.

Procedure

The beads were derivatized according to the procedure established previously by Ken Hassen.⁵³ A sample of beads was allowed to swell in 1,4-dioxane for approximately one hour. The 1,4 dioxane was removed and replaced with enough diethanolamine to completely cover the bead sample. The beads were then soaked in the diethanolamine for at least 48 hours, with occasional agitation, to allow the amination reaction to proceed to completion. The diethanolamine was removed, and the beads were washed first with water, then pH 4 acetate buffer, and again with water for 30 minutes each with stirring.

The beads were washed in acid because it was found earlier that beads would swell reproducibly only after the first swelling cycle. We assumed that the beads had to be conditioned in the acid because the microcracks that would possibly cause hysteresis would appear in the first swelling cycle.

Characterization

CHN analysis

CHN analysis were performed on samples placed in a 60°C oven overnight to insure dryness. All CHN analyses were performed by Nancy Cherim, UNH

Instrumentation Center, on a Perkin Elmer Series II, model 2400, CHNS/O Analyzer.

Diameter ratio and swell time

The diameter ratio and swell time were determined as described before, in pH 4 acetate buffer (IS=0.1M) and pH 10 ammonia buffer (IS=0.1M). The diameter ratio was found by measuring the diameter of the beads as they swelled in the acid at various time intervals, then dividing by the original diameter of the unswollen bead. Because some of the beads floated, it was often necessary to remove them from the acid solution and place them on a microscope slide for measuring. The diameters were recorded to +/- 0.025mm.

Penetration Modulus

Procedure

The penetration modulus was found for beads aminated with diethylamine⁵⁴ through stress/strain curves that were obtained in cooperation with Todd Gross, University of New Hampshire Department of Mechanical Engineering. A bead from each formulation whose diameter was measured and recorded was allowed to swell in pH 4 acetate buffer (IS = 0.1) for a period of 7 days.

The stress/strain data were collected using a Servohydraulic Instron equipped with a 500g load cell at 5% capacity, so that full scale equalled 25g. A schematic diagram of the Instron can be seen in Figure 3-5. The data resulted from measuring the force exerted by a fully swollen bead as it was being pressed, incrementally, by a stainless steel rod. A drilled out screw was connected to the load cell to serve as a solvent well for the bead. The bead was held in place by a dimple drilled into the bottom of the solvent well. The procedure for a run was as follows: A swollen bead was placed into the dimple of the solvent well. A slight force was then placed on the bead by bringing the stainless steel rod into contact with the bead. The solvent well was filled with buffer to insure that the bead was fully swollen. After approximately 30 seconds, the y-displacement of the stainless steel rod was begun, and the force data collected. The vertical displacement totalled 250 μ m, at a scan rate of 1 μ m/sec. The displacement was then reversed and the force measured as the stainless steel rod “released” the bead to test for hysteresis.

Mercury Porosimetry

The process of mercury porosimetry involves, first, the evacuation of all gas from the volume containing the sample. Mercury is then transferred into the sample container while under vacuum. Pressure is applied to force the mercury

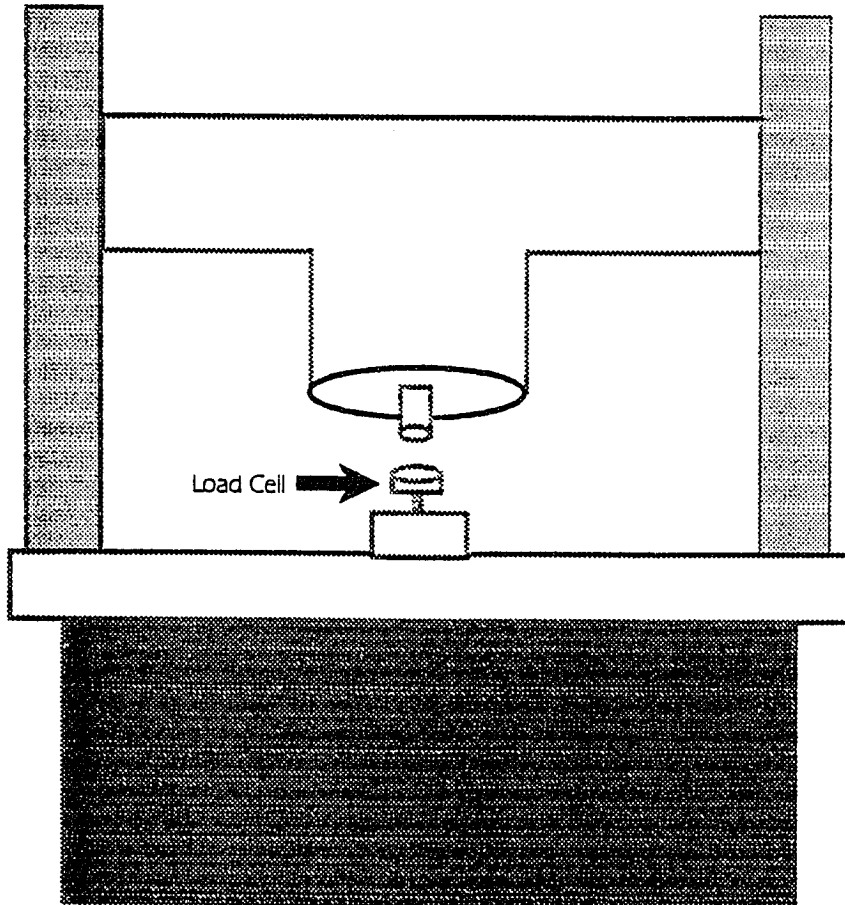


Figure 3-5 Schematic of the Servohydraulic Instron used to find the penetration modulus of the beads.

into the interparticle voids and intraparticle pores. The applied pressure increases as the pore size decreases. That is, at low pressures, intrusion occurs in the large interparticle voids; at higher pressures the mercury penetrates into the pores within the particles. Both the applied pressure and the intruded volume are monitored, as well as the extruded volume as the pressure is later decreased. The mercury porosimetry data is then plotted as the log differential intrusion vs. diameter, giving the pore size distribution of the sample, or the cumulative pore volume vs. diameter which shows the relative volume of different sized pores.

Approximately 1.5 - 2.0 grams of each bead sample were dried at 56 °C in a pistol drier for 24 hrs prior to the measurement. The mercury porosimetry data were collected using a Micromeritics Autopore II 9220. The Micromeritics Autopore II 9220 measure pore volumes and sizes, as well as densities, from 0.5 to 60,000 psi. The mercury was intruded in steps from subambient to 60,000 psi pressure. All mercury porosimetry work was performed by Richard Parmely, Juniata College, Huntingdon, PA.

CHAPTER IV

MORPHOLOGY

SEM MICROGRAPHS/MERCURY POROSIMETRY

Understanding the morphology of the polymer matrix is important in understanding what takes place during the polymerization process. The addition of the elastomeric additive and the porogenic solvents to the monomer mixture leads to a more complex polymerization process. SEM micrographs of the surface and cross-sections of the beads give a picture of the morphology of the modified polymer matrix. Using this information along with the pore distribution data obtained through mercury porosimetry, it was possible to construct a model of the processes involved in the polymerization.

Kraton G1652 was incorporated into the polystyrene matrix to serve as an impact modifier, a material that improves the polymer's resistance to stress. Kraton G1652 is a styrene-ethylene/butylene-styrene triblock polymer produced by Shell, Inc., and is commonly blended into polymers in the melt stage. The Kraton G1652 was added to the reaction mixture so that the polymerization of the poly(vinylbenzyl chloride) would take place in the presence of the elastomer.

Sardelis and coworkers⁵⁵ found that polymerizing polystyrene in the presence of block, graded block, or randomized copolymers of butadiene-styrene led to new polymer morphologies similar to toughened polystyrene, resulting from polymer-polymer interactions and a phase separation. The mechanical properties of the polystyrene were improved, but, still did not match the mechanical properties of conventional toughened polystyrene.

We believe that a similar process is occurring in our Kraton G1652 modified polymer. The monomer mixture consists of four main components: the monomer, vinylbenzyl chloride; the crosslinker, divinylbenzene; the porogenic solvents, dodecane and xylene; and Kraton G1652. The dodecane which is a non-solvating porogen, is not compatible with the forming polymer. Eventually, during polymerization, the dodecane and the forming polymer will separate into two distinct phases, introducing small regions of dodecane within the poly(vinylbenzyl chloride) matrix.

The Kraton G1652 consists of both an aliphatic and aromatic region and acts as a surfactant between the dodecane and the forming polymer saturated with monomer. During polymerization, the Kraton G1652 will concentrate at the interface so that the aliphatic block is in the dodecane phase and the aromatic blocks are in the polymer phase. Removal of the dodecane will result in pores that are lined with Kraton G1652.

Xylene will partition into both the aliphatic and aromatic region, that is, the region consisting of dodecane and the forming polymer, leaving the polymer phase microporous, and contributing to larger pores in the dodecane phase. both regions upon removal of the porogenic solvents.

The morphology of the beads was first studied by SEM microscopy. Cross-sections and surface shots of the beads were taken in an effort to discover the resulting morphology of the polymer matrix. Mercury porosimetry was also used to determine the pore size distribution of the beads.

The porosimetry data for beads of 0% Kraton G1652, 12% divinylbenzene, 33% dodecane and 40% total diluent are shown in Figure 4-1. These beads have a fairly narrow pore size distribution that is centered around 8 μ m. The pore size distribution for beads similar in composition, but with 6% divinylbenzene and 60% total diluent are presented in Figure 4-2. The pore size distribution of these beads centers mainly around two pore diameters, 9.5 and 3 μ m. The difference in pore sizes between the two bead samples is probably due to the effect of increasing the divinylbenzene which causes the phase separation to occur earlier in the polymerization process. The phase separation occurs because the aliphatic solvent is insoluble in the polymer. If the polymer is more highly crosslinked, the aliphatic solvent should be less soluble. The total pore area for the beads with 12% divinylbenzene and 40% total diluent is 0.133m²/g with a total percent porosity of 22.51%. The beads with 6% divinylbenzene and 60% total diluent

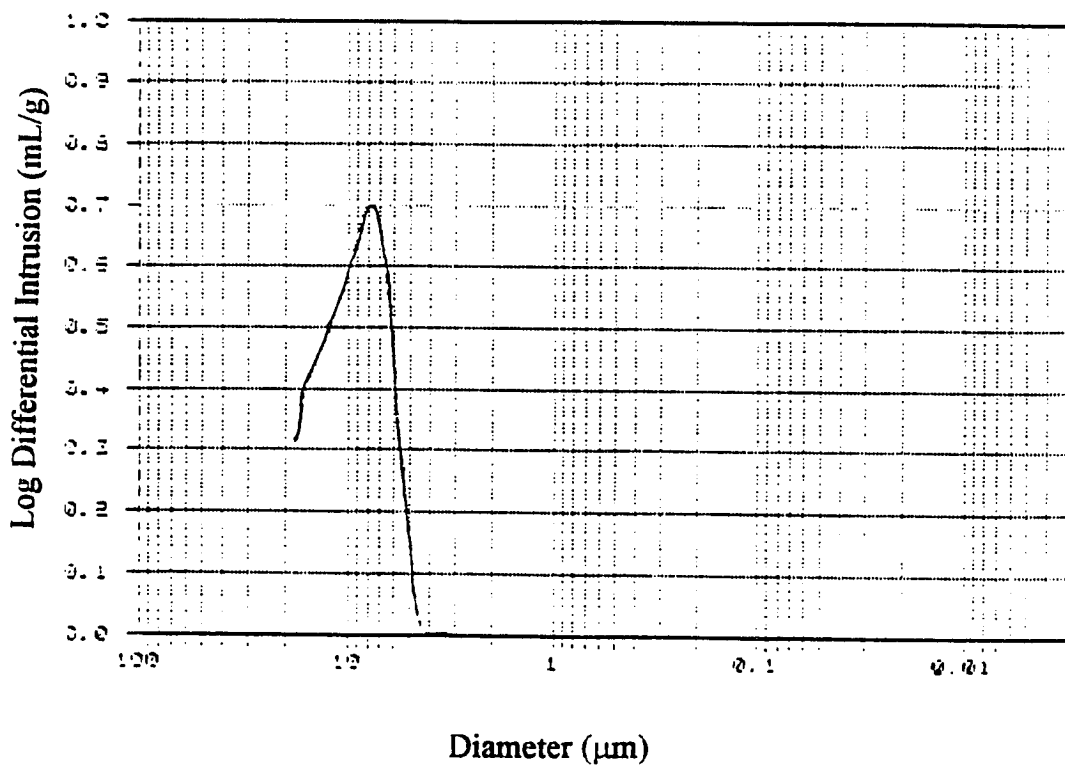


Figure 4-1 The pore size distribution of beads whose formulation is 0% Kraton G1652, 12% divinylbenzene, 33% dodecane and 40% total diluent.

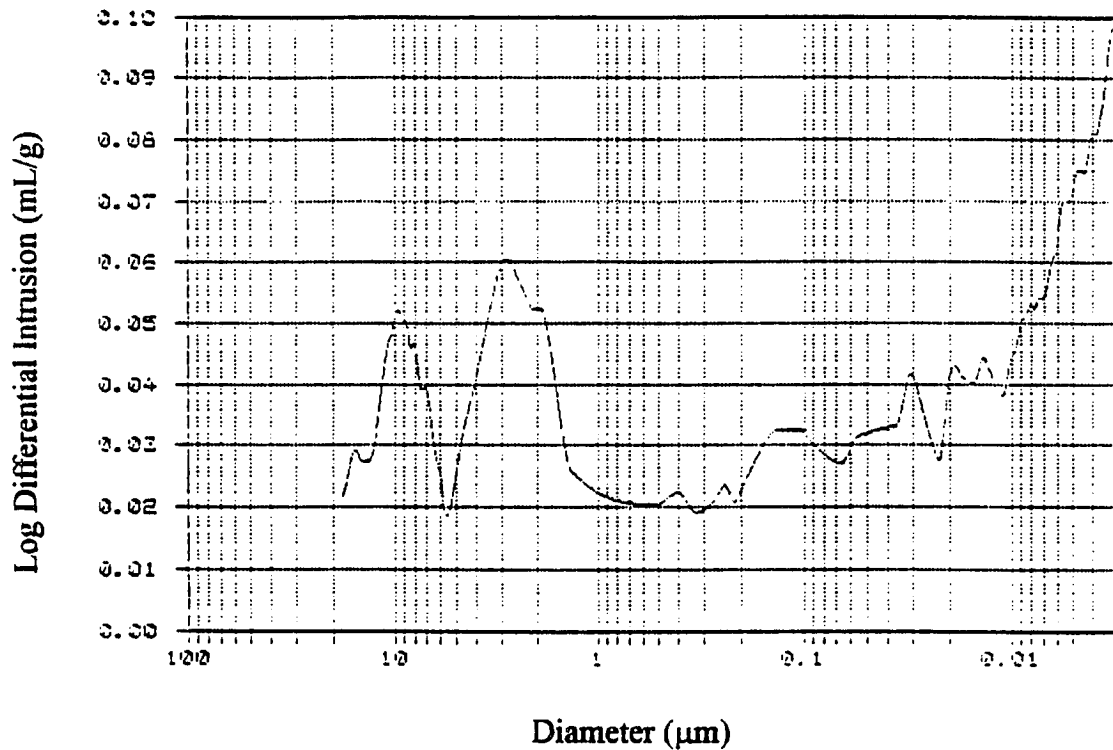


Figure 4-2 The pores size distribution for beads whose formulation is 0% Kraton G1652, 6% divinylbenzene, 33% dodecane and 60% total diluent.

have a total pore area of $36.0 \text{ m}^2/\text{g}$ with the total percent porosity of 15.6 %, indicating that there must be many smaller pores smaller than $0.01 \text{ }\mu\text{m}$.

Figure 4-3 shows the scanning electron micrograph of the cross-section of a bead whose formulation consists of 2% Kraton G1652, 12% divinylbenzene, 33% dodecane and 40% total diluent. The polymer matrix looks like a continuous phase with pores dispersed throughout the matrix.

The pore size distribution of beads with the same formulation is shown in Figure 4-4. The distribution ranges approximately from $0.15 \text{ }\mu\text{m}$ to 3 nm , with a significant pore distribution centered around $2.2 \text{ }\mu\text{m}$. The median pore diameter is 4.7 nm , suggesting that the highest pore density centers in the low pore size range. The relative volume of mercury in the different sized pores is shown in Figure 4-5, where Cumulative Volume is plotted vs. Diameter. The volume of mercury increases at approximately $2 \text{ }\mu\text{m}$, then continues to increase as the pore diameter decreases, supporting the assumption that the highest pore density centers on the low pore size range. The total pore area for the beads is $39.4 \text{ m}^2/\text{g}$ and the total percent porosity is 10.4 %, indicating that there must be many pores whose diameter is less than $0.01 \text{ }\mu\text{m}$. The difference in the porosity between the beads that have no Kraton G1652 and the beads that have 2% Kraton G1652 is significant. The beads that have no Kraton G1652 appear to have fewer smaller pores with their distributions centering around the relatively larger pore size ranges. In contrast, the beads that contain 2% Kraton G1652 have a significant

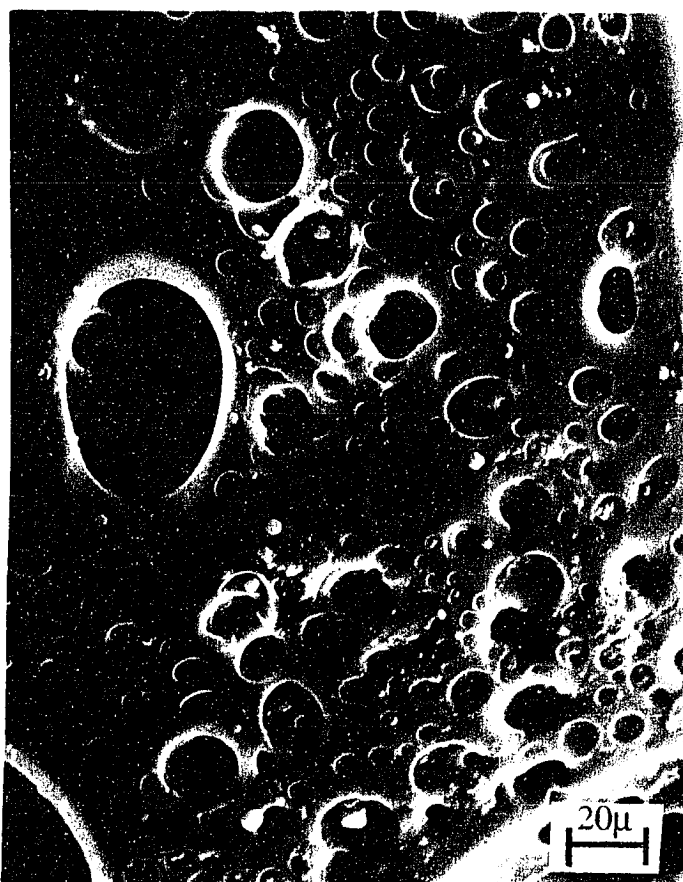


Figure 4-3 Scanning the electron micrograph of the cross-section of a bead whose formulation consists of 2% Kraton G1652, 12% divinylbenzene, 33% dodecane and 40% total diluent.

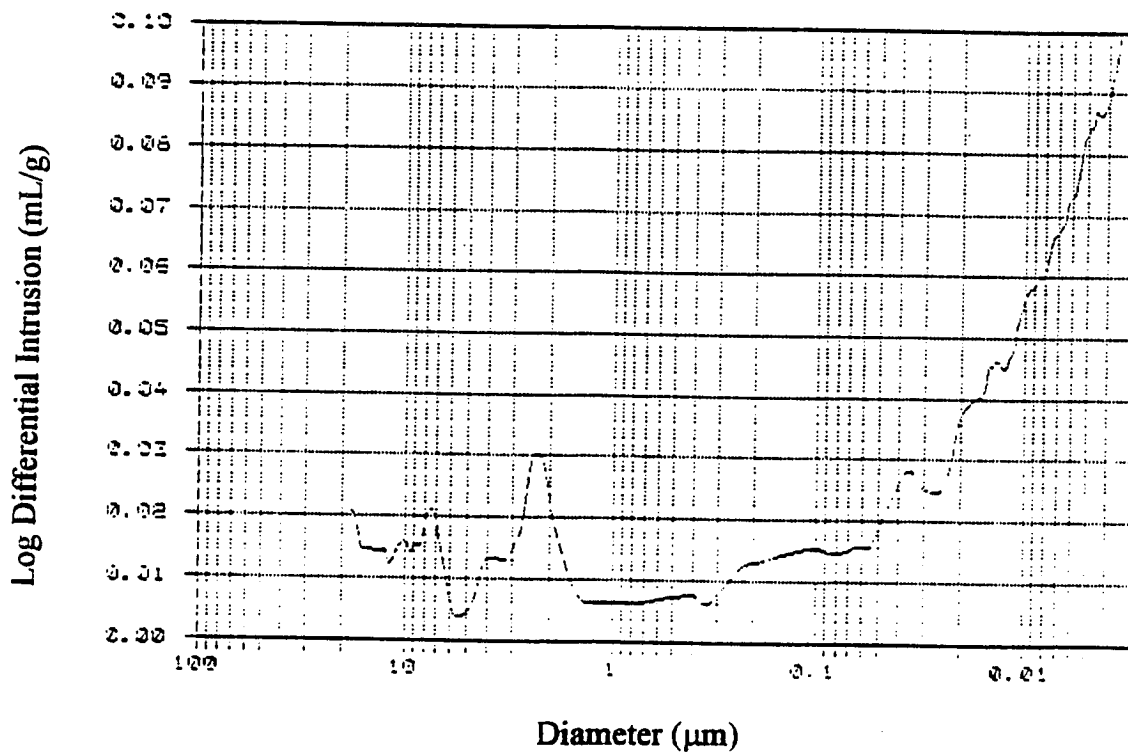


Figure 4-4 Pore size distributions of beads whose formulation consists of 2% Kraton G1652, 12% divinylbenzene, 33% dodecane and 40% total diluent.

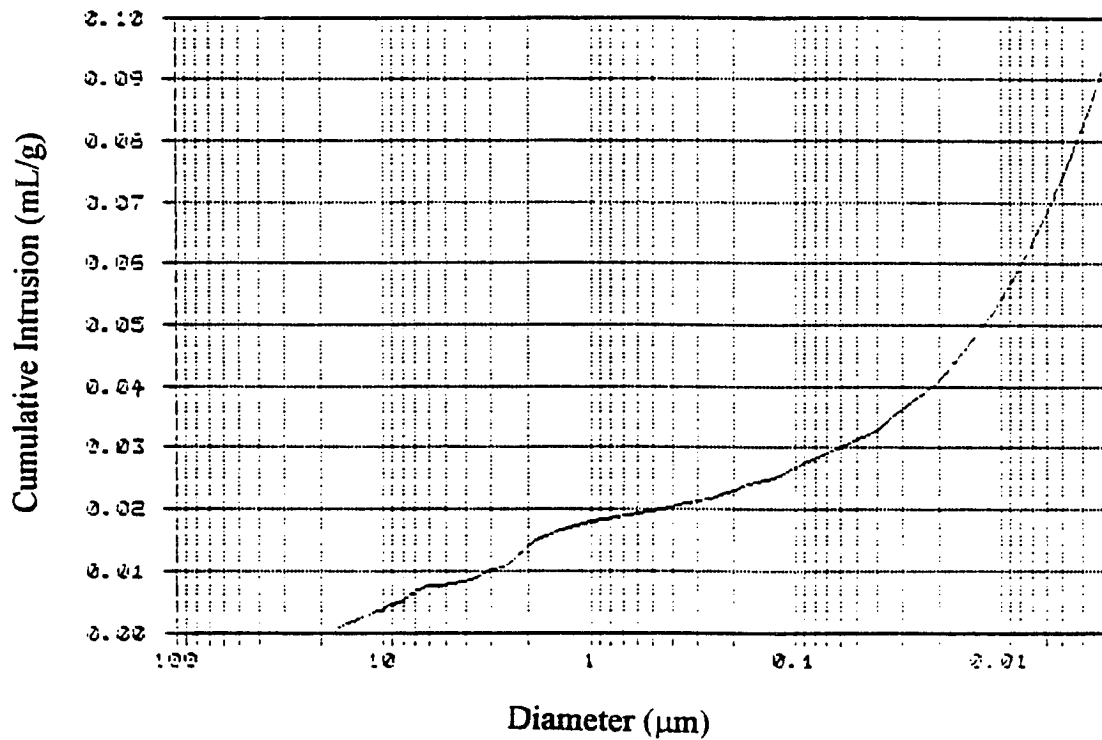


Figure 4-5 Cumulative volume of mercury vs. diameter for beads whose formulation consists of 2% Kraton G1652, 12% divinylbenzene, 33% dodecane and 40% total diluent.

number of pores located in the nanometer range. This suggests that Kraton G1652 is directly involved in stabilizing the interface between the dodecane and the forming polymer, resulting in an increased density of smaller pores.

Graphs of the pore size distribution for beads whose formulations are 2% Kraton, 12% divinylbenzene, 40% total diluent and 0%, or 66% dodecane are shown in Figures 4-6, and 4-7, respectively. The pore size distribution of beads with 0% dodecane is broad with pores ranging from 0.15 μm to approximately 3 nm. However, the median pore diameter was 4.8 nm, suggesting that the highest pore density centers in the low pore size range.

This is further illustrated in the plot of Cumulative Intrusion vs. Diameter listed in Figure 4-8. The volume of mercury present in the pores begins to increase at approximately 0.02 μm , and continues to increase as the pore diameter decreases, indicating that there are a larger number of smaller pores in the matrix. Because the only pore-forming solvent used in this case was xylene, a microporous porogen, the pore size distribution is consistent with the monomer mixture composition, i.e., only smaller pores are expected.

The distribution of beads with 33% dodecane shows there are both larger (~2nm) and smaller (~4.7 μm) pores in the matrix. The pore size distribution corresponds to the monomer mixture which contains a mixture of both xylene and dodecane.

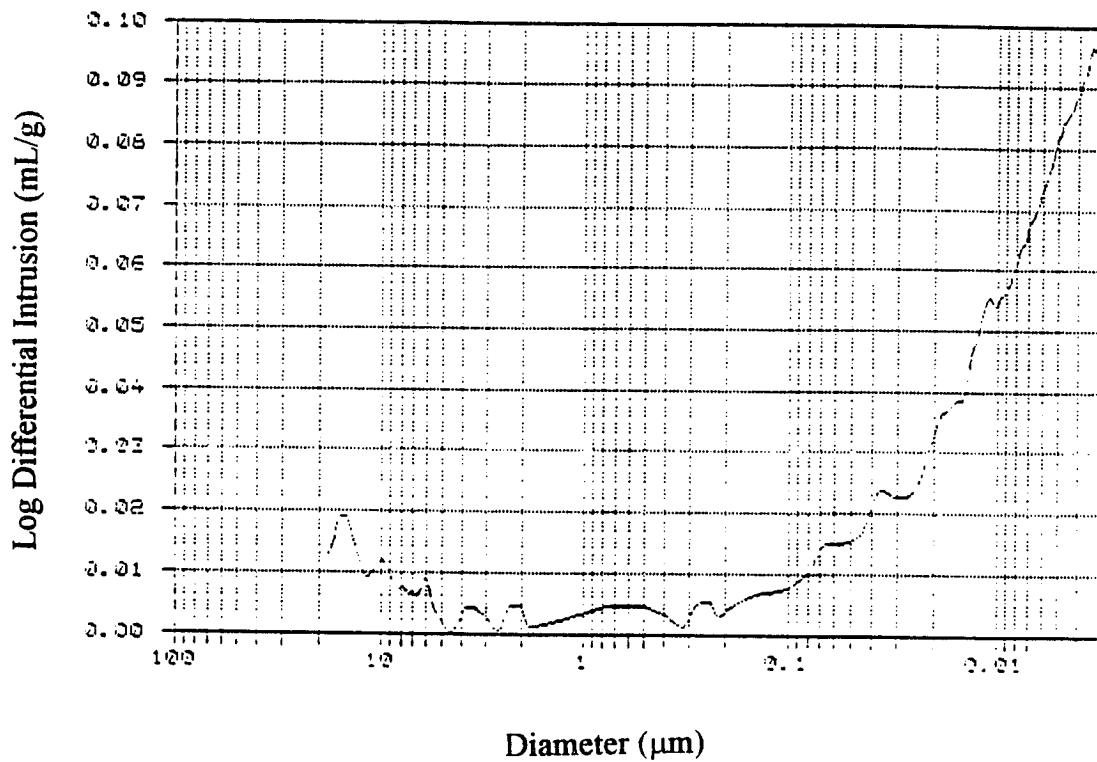


Figure 4-6 Pore size distribution for beads whose formulations are 2% Kraton, 12% divinylbenzene, 40% total diluent and 0% dodecane.

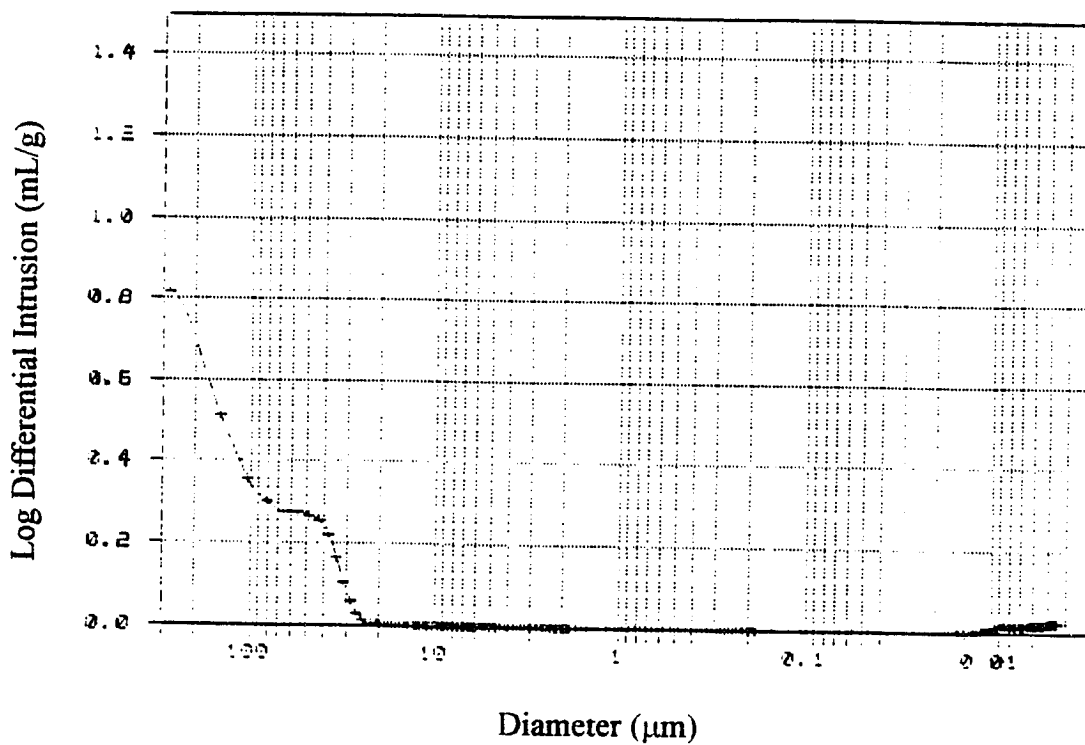


Figure 4-7 Pore size distribution for beads whose formulations are 2% Kraton, 12% divinylbenzene, 40% total diluent and 66% dodecane.

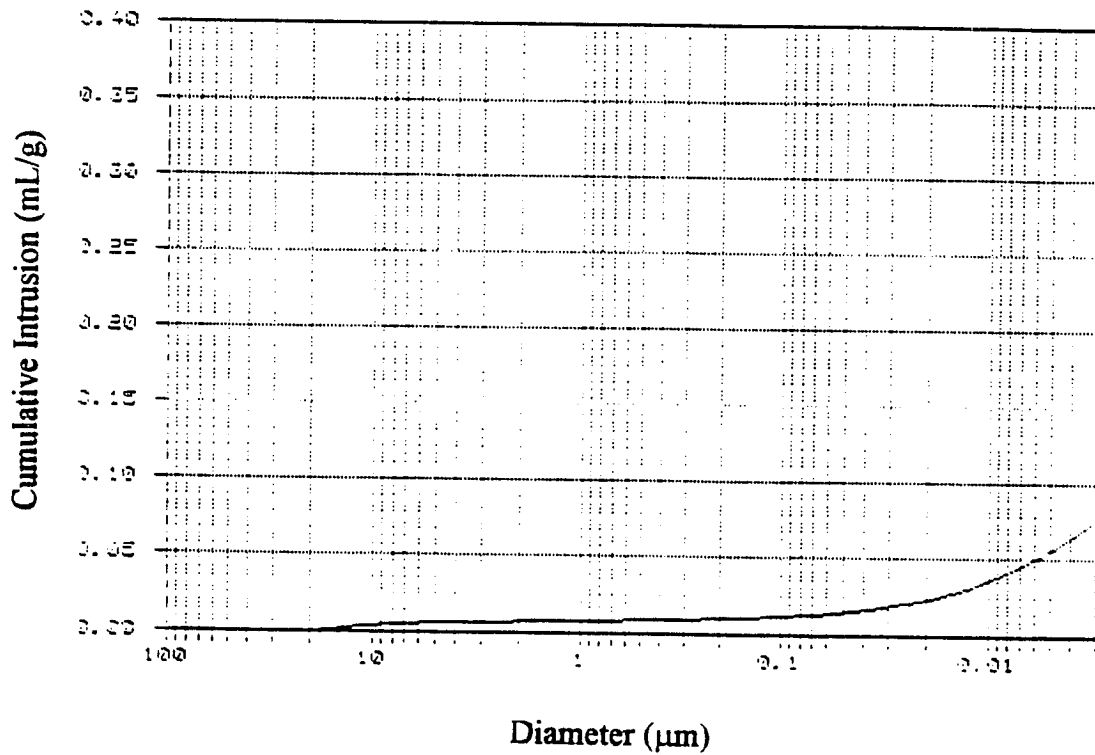


Figure 4-8 Cumulative volume of mercury vs. diameter for beads whose formulation is 2% Kraton, 12% divinylbenzene, 40% total diluent and 0% dodecane.

The pore size distribution of the beads with 66% dodecane in the monomer mixture is markedly different than the distributions found with 0 and 33% dodecane. The bead's distribution basically centers around two pore size ranges, one centered at 9nm and another from approximately 40 to 250 μm . The pore size centered around 9nm is probably due to the presence of xylene in the reaction mixture, similar to the 0 and 33% dodecane mixtures. The larger pore size is probably due to the presence of a higher percentage of dodecane in the mixture.

The volume of mercury intruded into the pores increases drastically at the larger pore diameter range shown in Figure 4-9. Although it is not possible to see whether or not the cumulative volume increases at the smaller pore sizes, the median pore size is approximately 6nm, suggesting that the majority of the pores are actually located in the smaller pore size range. It is interesting to note that the total % porosity increases from 8.64 to 10.35 to 30.4%, as you increase the percentage of dodecane from 0 to 33 to 66%, whereas the total pore area changes from 37.9 to 39.4 to 3.8 m^2/g , respectively. This indicates that with 0 and 33% dodecane, there are a larger number of pores with diameters less than 0.01 μm . Beads with 66% dodecane have less smaller pores and are predominantly macroporous.

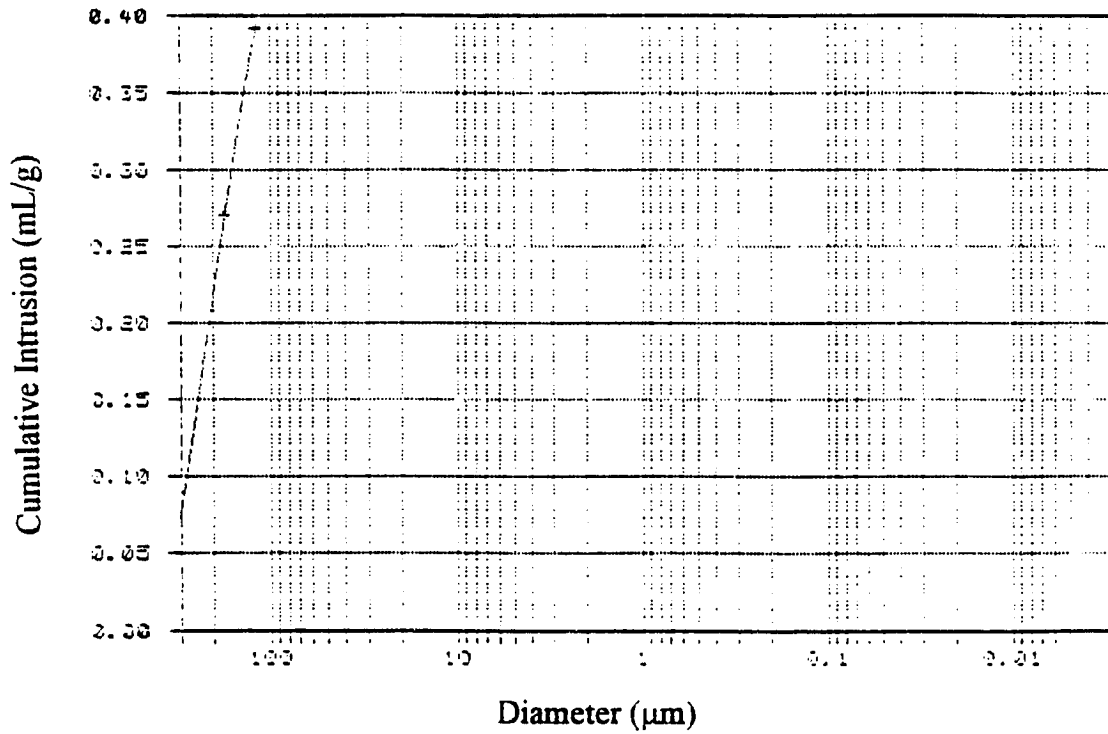


Figure 4-9 Cumulative volume vs. diameter of beads whose formulation is 2% Kraton G1652, 12% divinylbenzene, 66% dodecane, and 40% total diluent.

The addition of dodecane into the monomer mixture results in a polymer matrix with larger pores, as well as the smaller pores formed by the xylene. Figure 4-10 shows micrographs of beads whose formulations are 2% Kraton G1652, 12% divinylbenzene, 40% total diluent and 0%, 33%, and 66% dodecane. As the percentage of dodecane increases, the number and size distribution of the pores in the polymer matrix also increases. This effect also does not seem to depend on the amount of Kraton G1652 present. Figure 4-11 shows the same result with beads that are 8% Kraton G1652.

As the percentage of Kraton G1652 is increased, a different type of separation occurs. In this case, the Kraton G1652 is at a concentration high enough so that the aliphatic phase becomes the continuous phase. Increasing the Kraton G1652 to 8% and eventually to 14% essentially increases the surfactant content of the monomer mixture which, in turn, decreases the surface tension between the forming polymer and the dodecane during polymerization. The subsequent increase in the amount of dodecane at each Kraton G1652 level will increase the volume of the aliphatic phase (dodecane) surrounding the poly(vinylbenzyl chloride) regions. The poly(vinylbenzyl chloride) polymerizes in small inclusions throughout the aliphatic matrix. Therefore, formulations with a larger volume of Kraton G1652 adopts a morphology with a large surface area, leading to the formation of small poly(vinylbenzyl chloride spheres) throughout

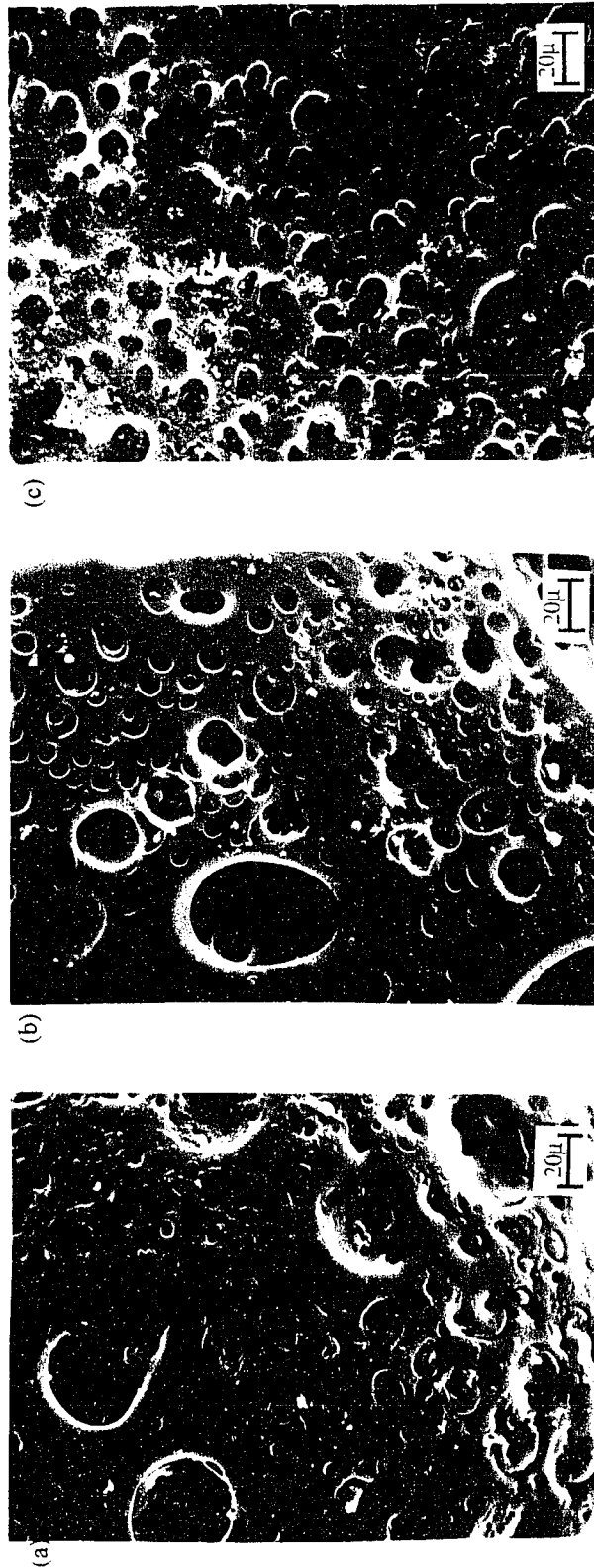


Figure 4-10 SEM micrographs of the surface of beads whose formulations are 2% Kraton G1652, 12% divinylbenzene, 40% total diluent and (a) 0%, (b) 33%, and (c) 66% dodecane.

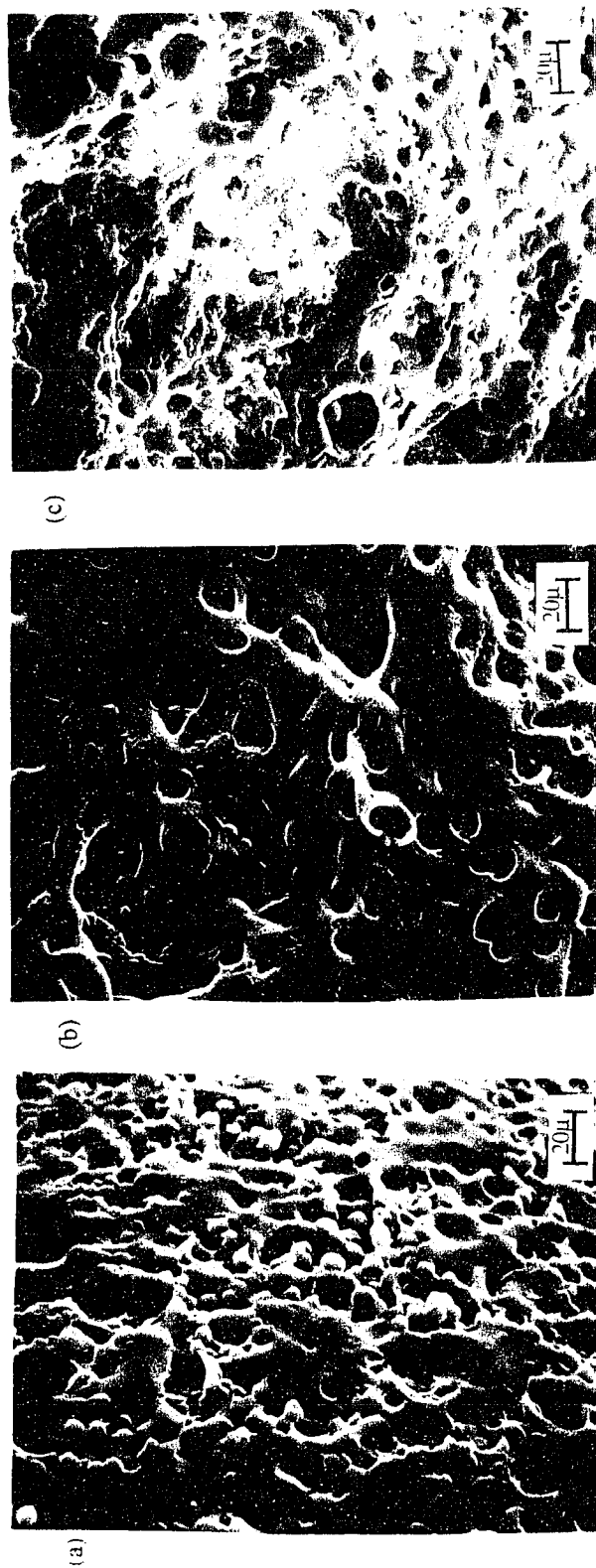


Figure 4-11 SEM micrographs of the surface of beads whose formulations are 8% Kraton G1652, 12% divinylbenzene, 40% total diluent and (a) 0%, (b) 33%, and (c) 66% dodecane.

the aliphatic matrix. This corresponds to a larger surface area than what is seen with 2% Kraton G1652 which results in a continuous porous matrix. Removal of the porogens results in a matrix of small polymer spheres situated throughout a porous “sea” of Kraton G1652.

This effect is illustrated in Figure 4-12, which shows cross-sections of beads whose formulations are 12% divinylbenzene, 33% dodecane, 40% total diluent and (a) 2%, (b) 8%, and (c) 14% Kraton G1652 poly(vinylbenzyl chloride). The bead with 2% Kraton G1652 appears as a porous continuous matrix. In contrast, the beads with 14% Kraton G1652, Figure 4-12 (c), clearly display that the poly(vinylbenzyl chloride) has polymerized in tiny spheres surrounded by Kraton G1652. In this case, the poly(vinylbenzyl chloride) and the dodecane phase separated leaving small spheres of polymer surrounded by the dodecane with Kraton G1652 present at the interfaces. When the dodecane is removed, the resulting morphology occurs. It is interesting to note that there are still a few pores scattered throughout the membrane. Figure 4-12 (b) shows a bead with 8% Kraton G1652. Although a phase separation of the poly(vinylbenzyl chloride) into small spheres can be seen, the morphology of the 8% Kraton G1652 seems to be at a point intermediate between the 2% and 14% Kraton G1652 beads.

The morphology of beads consisting of 14% Kraton G1652, 12% divinylbenzene, 33% dodecane and 40% total diluent is further illustrated in

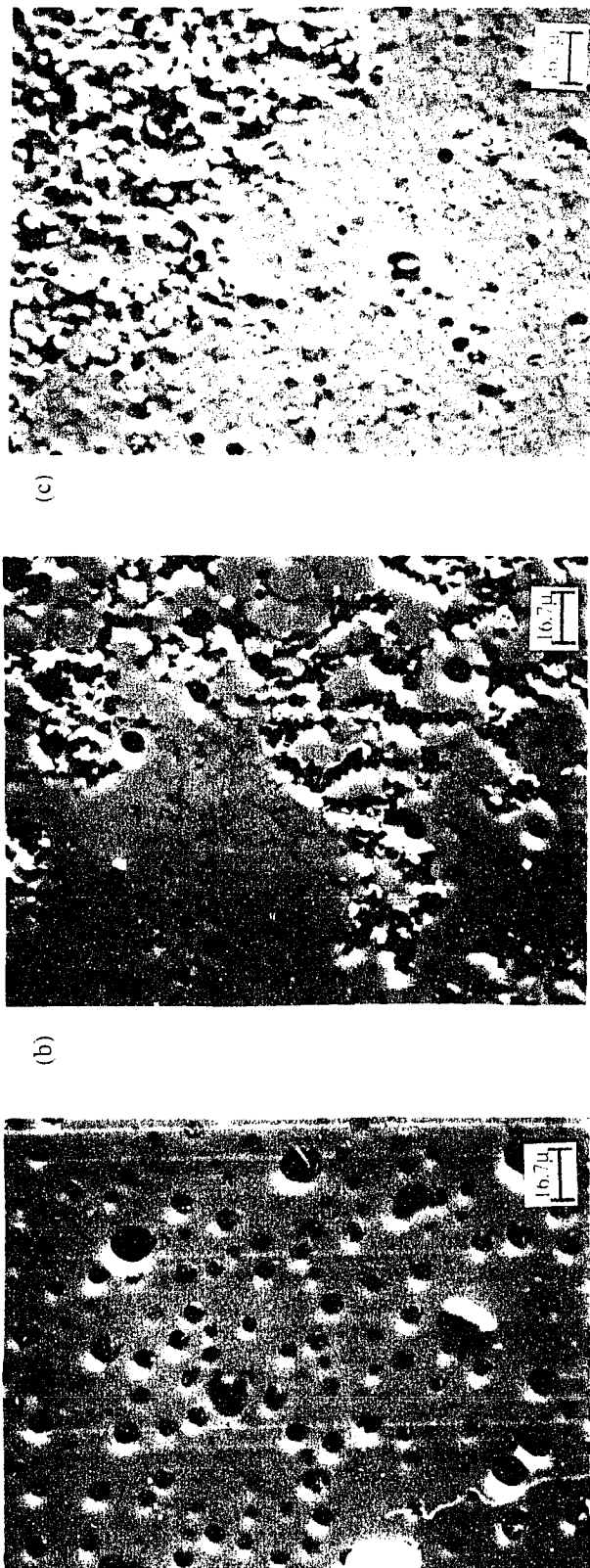


Figure 4-12 Cross-sections of beads whose formulations are 1.2% divinylbenzene, 3.3% dodecane, 40% total diluent and (a) 2%_w, (b) 8%_w, and (c) 14% Kraton G1652 poly(vinylbenzyl chloride).

Figure 4-13. Scanning electron micrographs taken of the surface of these beads show essentially the same morphology characteristics are present on the surface as is found in the cross-section. At low magnification, Figure (a), the phase separation that occurs within the bead is not readily apparent. However, as the magnification is increased, the small poly(vinylbenzyl chloride) spheres within the matrix are easily seen.

The pore distributions of beads with 8% and 14% Kraton G1652 are shown in Figures 4-14 and 4-15 respectively. The beads' formulations also include 12% divinylbenzene, 33% dodecane and 40% total diluent. Both graphs show narrow pore distributions centered around $2\mu\text{m}$ (8% Kraton G1652) and $1.5\mu\text{m}$ (14% Kraton G1652). The fact that the beads with 14% Kraton G1652 yield beads with smaller pore sizes is further evidence that the Kraton G1652 stabilizes the interface between the aliphatic and aromatic phases. We believe that the narrow pore distributions correspond to the space between the the closely and uniformly packed poly(vinylbenzyl chloride) spheres, which result from the phase inversion.

It is evident from both pore distributions that smaller pores do exist. The cumulative volume of intruded mercury vs. pore diameter for beads with 8% and 14% Kraton G1652 are shown in Figures 4-16 and 4-17. Both graphs show a sharp increase in the volume of mercury intruded at the larger diameter shown in Figures 4-14 and 4-15. However, the volume of intruded mercury continues

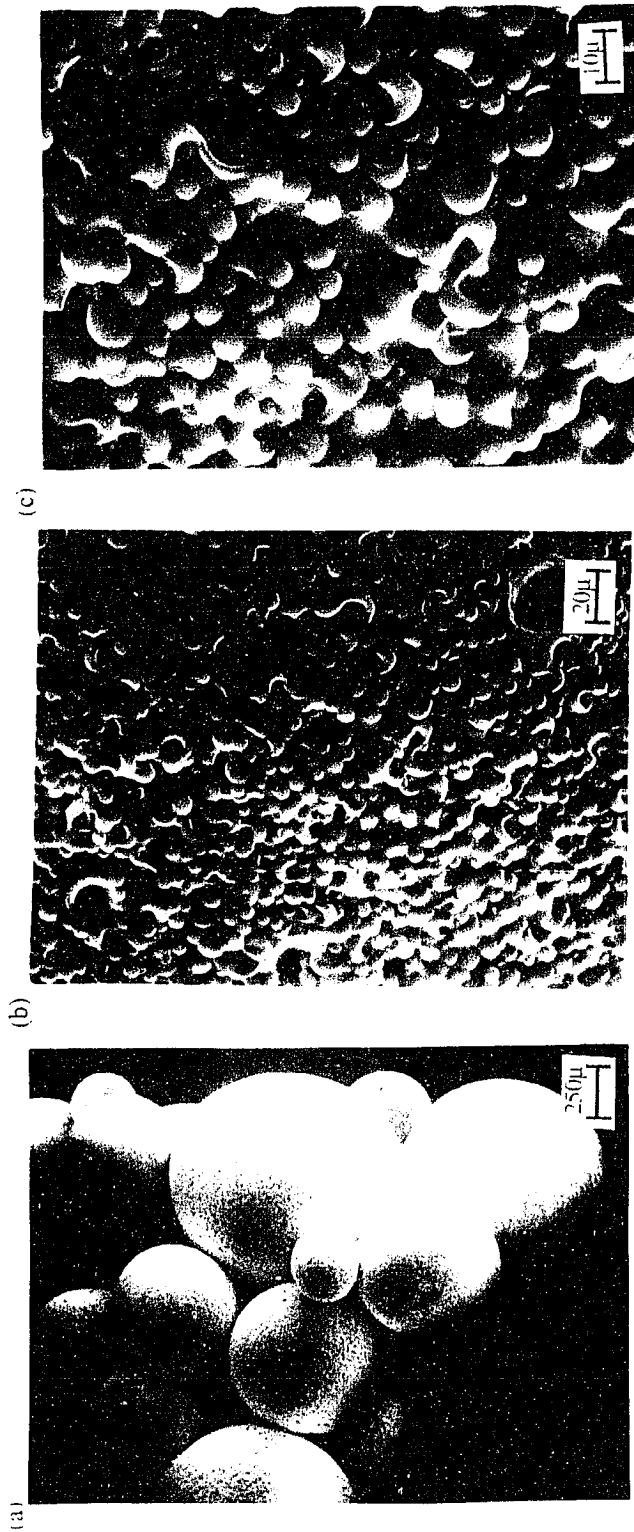


Figure 4-13 SEM micrographs of beads whose formulation 1.4% Kraton G1652, 1.2% divinylbenzene, 3.3% dodecane and 40% total diluent.

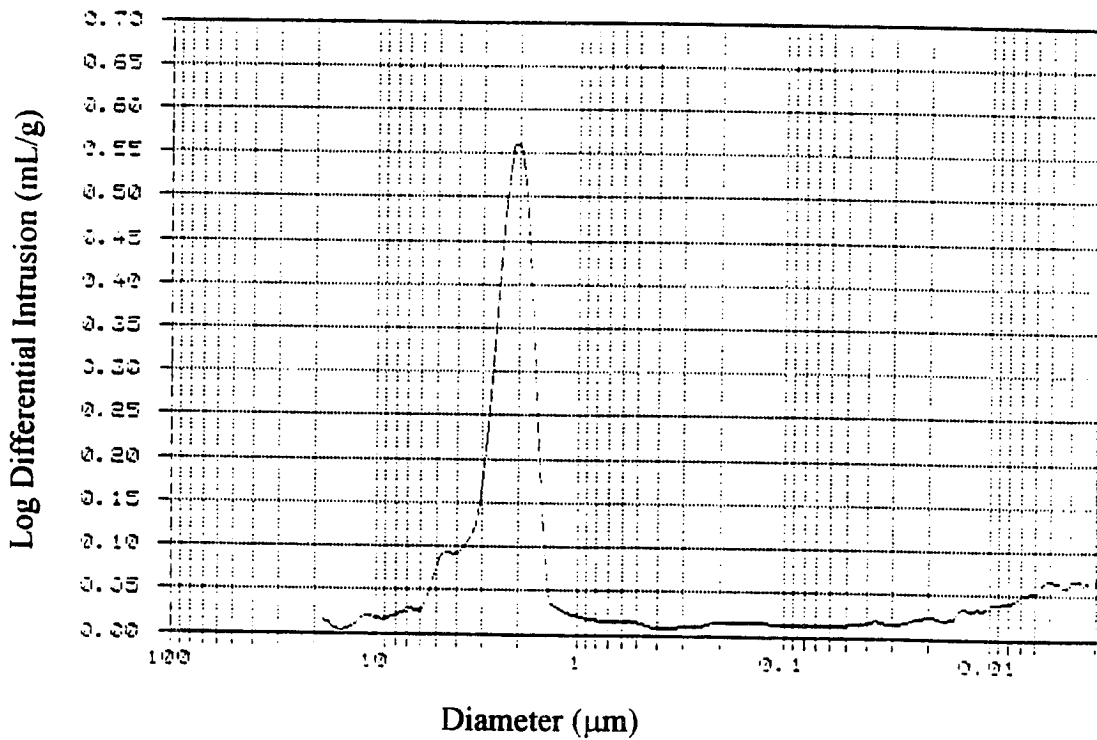


Figure 4-14 The pore size distribution of beads whose formulation consists of 8% Kraton G1652 , 12% divinylbenzene, 33% dodecane and 40% total diluent.

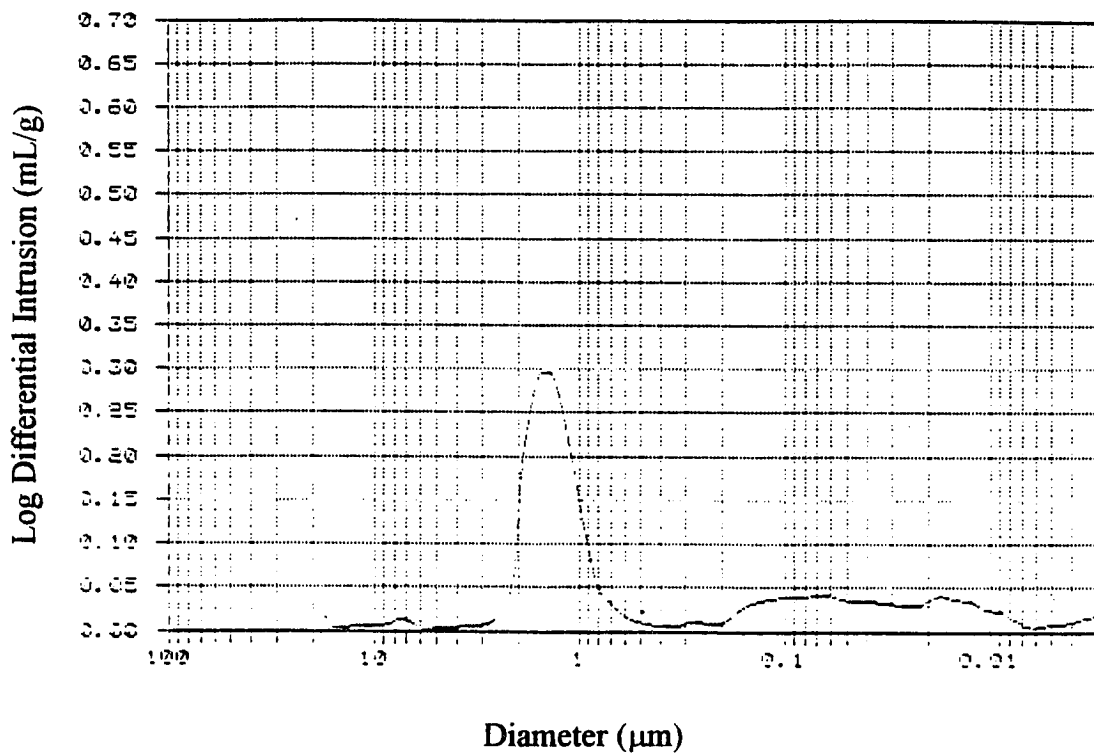


Figure 4-15 The pore size distribution of beads whose formulation consists of 14% Kraton G1652, 12% divinylbenzene, 33% dodecane and 40% total diluent.

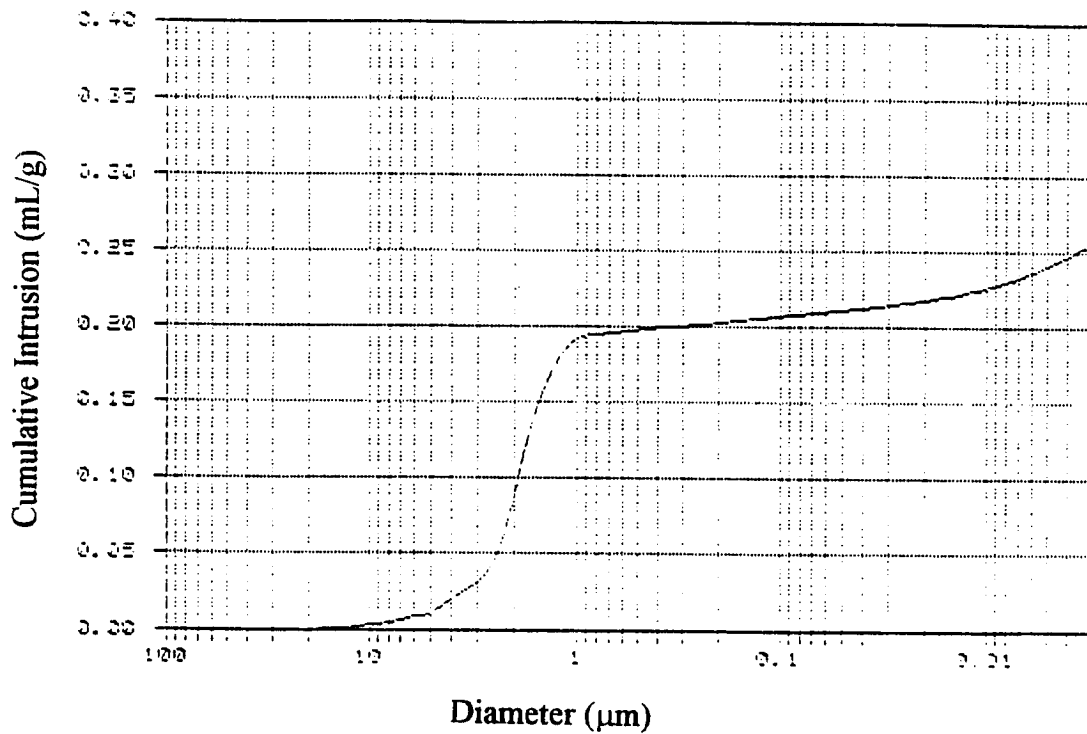


Figure 4-16 Cumulative volume of mercury vs. diameter of beads whose formulation consists of 8% Kraton G1652, 12% divinylbenzene, 33% dodecane and 40% total diluent.

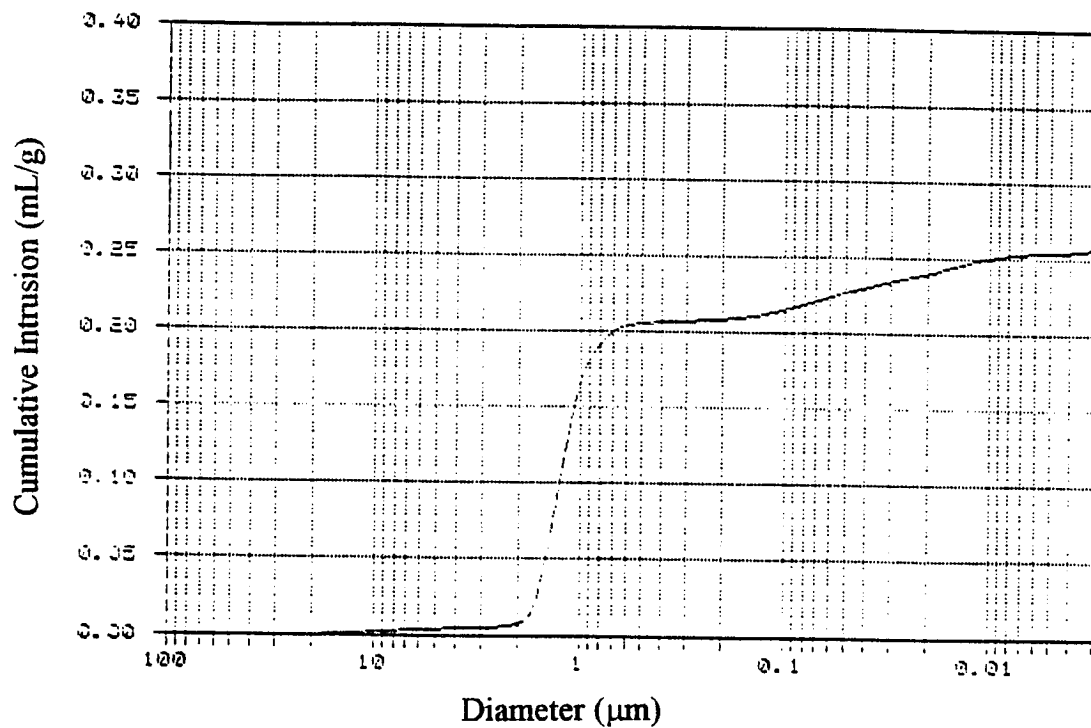


Figure 4-17 Cumulative volume of mercury vs. diameter of beads whose formulation consists of 14% Kraton G1652, 12% divinylbenzene, 33% dodecane and 40% total diluent.

increasing as the pore diameter decreases, suggesting that there are a large number of micropores throughout the matrix. The smaller pores may be due to the presence of xylene dissolved in the polymeric phase after polymerization is completed.

The morphology of the poly(vinylbenzyl chloride) matrix is directly affected by the addition of the porogenic solvents and the addition of Kraton G1652. Adding porogenic solvents to the monomer mixture (both macroporous and microporous) results in a porous polymer matrix. The addition of dodecane also caused a phase separation of the porogen and the forming polymer. At high levels, the Kraton G1652 sufficiently stabilized the interfacial surfaces so that the phase separation that occurred had a high surface area. The process of the polymerization of Kraton G1652 modified poly(vinylbenzyl chloride) with the addition of the porogenic solvents is complex, depending on the varying percentages of all components of the monomer mixture. The addition of Kraton G1652 into the monomer mixture before polymerization is a new approach to modifying the morphology of styrene-based resins.

CHAPTER V

SWELLING in TOLUENE

DIAMETER RATIOS and SWELL TIMES

The diameter ratios and the swelling times were recorded while exposing the beads to toluene. Toluene is a compatible solvent for all components of the polymer formulation (vinylbenzyl chloride, divinylbenzene and Kraton G1652). This test was performed to get an initial measurement, before amination, of the total swelling diameter and time since the polymer matrix itself was involved in the swelling process. This test also gave us further understanding as to how varying the formulation affected polymer properties.

The diameter ratios and the swelling times of the polymer beads prepared according to the formulation in the factorial design are listed in Table 5-1. There are no beads corresponding to formulations containing 66% dodecane and 40% total diluent. It was not possible to suspension polymerize material in the form of beads with this formulation. The resulting polymer was a flaky substance that crumbled with the application of even a small amount of pressure.

An analysis of variance⁵⁶ was performed on both the diameter ratios and swelling times of the factorial design. However, since one particular formulation was not available, the factorial was unbalanced. It was necessary to break the data

		% Kraton G1652									
		2			8			14			
		0	33	66	v% Dodecane in Diluent			0	33	66	
% Divinylbenzene	6	40	1.28 1.32 (7.10)	1.29 1.27 (7.5)	1.21 1.19 (15.6)	1.13 1.18 (10.4)	1.25 1.19 (10.5)	1.19 1.18 (2.3)	1.24 1.26 (10.20)	1.47 1.35 (3.3)	1.20 1.17 (3.5)
			60	1.45 1.48 (15.15)	1.28 1.12 (3.5)	/	1.38 1.33 (10.15)	1.29 1.18 (3.3)	/	1.41 1.36 (10.20)	1.25 1.17 (3.3)
	12	40	1.25 1.29 (25.20)	1.15 1.13 (10.10)	1.16 1.21 (1.6)	1.21 1.10 (3.3)	1.23 1.20 (5.3)	1.10 1.10 (1.2)	1.13 1.12 (5.10)	1.10 1.09 (2.2)	1.08 1.06 (1.2)
			60	1.30 1.19 (5.20)	1.21 1.11 (2.3)	/	1.20 1.14 (2.3)	1.40 1.26 (2.3)	/	1.25 1.19 (15.8)	1.25 1.05 (1.1)
	18	40	1.23 1.06 (20.15)	1.06 1.13 (3.20)	1.17 1.13 (2.1)	1.16 1.14 (2.2)	1.09 1.05 (1.1)	1.14 1.10 (1.1)	1.08 1.13 (1.10)	1.09 1.05 (1.2)	1.10 1.07 (5.1)
			60	1.30 1.24 (10.20)	1.09 1.04 (1.1)	/	1.24 1.17 (5.2)	1.18 1.04 (1.1)	/	1.12 1.15 (3.3)	1.12 1.09 (2.1)

Table 5-1 The diameter ratios and swelling times of the beads in toluene. Swelling times, in parenthesis, are reported in minutes.

set into two separate, smaller factorials. The first is a 3x2x3x2 design which is comprised of all data points except those whose formulation includes 66% dodecane. The second design excludes the beads whose formulation includes 60% total diluent which results in a 3x3x2 factorial. Performing two separate ANOVA's on the data set enabled us to include all the available data into the statistical analysis.

An analysis of variance is used to compare the means of data from several populations. The F-values, which represent the comparison of the standard deviations between the data for each effect (controlled factor) and the random error of the experiment, are listed in Table 5-2 and 5-3 for the analysis of the diameter ratio in toluene. Significant F-values mean that the variance of the effect (or changed variable) is significantly different than the random error variance.

Diameter Ratios/ Swelling in Toluene

The effect of varying % divinylbenzene, % dodecane, and % total diluent are statistically significant at the 99% confidence level on the diameter ratio of the beads swollen in toluene.

Varying the crosslinking density (divinylbenzene content) significantly affects the total diameter ratio. Typical results are shown in Figure 5-1 for beads whose formulations are 2% Kraton, 33% dodecane, 40% diluent and 6, 12, or 18% divinyl benzene. As the %DVB is increased, the diameter ratios decrease. This is

Variables	F-Value	P
% Kraton	1.46	0.246
% dodecane	14.52 **	0.001
% divinylbenzene	50.49 **	0.000
% total diluent	11.5 **	0.002
Interactions		
%K x %dod	8.13 **	0.001
%K x %dvh	3.23	0.023
% K x %td	1.14	0.331
%dod x %dvh	2.71	0.080
%dod x %td	11.50 **	0.002
%dvh x %td	0.09	0.916
% K x %dod x %dvh	2.09	0.103
%K x %dod x %td	1.15	0.327
%K x %dvh x %td	1.65	0.184
%dod x %dvh x %td	10.66 **	0.000
all	0.68	0.608

Table 5-2 Results of an ANOVA performed on diameter ratios of the beads in toluene, neglecting all data that includes 66% dodecane in the polymer formulation. * Significant at 95% confidence level, ** significant at 99% confidence level. Complete ANOVA tables are listed in Appendix A.

Variables	F-Value	P
%Kraton G1652 (Krat)	5.58 *	0.009
%dodecane (dod)	52.6 **	0.000
%divinylbenzene (dvb)	6.67 *	0.004
Interactions		
%Kraton x %dodecane	6.79 *	0.001
%Krat x %dvb	3.09	0.032
%dod x %dvb	7.04 *	0.001
%Krat x %dod x %dvb	2.55	0.033

Table 5-3 Results of an ANOVA performed on diameter ratios of the beads in toluene, neglecting all data that includes 60% total diluent in the polymer formulation. * Significant at 95% confidence level, ** significant at 99% confidence level. Complete ANOVA tables are listed in Appendix A.

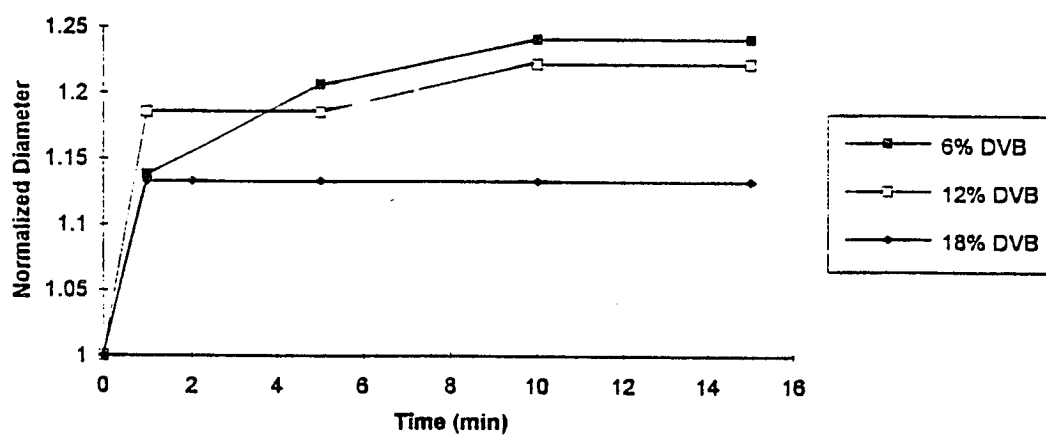


Figure 5-1 Normalized diameter vs. time for beads consisting of 2% Kraton G1652, 33% dodecane, 60% diluent, and 6, 12, or 18% divinylbenzene.

due to the fact that as the amount of crosslinking increases, the individual strands of the polymer become more interconnected. As swelling occurs, the forces due to the stretching of the bonds increase more quickly as the polymer chains become solvated. The crosslinks, by causing a three-dimensional network, effectively prevent the chains from completely solvating. The Kraton G1652 content, as well as the porogenic solvent composition, do not seem to have an effect on varying divinylbenzene content. Figure 5-2 shows the same general trend with beads whose formulations are 8% Kraton G1652, 33% dodecane, 40% total diluent and 6, 12, or 18% divinyl benzene. Each diameter ratio corresponds to a particular formula in the factorial design, and therefore the diameter ratio is influenced by more than one parameter. However, by plotting all the data points of the factorial, it is possible to see the general trends present in the data. All diameter ratios for the factorial formulations are plotted against the crosslinking content to better illustrate the trend in Figure 5-3. There is a definite decrease in the average diameter ratio as the % crosslinking is increased. The polymer networks are behaving as predicted by Flory in equation (1), Chapter II.

The % dodecane content of the total diluent leads to a slight decrease in the diameter ratio. Typical results are shown in Figure 5-4 for beads whose formulations are 14% Kraton, 12% DVB, 40% total diluent, and 0, 33, or 66% dodecane P(VBC). The cause of the decrease in diameter ratio is unknown.

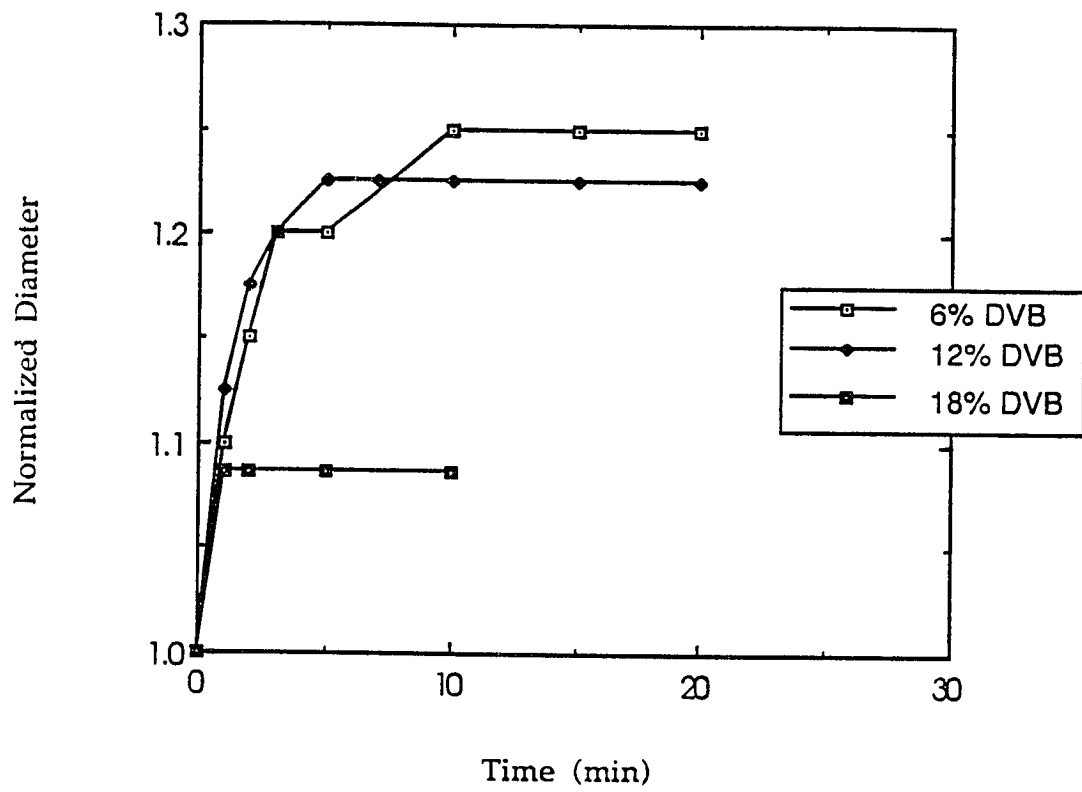


Figure 5-2 Normalized diameter vs. time for beads consisting of 8% Kraton G1652, 33% dodecane, 40% total diluent, and 6, 12, or 18% divinylbenzene.

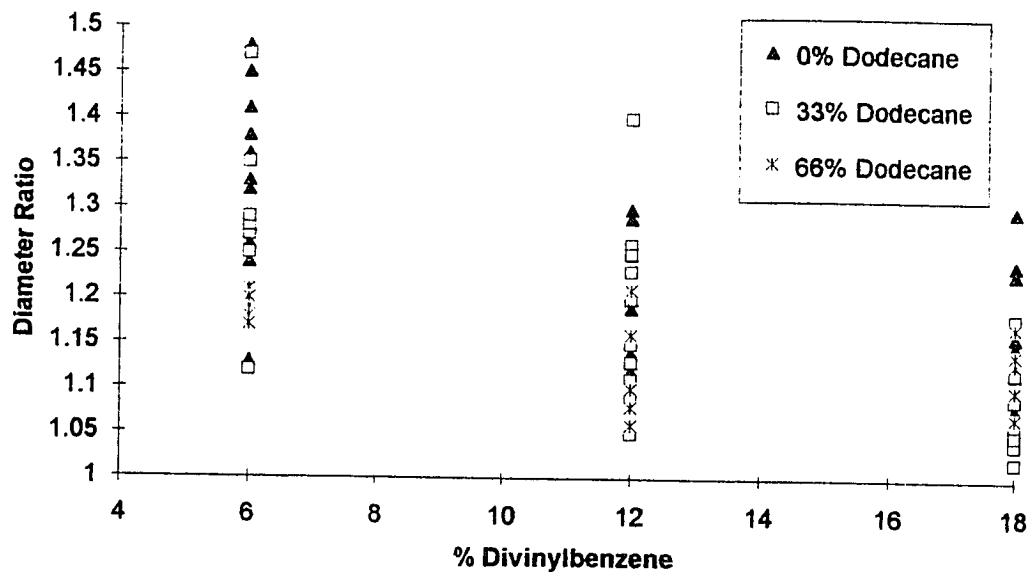


Figure 5-3 All diameter ratios in toluene vs. % divinylbenzene.

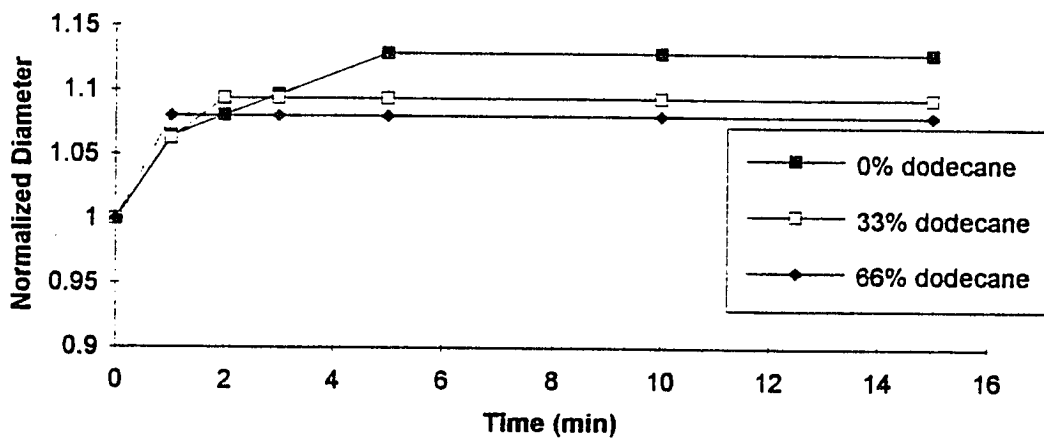


Figure 5-4 Normalized diameter vs. time for beads consisting of 14% Kraton G1652, 12% divinylbenzene, 40% total diluent, and 0, 33, or 66% dodecane.

However, it is possible to speculate that the effect may be due to the morphological changes associated with the addition of dodecane. Since dodecane is not compatible with the forming polymer, a high dodecane content will lead to a phase separation, causing the formation of a macroporous polymer. As polymerization proceeds, the dodecane phase separates from the forming polymer which is swollen in monomer. Because of this, the growing chains have a limited pool of monomer from which to propagate. Eventually, the monomer will be exhausted and polymerization will terminate, resulting in a polymer whose structure consists of regions of entangled strands connected to each other by fewer relatively untangled chains.⁵⁷ Because small regions of the polymer are highly entangled, they will swell but will not be fully elongated, possibly leading to a slight decrease in the equilibrium diameter ratio. This general trend was seen regardless of the %Kraton G1652, %DVB, or the total diluent content in the monomer mixture. To further illustrate this overall trend, all diameter ratios were plotted vs. % dodecane in Figure 5-5, which shows that the average diameter ratio slightly decreases as the % dodecane increases.

Increasing the total diluent in the monomer mixture resulted in a slight increase in the diameter ratio. Typical results are shown in Figure 5-6 for beads whose formulations are 14% Kraton G1652, 12% DVB, 33% dodecane, and 40 or 60% total diluent P(VBC). Again, the exact explanation of this effect is not known. However, it is known⁵⁸ that the presence of a compatible solvent during

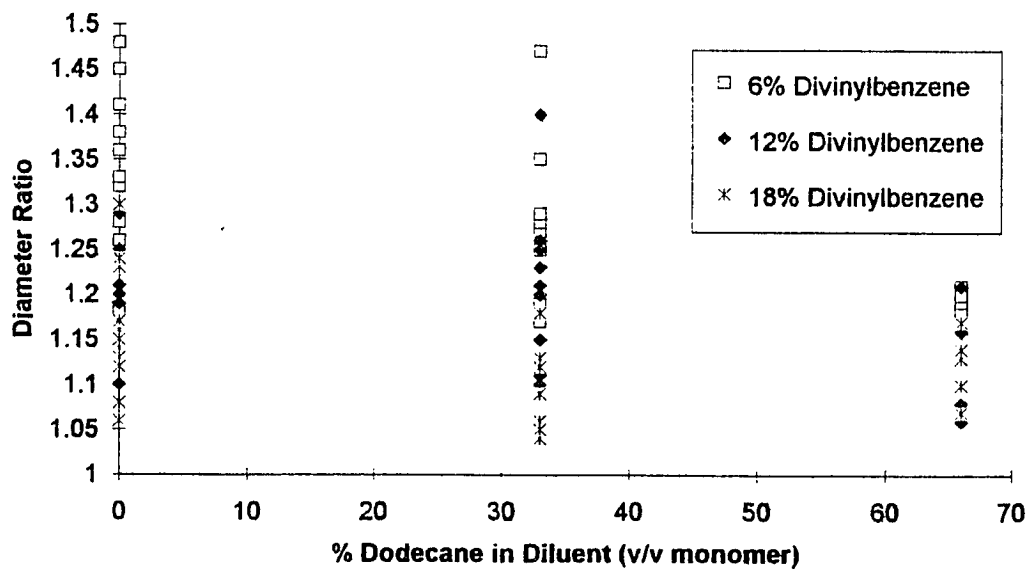


Figure 5-5 All diameter ratios vs. percent dodecane.

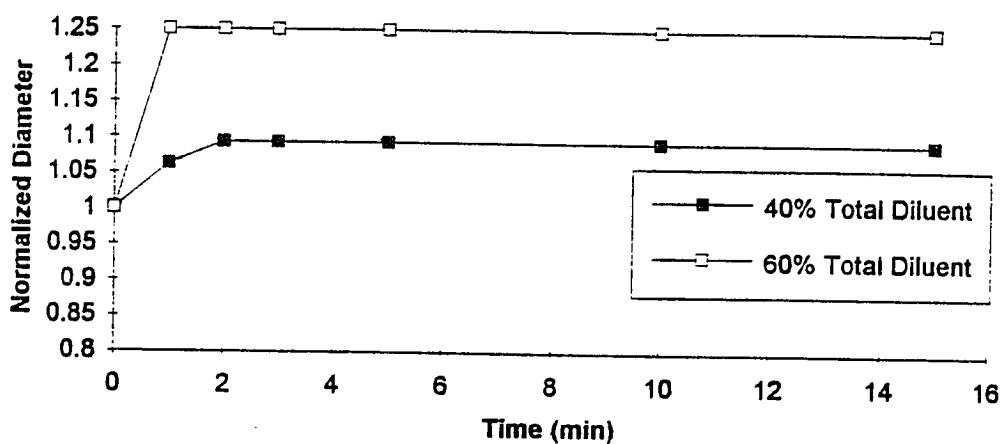


Figure 5-6 Normalized diameter vs. swelling time of beads whose formulations are 14% Kraton G1652, 12% divinylbenzene, 33% dodecane, 40% or 60% total diluent poly(vinylbenzyl chloride).

polymerization will lead to a polymer that is fully solvated at all times. With increasing dilution the growing chains reach greater lengths before termination occurs. The removal of the diluent causes collapse of the pores, however, swelling in a compatible solvent will restore the original porous structure. A plot of all diameter ratios vs. total diluent content is shown in Figure 5-7, illustrating this overall increasing trend.

Table 5-3 also shows that the %Kraton G1652 is significant at the 95% confidence level when the diameter ratios for the beads with 60% total diluent are excluded. All data consisting of 40% total diluent are plotted vs. the % Kraton G1652 in Figure 5-8. The formulations with 40% total diluent have a higher percentage of Kraton in the monomer mixture than those with 60% total diluent. As discussed in Chapter IV, the morphology of the polymer matrix changes as the percent Kraton G1652 is increased. The effect of Kraton G1652 on diameter ratio of beads with 40% total diluent in toluene is slight compared to the other significant factors. higher percentage of Kraton in the monomer mixture than those with 60% total diluent. The significant interactions, also listed in Tables 5-2 and 5-3, support the conclusions drawn from the discussion of the main effects.

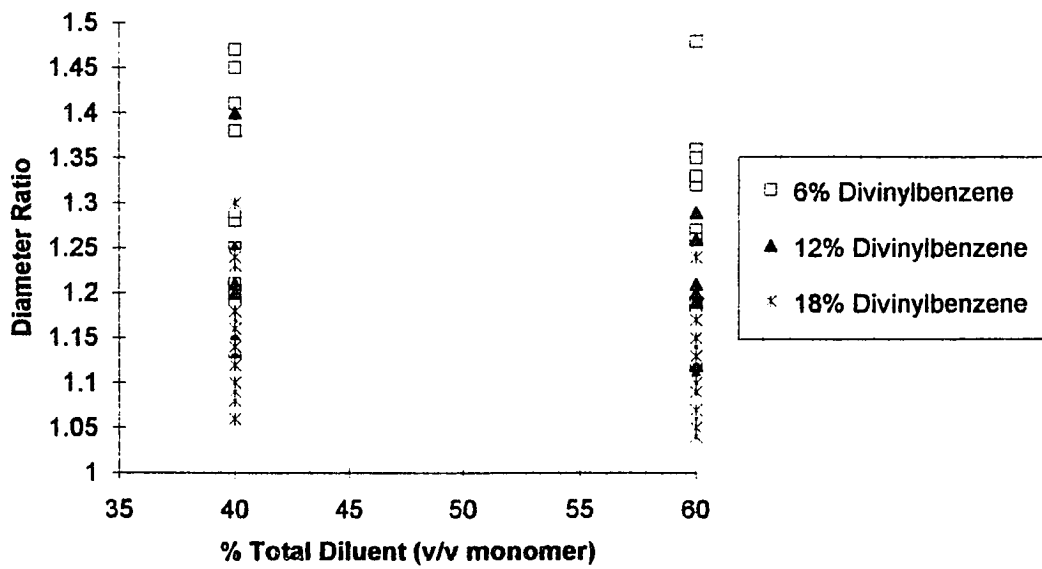


Figure 5-7 All diameter ratios vs. percent total diluent of bead formulation.

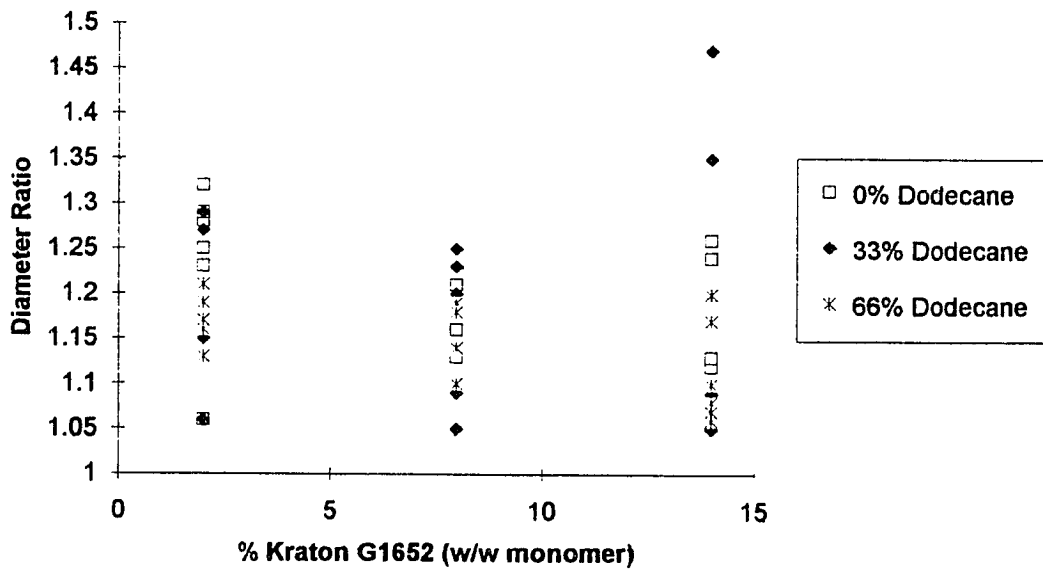


Figure 5-8 All data consisting of 40% total diluent vs. % Kraton G1652.

Swelling Times

Tables 5-4 and 5-5 list the F-values of the analysis of variance performed on the swelling times of the beads in toluene. The %Kraton G1652 and the % dodecane are statistically significant at the 99% confidence level. As discussed in Chapter IV, the morphology of the polymer matrix is controlled by a phase separation that occurs between its aliphatic and aromatic portions. At low Kraton G1652 levels, the aliphatic phase separates into inclusions within the matrix as the polymer forms. After polymerization the dodecane is removed, leaving what appears as pores throughout the matrix, with the aliphatic portion of the Kraton G1652 lining the pores. At higher concentrations a phase separation occurs, resulting in a matrix that consists of spheres of poly(vinylbenzyl chloride) surrounded by the aliphatic phase of the Kraton G1652.

It is not surprising that swell times are dependent upon the dodecane and Kraton G1652, i.e., the morphology, of the polymer matrix. Increasing the % dodecane in the monomer mixture leads to an overall decrease in the swelling time of the polymer, regardless of the percentage of Kraton G1652 present. Dodecane, as discussed before, is a non-solvating pore-forming solvent that causes a macroporous polymer matrix when present during polymerization at the 2% Kraton G1652 level. The addition of larger pores will give the solvent better access into the bead's interior, thus decreasing the swell time of the bead.

Variables	F-Value	P
% Kraton	16.73 **	0.000
% dodecane	44.29 **	0.000
% divinylbenzene	3.59	0.038
% total diluent	2.46	0.126
Interactions		
%K x %dod	5.64 *	0.007
%K x %dvh	3.98	0.009
% K x %td	2.33	0.112
%dod x %dvh	0.85	0.436
%dod x %td	2.84	0.100
%dvh x %td	1.62	0.212
% K x %dod x %dvh	1.74	0.162
%K x %dod x %td	0.45	0.642
%K x %dvh x %td	1.57	0.204
%dod x %dvh x %td	0.66	0.522
all	0.94	0.454

Table 5-4 Results of an ANOVA performed on the swelling times of the beads in toluene, neglecting all data that includes 66% dodecane in the polymer formulation. * Significant at 95% confidence level, ** significant at 99% confidence level. Complete ANOVA tables are listed in Appendix A.

Variables	F-Value	P
%Kraton G1652 (Krat)	17.69 **	0.000
%dodecane (dod)	16.16 **	0.000
%divinylbenzene (dvb)	1.91	0.168
Interactions		
%Kraton x %dodecane	2.96	0.038
%Krat x %dvb	2.17	0.099
%dod x %dvb	0.72	0.583
%Krat x %dod x %dvb	2.73	0.024

Table 5-5 Results of an ANOVA performed on swelling time of the beads in toluene, neglecting all data that includes 60% total diluent in the polymer formulation. * Significant at 95% confidence level, ** significant at 99% confidence level. Complete ANOVA tables are listed in Appendix A.

Figure 5-9, a graph of Normalized Diameter vs. Time (min) of beads with the formulation of 2% Kraton G1652, 12% DVB, 40% total diluent and 0, 33, or 66% dodecane, shows the decrease in the swelling time of the beads in toluene as the dodecane percentage is increased. The swelling time decreases from twenty minutes with 0% dodecane to ten minutes with 33% dodecane. The swelling time further decreased to one minute with the addition of 66% dodecane. Figure 5-10 clearly depicts the decreasing trend of swelling time as the dodecane is increased.

The effect of the addition of Kraton G1652 into the reaction mixture is slightly different. As the percentage of Kraton G1652 is increased, the change in morphology begins to govern the response of the polymer. Increasing the Kraton G1652 to 8% and eventually to 14% results in a matrix where small poly(vinylbenzyl chloride) spheres are situated throughout a porous “sea” of Kraton G1652. Relatively large, uniform pores are created by the space between the poly(vinylbenzyl chloride) spheres. Therefore, in beads modified with 8 and 14% Kraton G1652, all pores are interconnected, providing a path for the solvent throughout the polymer matrix, decreasing the swelling times. In contrast, beads modified with 2% Kraton G1652 do not have interconnected pores, and subsequently, have longer swelling times.

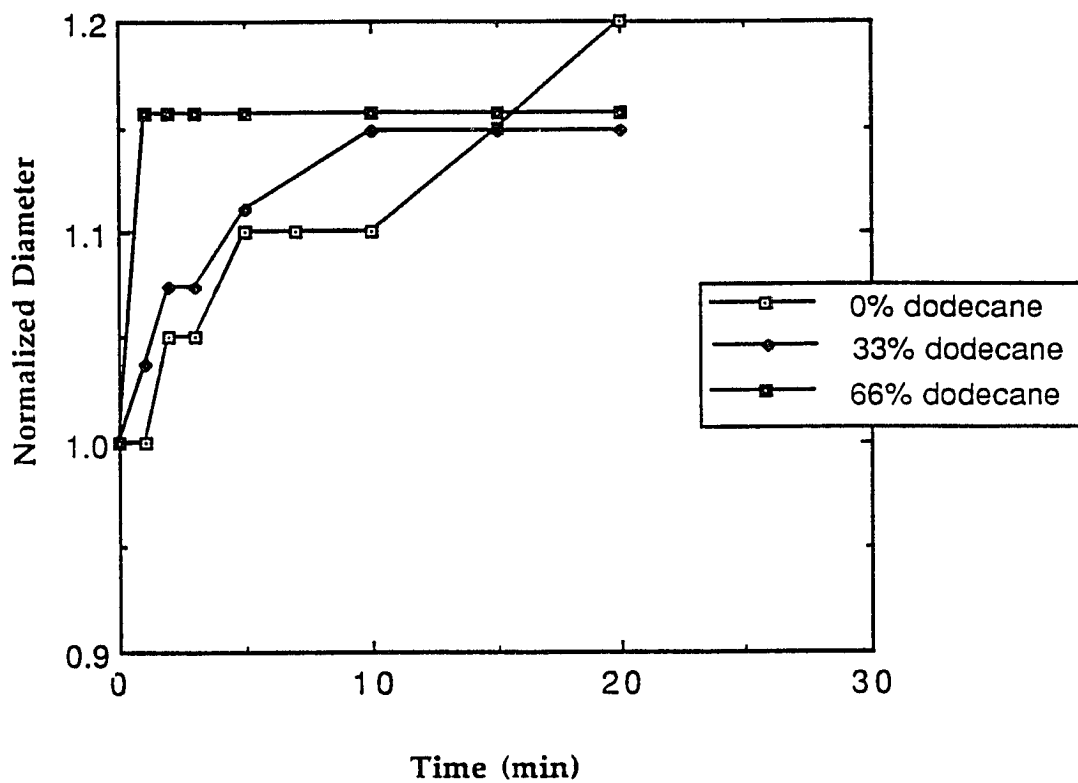


Figure 5-9 Normalized diameter vs. time of beads whose formulations are 2% Kraton G1652, 12% divinylbenzene, 40% total diluent, and 0, 33, or 66% dodecane.

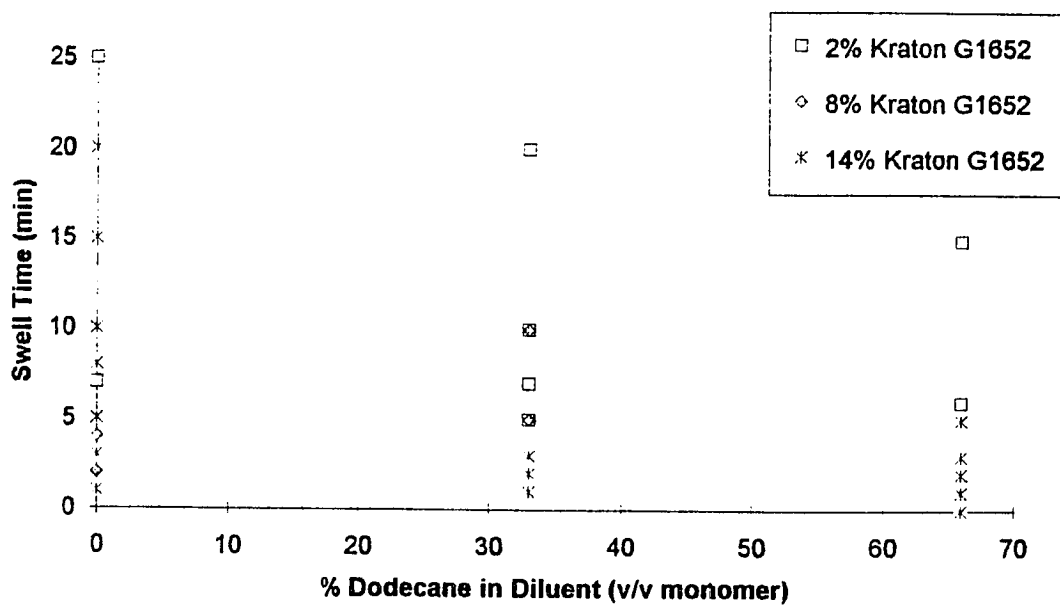


Figure 5-10 Swell times of all formulations vs. percent dodecane.

However, the fastest swelling times in the factorial, on average, are seen in beads with 8% Kraton G1652 their formulation. This result may be an effect of the morphology changes. As seen in Chapter IV, scanning electron micrographs of the varying Kraton G1652 levels show that the morphology of the beads with 8% Kraton G1652 seem to be intermediate between those with 2 and 14%. The morphology of the beads with 8% Kraton G1652 is a phase separated matrix with some dispersed larger pores. The pore-size distribution shows a slightly larger mean pore size with two definite peaks centering around approximately 2 and 4.5 nm. This may make the solvent more accessible into the bead's interior causing this polymer formulation to swell more quickly. Figure 5-11 shows the overall trend in swell times as a function of the percent Kraton G1652 in the monomer mixture.

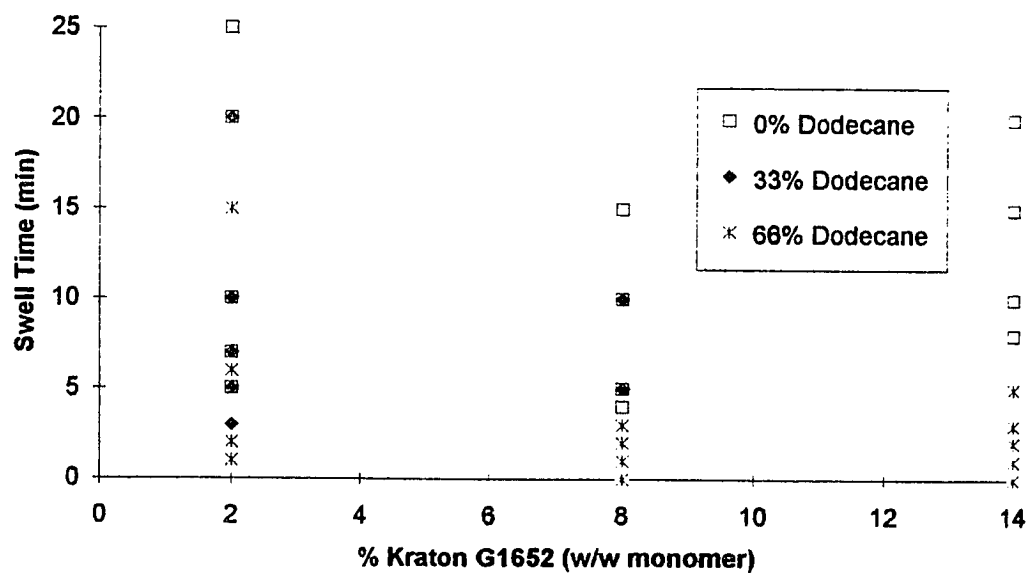


Figure 5-11 Swell times of all formulations vs. percent Kraton G1652.

CHAPTER VI
SWELLING in ACID
DIAMETER RATIOS and SWELLING TIMES

The beads were aminated with diethanolamine according to the procedure that was developed earlier in this laboratory, and described in Chapter III. It was found that after derivatizing with diethanolamine, the beads would swell in the presence of acid. The swelling of the polymer was caused by the electrostatic forces due to the protonation of the polymer matrix. The amination reaction is shown in Figure 6-1.

CHN Analyses of the Beads

To test the completion of the amination reaction, carbon, hydrogen and nitrogen (CHN) analyses were performed on each bead formulation. The percentages of nitrogen in the aminated beads are listed in Table 6-1. The theoretical values, corrected for the divinylbenzene and Kraton G1652 content are listed in parenthesis. The percentages of nitrogen found for the bead formulations are lower than the theoretical percentages due to an incomplete reaction of the

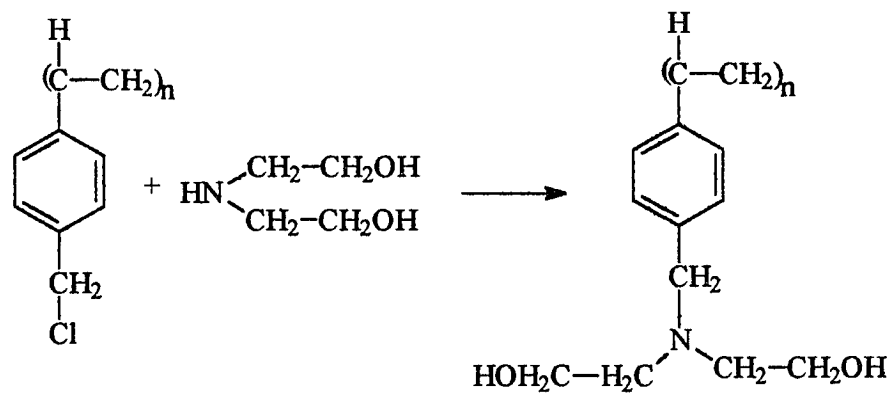


Figure 6-1 Amination of poly(vinylbenzyl chloride) with diethanolamine.

		% Kraton G1652										
		2			8			14				
		0	33	66	v% Dodecane in Diluent			0	33	66		
% Divinylbenzene	6	% Diluent	40	4.28 (5.84)	4.07	4.99	4.32 (5.49)	4.37	4.34	4.62 (5.18)	4.28	4.24
			60	4.37	4.52	/	4.53	4.57	/	4.38	4.15	/
	12	% Diluent	40	3.81 (5.63)	3.97	4.94	4.40 (5.30)	3.15	4.96	3.39 (5.01)	3.42	3.10
			60	3.79	4.02	/	4.45	3.74	/	3.28	3.99	/
	18	% Diluent	40	3.55 (5.42)	3.67	3.12	4.38 (5.12)	4.34	3.60	2.46 (4.85)	2.19	2.20
			60	3.57	3.56	/	4.29	3.98	/	3.16	2.75	/

Table 6-1 Percent nitrogen of each formulation from CHN analyses. The theoretical %N, corrected for the Kraton G1652 and divinylbenzene content, are listed in parenthesis.

diethanolamine with the vinylbenzyl chloride.

Some general trends in the percentage of nitrogen were noticed. Figure 6-2 is a graph showing all percent nitrogen data plotted against the percent divinylbenzene to illustrate the effect of increasing the crosslinking density on the percent nitrogen. The percent nitrogen decreases as the crosslinking increases. The actual values of percent nitrogen are consistently lower than the theoretical values corrected for the addition of divinylbenzene and Kraton G1652 in the matrix, suggesting that the difference is due to an incomplete reaction of the diethanolamine with the vinylbenzyl chloride. This could be caused by the decrease in the swelling of the polymer due to the increasing constraints between the bonds. The diethanolamine has better access into the bead's interior at lower crosslinking concentrations.

Figure 6-3 shows all percent nitrogen data plotted against the percent Kraton G1652 of the monomer mixture. Although the variation is slight, there is a decrease in the percentage of nitrogen as the percentage of Kraton G1652 is increased. The percent nitrogen decreases more than expected from the increase in divinylbenzene at high Kraton G1652 levels. The highest variation between the theoretical value and the actual values occurs at 14% Kraton G1652 and 18% divinylbenzene, suggesting that the change in morphology has a direct effect on the completeness of the diethanolamine reaction. Because the

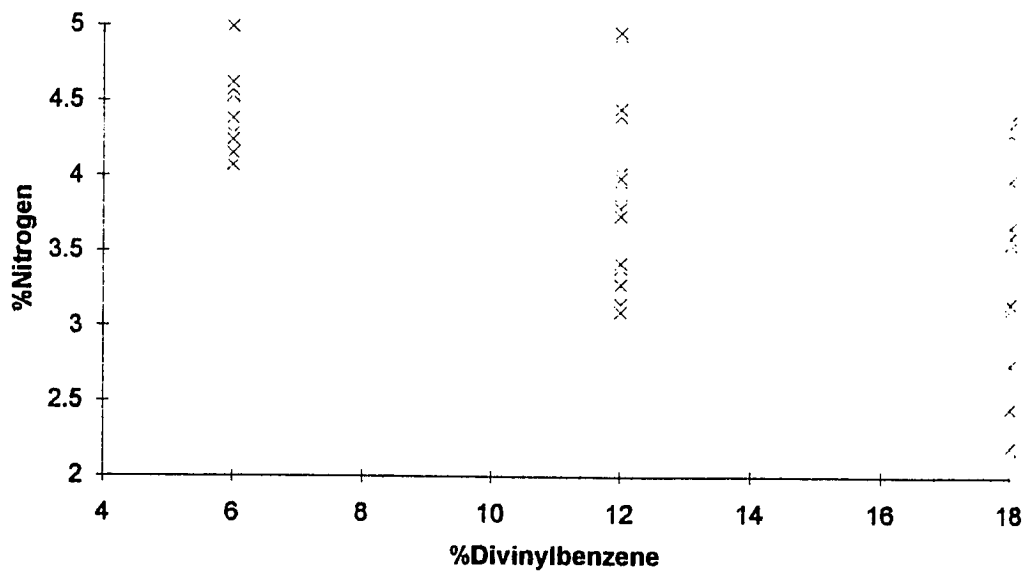


Figure 6-2 All percentages of nitrogen vs. % divinylbenzene in polymer formulation.

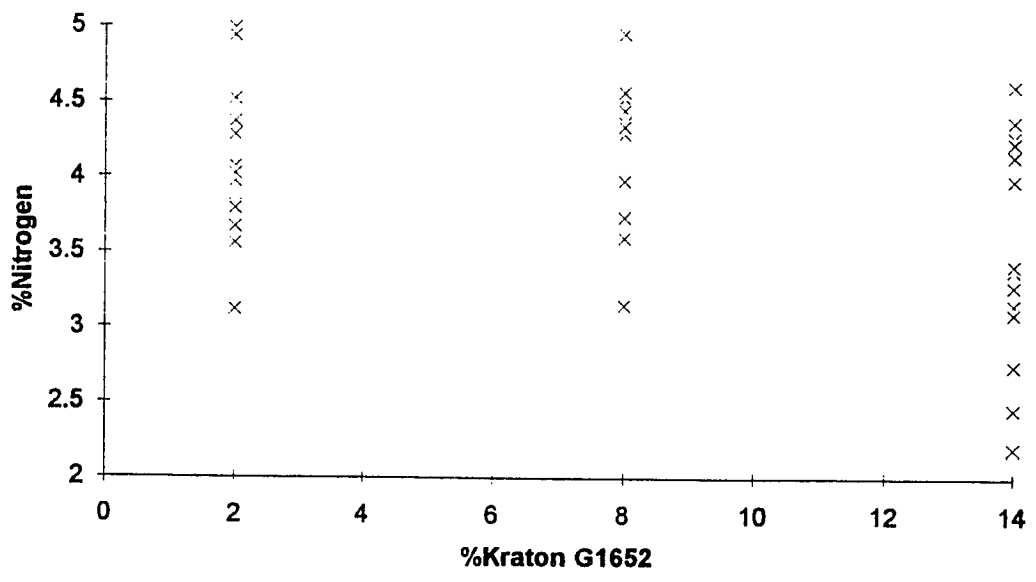


Figure 6-3 All percentages of nitrogen vs. %Kraton G1652.

morphology of the polymer matrix changes with high concentrations of Kraton G1652, the decrease in the percent nitrogen could be due to the fact that the diethanolamine is not able to efficiently swell the poly(vinylbenzyl chloride) in the matrix. That is, the diethanolamine can easily penetrate the pores situated between the poly(vinylbenzyl chloride) spheres, but cannot penetrate the microporous spheres as readily. Figures 6-4 and 6-5 shows that % dodecane and % total diluent in the monomer mixture have little or no effect on the resulting percent nitrogen after amination.

The beads were swollen to equilibrium in 0.1M, pH 4 acetate buffer (IS = 0.1M), while recording diameter and time. The diameter ratios and swelling times of the diethanolamine derivatized beads are listed in Table 6-2. An analysis of variance (ANOVA) was performed on the data. However, because some beads are not mechanically tough and crack upon swelling, some data points are missing. It was only possible to do the ANOVA on all data points except those formulations containing 66% dodecane. However, there is only one data point available for beads with the formulation 2% Kraton G1652, 12% divinylbenzene, 0% dodecane and 60% total diluent. To complete the ANOVA, the grand average of all diameter ratios and swelling times was used as the replicate data point.

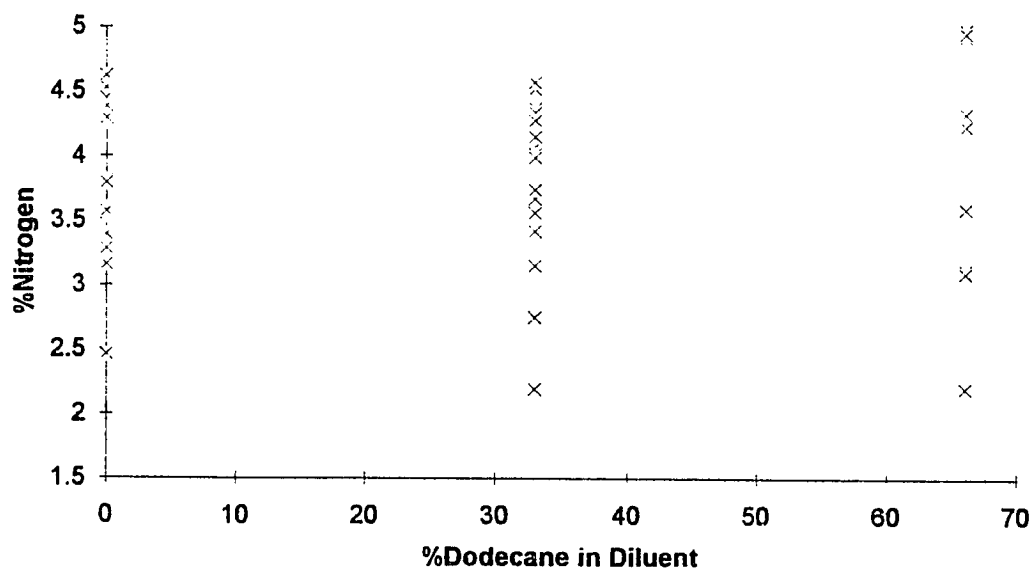


Figure 6-4 All percentages of nitrogen vs. % dodecane.

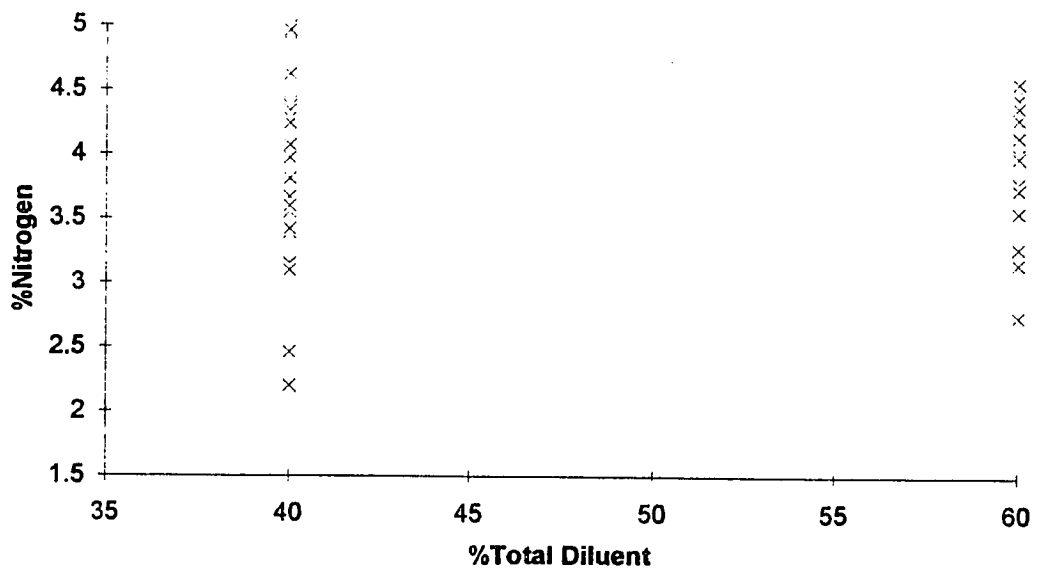


Figure 6-5 All percentages of nitrogen vs. % total diluent.

		% Kraton G1652									
		2			8			14			
		v% Dodecane in Diluent			v% Dodecane in Diluent			v% Dodecane in Diluent			
		0	33	66	0	33	66	0	33	66	
% Divinylbenzene	6	40	1.44 1.44 (4.5)	1.24 1.59 (10, 10)	crack	1.21 1.38 (15.5)	1.28 1.27 (5.3)	crack	1.17 1.13 (3.3)	1.15 1.18 (1.1)	1.36 1.10 (5.10)
			60	1.50 1.48 (3.1)	1.25 1.06 (5.5)	/	1.17 1.41 (15.10)	1.18 1.24 (3.3)	/	1.38 1.43 (5.5)	1.22 1.33 (5.15)
	12	40		1.23 2.00 (3.3)	1.22 1.17 (10.10)	1.10 1.25 (3.3)	1.09 1.14 (3.1)	1.21 1.22 (1.1)	1.08 1.09 (3.5)	1.13 1.18 (10.10)	1.04 1.05 (3.3)
			60	1.35 1.44 (1.2)	1.31 1.15 (5.3)	/	1.18 1.20 (3.3)	1.21 1.86 (1.5)	/	1.04 1.98 (1.5)	1.16 1.30 (10.10)
	18	40		1.18 1.09 (5.2)	1.13 1.12 (5.3)	crack	1.08 1.07 (1.3)	1.09 1.12 (3.3)	1.18 1.14 (2.3)	1.15 1.11 (10.1)	1.08 1.10 (5.3)
			60	1.24 (10)	1.18 1.22 (1.1)	/	1.10 1.25 (1.10)	1.07 1.17 (5.15)	/	1.06 1.06 (1.3)	1.06 1.03 (3.1)

Table 6-2 The diameter ratios and swelling times of the diethanolamine derivatized beads in 0.1M, pH 4 acetate buffer (IS=0.1M). Swelling times are listed in parenthesis.

Diameter Ratios of the Beads in Acid

The F-values, which represent the comparison of the standard deviations between the data for each effect (controlled factor) and the random error of the experiment, are listed in Table 6-3 for the analysis of the diameter ratio of the derivatized beads in acid. The results indicate that % divinylbenzene is statistically significant at the 99% confidence limit and %Kraton G1652 is significant at the 95% confidence limit.

Figure 6-6 illustrates the effect of % divinylbenzene on the diameter ratio of the aminated beads in acid. All diameter ratios are plotted against the % divinylbenzene. As expected, the diameter ratio decreases with increasing crosslinking content. Typical data is presented in Figure 6-7 for beads whose formulations are 2% Kraton G1652, 0% dodecane, 60% total diluent, and 6, 12, or 18% divinylbenzene.

Varying the percent Kraton G1652 in the monomer mixture has a significant effect on the diameter ratio of the aminated beads in acid. Figure 6-8 is a graph of all diameter ratios plotted against the percent Kraton G1652. This shows that there is a slight decrease in diameter ratio as the percentage of Kraton G1652 is increased. It is not completely clear why this occurs. The decrease in swelling is most likely due to the varying nitrogen content in the beads shown in Table 6-1, caused by the increasing Kraton G1652 and

Variables	F-Value	P
% Kraton	6.29 *	0.005
% dodecane	2.80	0.103
% divinylbenzene	9.07 **	0.001
% total diluent	1.01	0.322
Interactions		
%K x %dod	3.38	0.045
%K x %dvh	0.32	0.866
% K x %td	1.09	0.348
%dod x %dvh	0.67	0.517
%dod x %td	0.01	0.929
%dvh x %td	0.44	0.648
% K x %dod x %dvh	1.69	0.174
%K x %dod x %td	0.10	0.905
%K x %dvh x %td	1.52	0.217
%dod x %dvh x %td	3.06	0.059
all	0.24	0.915

Table 6-3 Results of ANOVA performed on data obtained upon swelling the beads in acid, neglecting all data that includes 66% dodecane in the polymer formulation. *Significant at 95% confidence level, **significant at 99% confidence level. The complete ANOVA table is listed in Appendix B.

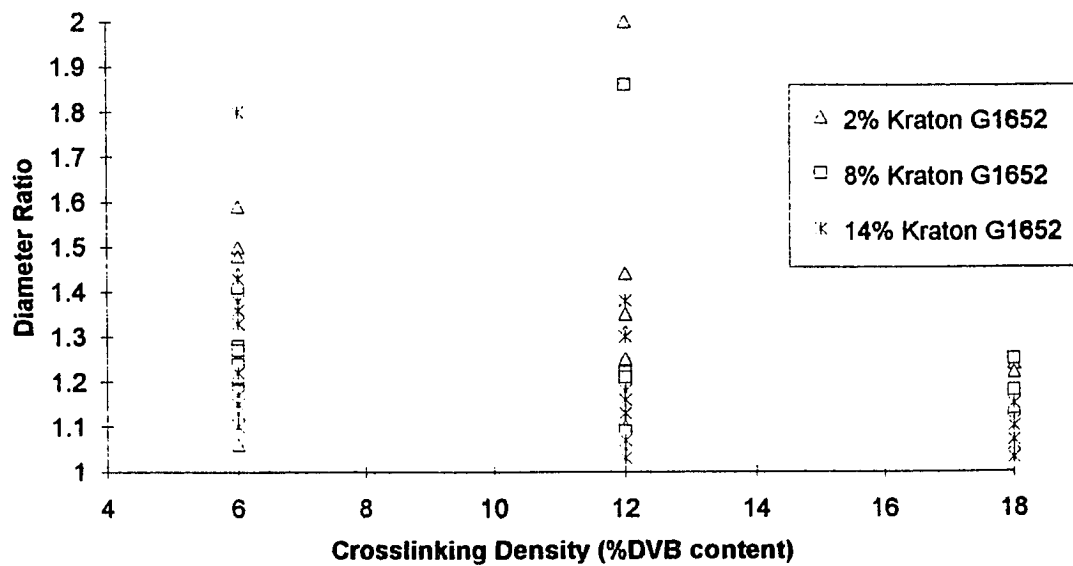


Figure 6-6 All diameter ratios in acid vs. % divinylbenzene.

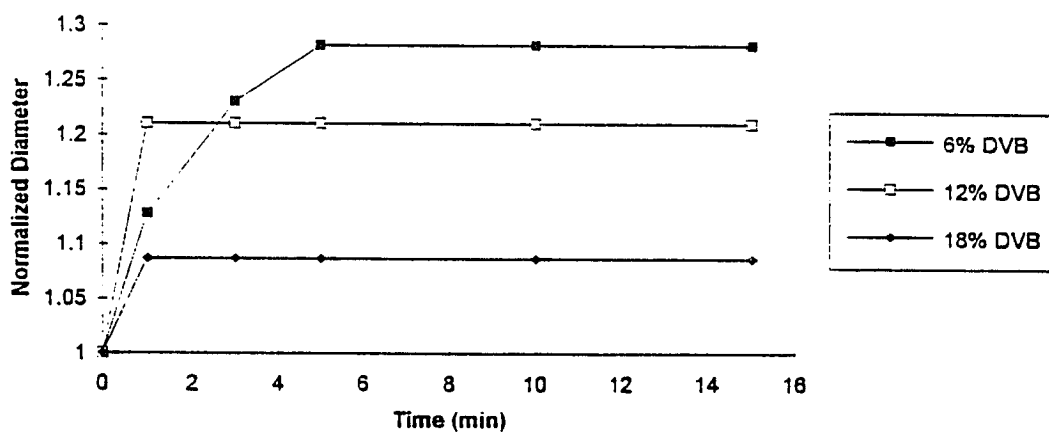


Figure 6-7 Normalized diameter ratio vs. time for beads whose formulations are 2% Kraton G1652, 0% dodecane, 60% total diluent and 6, 12, or 18% divinylbenzene.

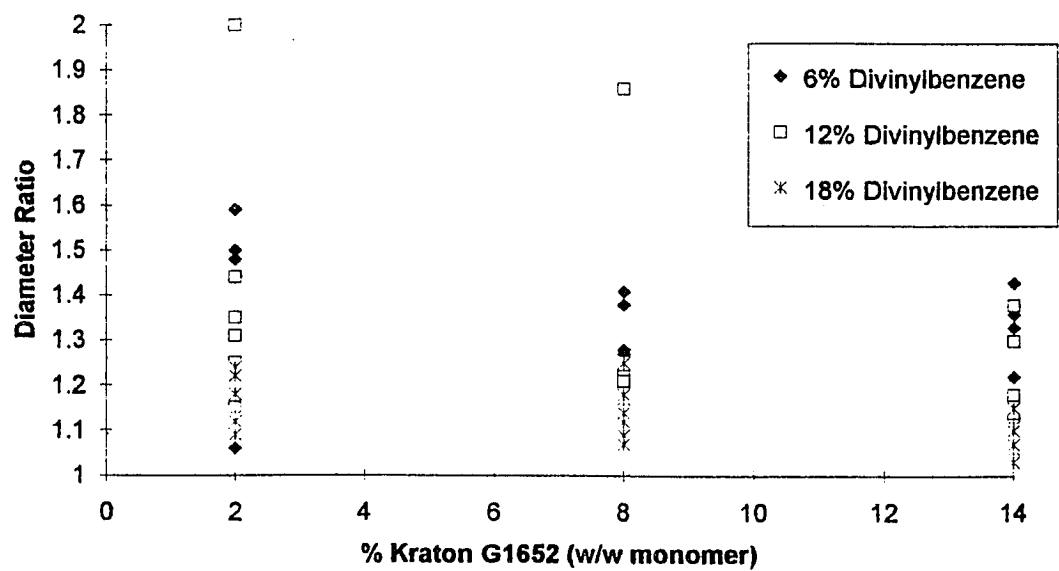


Figure 6-8 All diameter ratios in acid vs. %Kraton G1652.

divinylbenzene content in the polymer matrix. Kraton G1652 is not a significant factor on the diameter ratio when swelling occurs in toluene in the comparable ANOVA listed in Table 5-2, Chapter V. If the increasing Kraton G1652 content relative to poly(vinylbenzyl chloride) was the reason for the decreasing diameter ratio, then the same effect should have been seen in toluene.

Swelling Times of Beads in Acid

An analysis of variance was performed on the time it took the beads to swell to equilibrium when placed in 0.1M, pH 4 acetate buffer (0.1M IS). Whenever possible, the initial radius of the beads chosen for testing were close to 0.500mm so that the swelling times between formulations were directly comparable. However, the bead size distribution of some of the formulations did not include radii close to 0.500mm. The varying initial diameter of the beads will cause an increase in the random error of the swelling time data because larger beads take longer to swell to equilibrium.

The F-values, along with the probabilities are listed in Table 6-4 for all data excluding those formulations including 66% dodecane. None of the four

Variables	F-Value	P
% Kraton	0.26	0.771
% dodecane	1.84	0.183
% divinylbenzene	1.30	0.285
% total diluent	2.67	0.111
Interactions		
%K x %dod	0.53	0.591
%K x %dvh	2.37	0.071
% K x %td	5.95 *	0.006
%dod x %dvh	0.08	0.927
%dod x %td	1.32	0.259
%dvh x %td	1.71	0.195
% K x %dod x %dvh	2.27	0.080
%K x %dod x %td	6.69 *	0.003
%K x %dvh x %td	1.05	0.394
%dod x %dvh x %td	1.29	0.753
all	0.50	0.738

Table 6-4 Results of ANOVA performed on swelling times of the beads in acid, neglecting all data that included 66% dodecane in the polymer formulation. *Significant at 95% confidence level, **significant at the 99% confidence level. The complete ANOVA table is listed in Appendix B.

major effects are significant. The only significant interactions, at the 95% confidence level, are (% Kraton G1652 x % total diluent) and the (% Kraton G1652 x % dodecane x % total diluent).

There are no significant major effects in the ANOVA of swelling times in acid. However, the factors that seem to have the most effect are the % dodecane, % divinylbenzene and the % total diluent, even though they are not statistically significant. In contrast, the % Kraton G1652 and the % dodecane were found to be statistically significant at the 99% confidence level for the swelling times of the beads in toluene. The morphology of the beads, i.e., their phase separation, was governing the swelling process in compatible solvent. In acid, it is not evident that the pore structure affects the swelling time in the same way. Furthermore, the average swelling time in acid is much longer than the swelling time in toluene, also indicating a different swelling mechanism. Further study is necessary in order to conclude which parameters have a direct effect on swelling times in acid.

It seems as though increasing percent diluent may decrease the swelling time of the polymer. Increasing the percentage of total diluent increases the amount of xylene in the monomer mixture. During polymerization, xylene is partitioning between the dodecane and the forming polymer swollen in monomer. After polymerization is complete, removal of the xylene results in

microporous polymer spheres situated throughout a “sea” of macro and microporous Kraton G1652. An increase in the percentage of xylene in the monomer mixture will increase the amount of xylene that partitions into the aromatic phase, thus increasing the porosity of the poly(vinylbenzyl chloride), and affecting the swelling time of the polymer.

CHAPTER VII

PENETRATION MODULUS

Strain is defined as the polymer's reaction to stress. The modulus describes the particular type of strain exerted. The penetration modulus is a measure of the stress distribution of a bead in contact with two planes. It is a measurement of the force exerted by the bead during deformation. A bead, which is placed between two planes, is deformed by the horizontal movement of the upper plane. The force that the bead exerts on the lower plane as it deforms is measured. This force, in effect, is a measure of the mechanical strength of the bead in its swollen state.

The relationship of the total pressure force, F , of a bead compressed between two planes that have a high Young's modulus is defined as^{59,60} (Equation (3)):

$$F = 16/3 A r^{1/2} (\Delta y/2)^{3/2}$$

where A = penetration modulus

r = radius of the bead

$\Delta y = (y_o - y)$ change in the distance of the deformation plane from the deformed state to the undeformed state.

Rearranging Equation (3) produces the following (Equation (4)).

$$F_t^{2/3} = 1/2(16/3Ar^{1/2})^{2/3} \Delta y$$

The penetration modulus can then be found from the slope, S , of the line resulting from the graph of Δy vs. $F_t^{2/3}$, where (Equation (5))

$$A = 3(2S)^{3/2}/16r^{1/2}.$$

A low penetration modulus signifies a bead that is easily deformed, whereas, a high modulus indicates a bead that is harder and not easily deformed. The penetration moduli were found for all possible bead formulations derivatized with diethylamine by Ken Hassen, and are listed in Table 7-1. Some bead formulations, when swollen, crumbled with the application of a small amount of force when transferring with a pair of tweezers, making it impossible to obtain data.

		% Kraton G1652									
		2			8			14			
		v% Dodecane in Diluent			v% Dodecane in Diluent			v% Dodecane in Diluent			
% Divinylbenzene		0			33			66			
		0			33			66			
18	6	40	/	/	/	0.0144 MPa	0.0424 MPa	0.0909 MPa	0.0898 MPa	0.0651 MPa	0.0581 MPa
		60	0.0139 MPa	/	/	0.0113 MPa	0.0217 MPa	/	0.0257 MPa	0.0447 MPa	/
	12	40	0.136 MPa	0.112 MPa	0.106 MPa	0.131 MPa	0.0411 MPa	0.0868 MPa	0.193 MPa	0.306 MPa	0.0621 MPa
		60	0.0166 MPa	0.209 MPa	/	0.0262 MPa	0.0164 MPa	/	0.246 MPa	0.0693 MPa	/
	18	40	/	0.590 MPa	/	0.0438 MPa	0.319 MPa	0.242 MPa	0.441 MPa	0.242 MPa	0.256 MPa
		60	0.239 MPa	0.197 MPa	/	0.152 MPa	0.0922 MPa	/	0.0880 MPa	0.111 MPa	/

Table 7-1 Penetration moduli in MPa.

The penetration moduli computed for the beads from our factorial are 1-3 orders of magnitude lower than those published by Wieczorek et al.⁶¹ for comparable beads with 10% divinylbenzene. This is probably a result of the addition of Kraton G1652 and microcracking in our polymer matrix, which causes our beads to swell with less force.

Figure 7-1 shows a typical plot of Δy vs. $F_t^{2/3}$ for the formulation 2% Kraton G1652, 18% divinylbenzene, 0% dodecane and 40% total diluent as the force is increased. The result is a straight line, with, according to Equation (4), the slope being equal to $1/2(16/3Ar^{1/2})^{2/3}$.

The data collected while increasing then subsequently decreasing the displacement for the same bead is shown in Figure 7-2. The force exerted by the bead when initially deformed is not the same as the force exerted as the upper plane releases the bead. The bead is exhibiting hysteresis, an expected property of viscoelastic solids. As the upper plane exerts force on the polymer bead, work is being done on the bead. If you attempt to recover that work, there is always some mechanical loss.⁶²

Because there are a large amount of missing values, it was not possible to do an analysis of variance that would include all the data obtained. An ANOVA was performed on all data excluding those formulations containing 2% Kraton G1652 and 66% dodecane. Since there was only one data point per formulation, it was necessary to use the interactions as an estimate of the random error of the

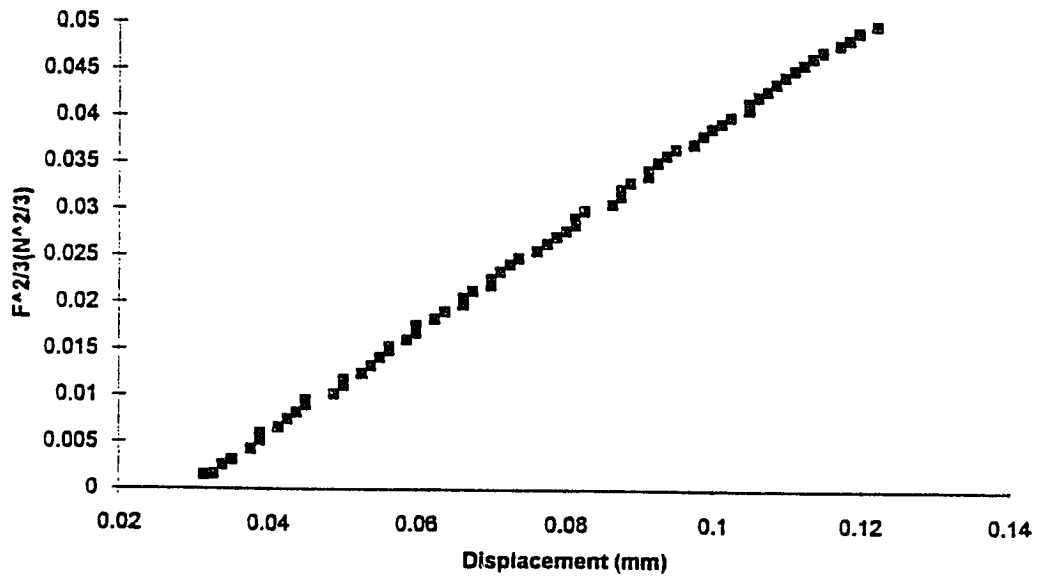


Figure 7-1 A plot of the change in displacement (Δy) vs. Force^{2/3} for the formulation 2% Kraton G1652, 18% divinylbenzene, 0% dodecane, and 40% total diluent. The slope is equal to $1/2(16/3Ar^{1/2})^{2/3}$.

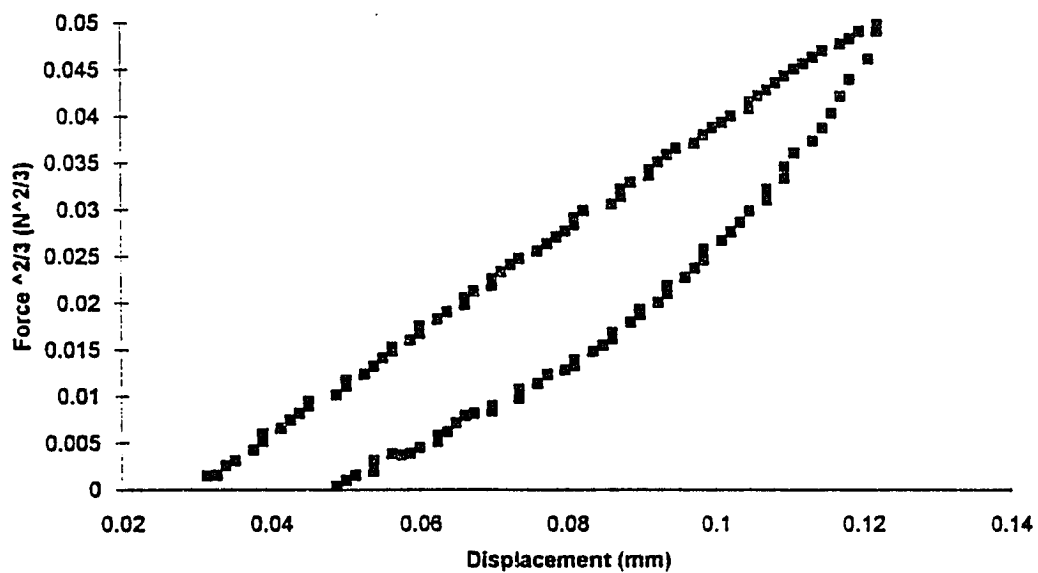


Figure 7-2 Force^{2/3} vs. displacement for a bead with the formulation 2% Kraton G1652 18% divinylbenzene, 0% dodecane, and 40% total diluent.

system, with 18 degrees of freedom. The F-values for the main effects are listed in Table 7-2. The entire ANOVA table can be found in Appendix C. The %Kraton G1652, % divinylbenzene and the % total diluent are all statistically significant at the 99% confidence level.

Figure 7-3 shows all penetration moduli plotted against the % Kraton G1652. As the Kraton G1652 content increases, the penetration modulus also increases. This is an unexpected result because it was assumed that the addition of the elastomer would cause the polymer matrix to deform more easily. The increase in the penetration modulus as the Kraton G1652 is increased may be due to a morphological effect. At higher levels of Kraton G1652, the morphology of the matrix changes, resulting in poly(vinylbenzyl chloride) spheres surrounded by the aliphatic region of the Kraton G1652 (See ChapterIV). These spheres are closely packed together to eventually form the polymer bead. The packing may add to the strength of the polymer matrix, possibly by restricting deformation.

Figure 7-4 shows all penetration moduli plotted against the changing divinylbenzene concentration. The penetration modulus increases as the percent divinylbenzene increases. As crosslinking increases, the polymer strands become more interconnected, resulting in a polymer matrix that is more resistant to deformation.

The % total diluent has the opposite effect on the penetration modulus. As shown in Figure 7-5, the penetration modulus decreases as the % total

Effects	F-Value
% Kraton G1652	16.1**
% Dodecane	0.165
% Divinylbenzene	17.4**
% Total Diluent	17.3**

Table 7-2 Results of the ANOVA performed on the penetration moduli of all beads excluding those with 2% Kraton G1652 and 66% dodecane. The interactions were used as an estimate of the random error of the system. ** Significant at 99% confidence level. The complete ANOVA table is listed in Appendix C.

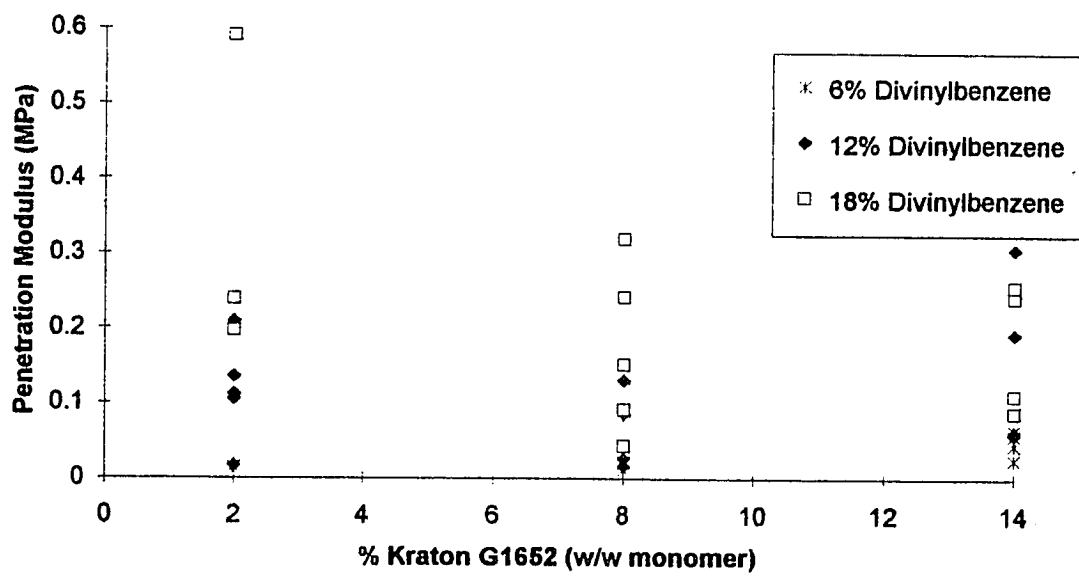


Figure 7-3 Penetration moduli vs. %Kraton G1652.

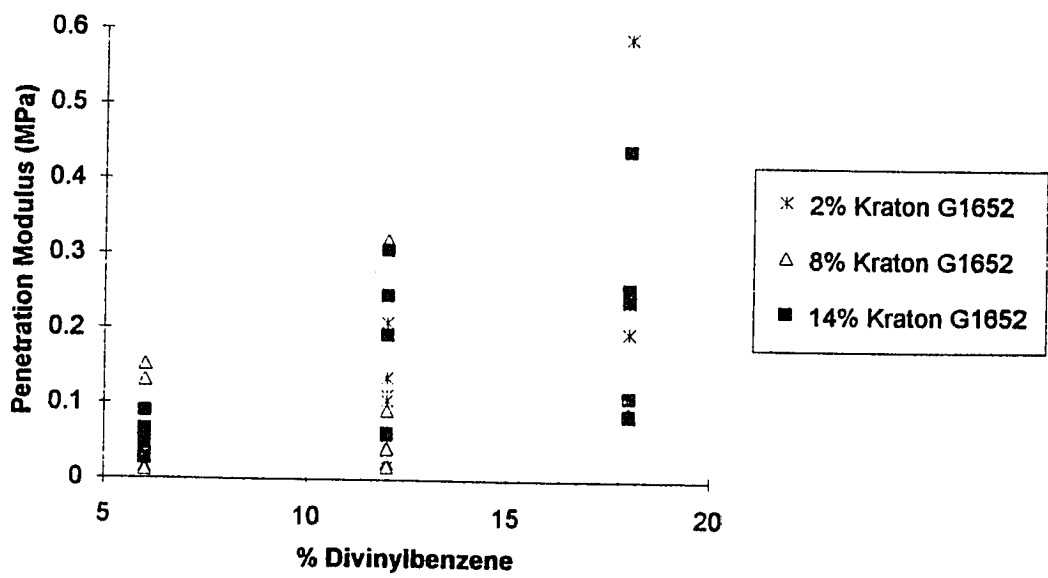


Figure 7-4 All penetration moduli vs. % divinylbenzene.

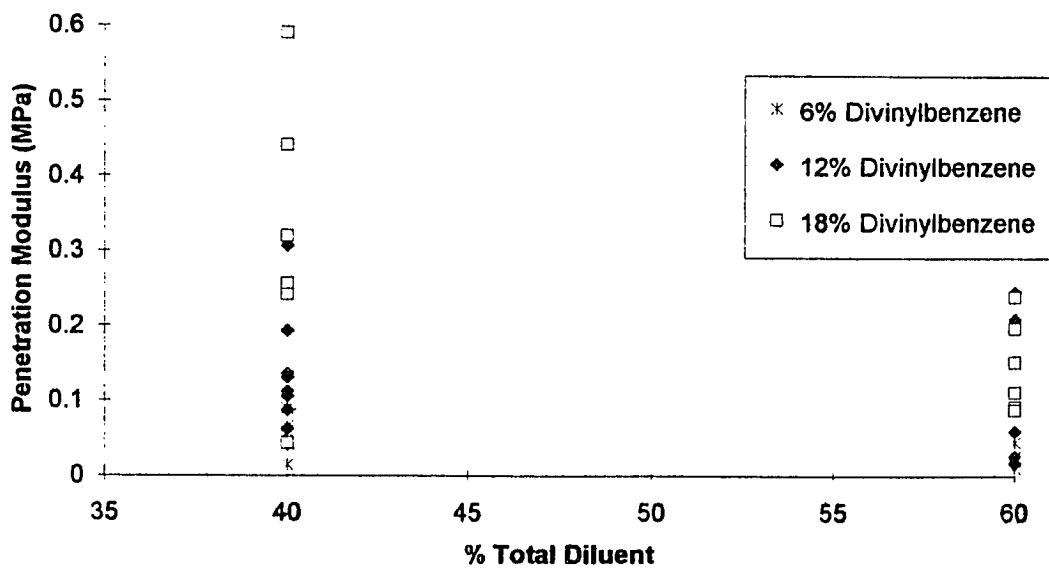


Figure 7-5 All penetration moduli vs. % total diluent.

diluent increases from 40 to 60%. As the pore space increases in the polymer, the volume of the polymer between the pores decreases. Therefore, there is less polymer to deform, leading to a lower penetration modulus.

Changing the percent dodecane in the monomer mixture does not seem to affect the penetration modulus. In Figure 7-6, the means of the 0 and 33% range are very similar, supporting the result obtained in the ANOVA. There are fewer available data points available for the 66% dodecane formulations, making it difficult to make direct comparisons. However, with the exception of the two outliers in the 0 and 33% dodecane range, the three means do not seem significantly different.

Increasing the crosslinking content of a bead will increase the penetration modulus of the bead. That is, beads with higher crosslinking content will swell with more force. Surprisingly, increasing the Kraton G1652 also increases the penetration modulus of the beads. The morphological changes associated with the addition of Kraton G1652 into the matrix may be responsible, however, more study is needed. Varying total diluent also has an effect on the penetration modulus. The higher degree of pore space leads to a lower penetration modulus. The swelling force of the bead is highly dependent upon the morphological structure of the polymer matrix.

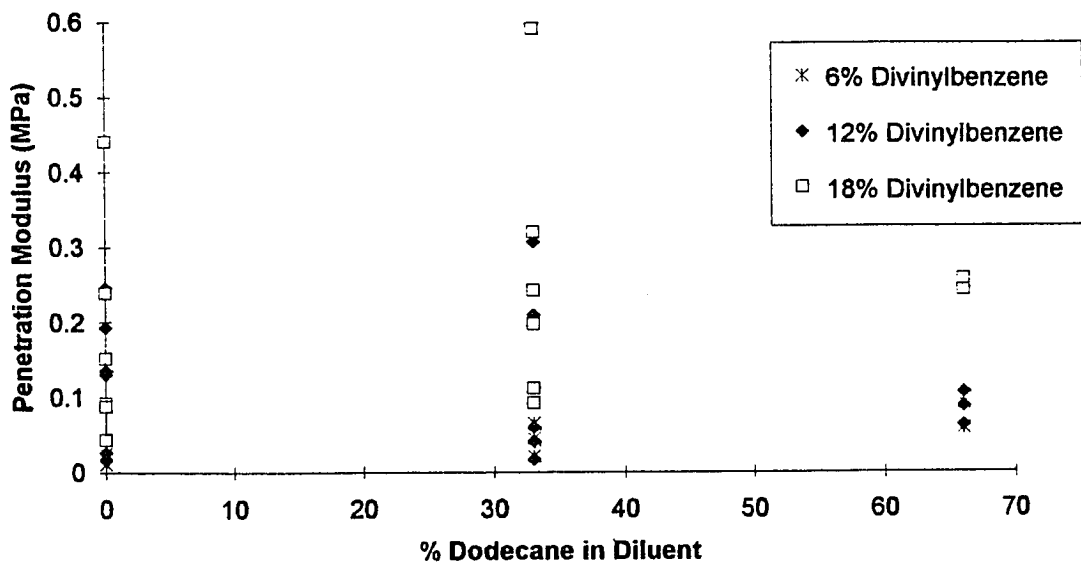


Figure 7-6 All penetration moduli vs. % dodecane.

CHAPTER VIII

CONCLUSION

The polymerization of Kraton G1652 modified poly(vinylbenzyl chloride) in the presence of xylene and dodecane is complex. The SEM and porosimetry data suggest a model of the polymerization process. As polymerization proceeds, the forming poly(vinylbenzyl chloride) and the porogenic solvent, dodecane, separate into distinct aromatic and aliphatic phases. The Kraton G1652 acts as a surfactant between the dodecane and the forming polymer swollen in monomer, and is directly involved in stabilizing the interface. As the percentage of Kraton G1652 is increased, our results indicate that it eventually reaches a concentration high enough so that the aliphatic phase becomes the continuous phase. Increasing the Kraton G1652 increases the surfactant content of the monomer mixture which decreases the surface tension between the forming polymer and the dodecane during polymerization. Formation with a larger volume of Kraton G1652 results in a morphology consisting of small poly(vinylbenzyl chloride) spheres situated throughout the aliphatic matrix. We believe that because the Kraton G1652 has a stabilizing effect, the resulting morphology is due to the drive to increase the surface area between the two phases.

The other porogenic solvent, xylene, partitions into both the aliphatic and aromatic regions, that is, the regions consisting of dodecane and the forming polymer. Removal of both porogenic solvents results in a matrix that consists of microporous poly(vinylbenzyl chloride) spheres surrounded by a “sea” of micro- and macroporous Kraton G1652.

The morphology of the matrix governs the properties of the polymer. The diameter ratio of the modified polymer in toluene is determined by the amount of divinylbenzene, dodecane and total diluent in the monomer mixture. The exact swelling process is unknown, however we know that adding divinylbenzene and dodecane will decrease the diameter ratio. Whereas, increasing the total diluent increases the diameter ratio. It is not surprising that increasing the crosslinking decreases the swelling ratio. However, further study into the morphology of the polymer will result in a better understanding of the swelling process and its dependence on the two porogenic solvents.

The swelling times in toluene are dependent upon the Kraton G1652 and the dodecane, i.e., the morphology of the polymer matrix. The larger pores corresponding to the space between the poly(vinylbenzyl chloride) pores will allow the solvent better access into the bead's interior.

The swelling process after amination with diethanolamine in acid is somewhat different. The diameter ratio depends upon the amount of divinylbenzene and Kraton G1652 present in the monomer mixture. The

percentage of nitrogen of the beads after amination is also dependent upon the amount of Kraton G1652 and divinylbenzene in the polymer matrix. This suggests that the diameter ratio in acid is dependent upon the amount of available sites that can be protonated throughout the matrix.

Due to a large random error in the sample, it was not possible to determine the exact cause of the swelling time in acid. However, it is interesting to note that the swelling time in acid is not determined by the same parameters as the time in toluene. It is not evident that the pore structure affects the swelling time in the same way as it does in toluene. This indicates that the swelling processes in acid and toluene are distinct.

The penetration modulus is dependent upon the amount of Kraton G1652, divinylbenzene and total diluent in the monomer mixture. Increasing the Kraton G1652 increases the penetration modulus. This increase may be due to a morphological effect. As crosslinking increases, the polymer strands become more interconnected, resulting in a polymer matrix that is more resistant to deformation. Increasing the total diluent increases the overall pore space of the polymer. The volume of the polymer between the pores decreases leaving less polymer to deform, decreasing the penetration modulus.

While we were able to increase the mechanical strength and the response time of the sensor, we were not able to synthesize a polymer that would swell with enough strength to adequately push the diaphragm of the fiber optic sensor.

However, we now more fully understand the polymerization process of Kraton G1652 modified poly(vinylbenzyl chloride), and are better able to predict the outcome of future modifications.

It became evident that it would not be possible to synthesize a bead that would be able to swell with enough force to push the diaphragm of the chemical sensor. The beads, when placed in contact with the diaphragm and swelled, would deform. Although they did displace the diaphragm slightly, the resulting loss of sensitivity for the sensor was unacceptable. When the search for a diaphragm that could more easily be displaced by the bead proved futile, the fiber optic chemical sensor based on swelling of polymer beads was abandoned.

During swelling tests conducted by Sizhong Pan, it was noticed that beads with 2% Kraton G1652 became more clear as they swelled in acid. We are still investigating why the addition 2% Kraton G1652 causes the beads to become more clear. Research is now in progress that uses the changing optical properties of the polymer as a basis for a sensor. The polymer can be dipcoated onto the end of the optical fibers, or polymer membranes of the same basic formulations are synthesized then connected to the end of the fibers.

APPENDIX A

Variables	DF	SS	MS	F-Value	P
% Kraton	2	0.009244	0.004622	1.46	0.246
% dodecane	1	0.046006	0.046006	14.52 **	0.001
% divinylbenzene	2	0.320036	0.160018	50.49 **	0.000
% total diluent	1	0.036450	0.036450	11.5 **	0.002
Interactions					
%K x %dod	2	0.051511	0.025756	8.13 **	0.001
%K x %dvh	4	0.040922	0.010231	3.23	0.023
% K x %td	2	0.007233	0.003617	1.14	0.331
%dod x %dvh	2	0.017169	0.008585	2.71	0.080
%dod x %td	1	0.036450	0.036450	11.50 **	0.002
%dvh x %td	2	0.000558	0.000279	0.09	0.916
% K x %dod x %dvh	4	0.026439	0.006610	2.09	0.103
%K x %dod x %td	2	0.007300	0.003650	1.15	0.327
%K x %dvh x %td	4	0.020883	0.005221	1.65	0.184
%dod x %dvh x %td	2	0.067558	0.033779	10.66 **	0.000
all	4	0.008667	0.002167	0.68	0.608
Error	36	0.114100	0.003169		
Total	71	0.810528			

Complete results of the ANOVA performed on diameter ratios of the beads in toluene, neglecting all data that includes 66% dodecane in the polymer formulation. *Significant at 95% confidence level, ** significant at 99% confidence level.

Variables	DF	SS	MS	F-Value	P
%Kraton G1652 (Krat)	2	0.017715	241.72	5.58 *	0.009
%dodecane (dod)	2	0.167026	219.50	52.6 **	0.000
%divinylbenzene (dvb)	2	0.021181	26.06	6.67 *	0.004
Interactions					
%Kraton x %dodecane	4	0.043096	40.07	6.79 *	0.001
%Krat x %dvb	4	0.019607	29.69	3.09	0.032
%dod x %dvb	4	0.044696	9.89	7.04 *	0.001
%Krat x %dod x %dvb	8	0.032415	37.28	2.55	0.033
Error	27	0.042850	13.67		
Total	53	0.388587			

Complete results of an ANOVA performed on diameter ratios of the beads in toluene, neglecting all data that includes 60% total diluent in the polymer formulation. * Significant at 95% confidence level, ** significant at 99% confidence level.

Variables	DF	SS	MS	F-Value	P
% Kraton	2	531.03	265.51	16.73 **	0.000
% dodecane	1	703.12	703.12	44.29 **	0.000
% divinylbenzene	2	114.11	57.06	3.59	0.038
% total diluent	1	39.01	39.01	2.46	0.126
Interactions					
%K x %dod	2	179.08	89.54	5.64 *	0.007
%K x %dvh	4	252.72	63.18	3.98	0.009
% K x %td	2	73.86	36.93	2.33	0.112
%dod x %dvh	2	27.00	13.50	0.85	0.436
%dod x %td	1	45.12	45.12	2.84	0.100
%dvh x %td	2	51.44	25.72	1.62	0.212
% K x %dod x %dvh	4	110.67	27.67	1.74	0.162
%K x %dod x %td	2	14.25	7.13	0.45	0.642
%K x %dvh x %td	4	99.56	24.89	1.57	0.204
%dod x %dvh x %td	2	21.00	10.50	0.66	0.522
all	4	59.50	14.88	0.94	0.454
Error	36	571.50	15.88		
Total	71	2892.9			

Results of an ANOVA performed on the swelling times of the beads in toluene, neglecting all data that includes 66% dodecane in the polymer formulation. *Significant at 95% confidence level, ** significant at 99% confidence level.

Variables	DF	SS	MS	F-Value	P
%Kraton G1652 (Krat)	2	483.44	241.72	17.69 **	0.000
%dodecane (dod)	2	439.00	219.50	16.16 **	0.000
%divinylbenzene (dvb)	2	52.11	26.06	1.91	0.168
Interactions					
%Kraton x %dodecane	4	161.89	40.07	2.96	0.038
%Krat x %dvb	4	118.78	29.69	2.17	0.099
%dod x %dvb	4	39.56	9.89	0.72	0.583
%Krat x %dod x %dvb	8	298.22	37.28	2.73	0.024
Error	27	369.00	13.67		
Total	53	1962.0			

Complete results of an ANOVA performed on swelling time of the beads in toluene, neglecting all data that includes 60% total diluent in the polymer formulation. * Significant at 95% confidence level, ** significant at 99% confidence level.

APPENDIX B

Variables	DF	SS	MS	F-Value	P
% Kraton	2	0.26236	0.13118	6.29 *	0.005
% dodecane	1	0.05837	0.05837	2.80	0.103
% styrene	2	0.37841	0.18920	9.07 **	0.001
% total diluent	1	0.02101	0.02101	1.01	0.322
Interactions					
%K x %dod	2	0.14097	0.07048	3.38	0.045
%K x %dvh	4	0.02631	0.00658	0.32	0.866
% K x %td	2	0.04532	0.02266	1.09	0.348
%dod x %dvh	2	0.02805	0.01403	0.67	0.517
%dod x %td	1	0.00017	0.00017	0.01	0.929
%dvh x %td	2	0.01833	0.00916	0.44	0.648
% K x %dod x %dvh	4	0.14100	0.03525	1.69	0.174
%K x %dod x %td	2	0.00417	0.00208	0.10	0.905
%K x %dvh x %td	4	0.12673	0.03168	1.52	0.217
%dod x %dvh x %td	2	0.12777	0.06388	3.06	0.059
all	4	0.01988	0.00497	0.24	0.915
Error	36	0.75115	0.02087		
Total	71	2.14999			

Complete results of ANOVA performed on data obtained upon swelling the beads in acid, neglecting all data that includes 66% dodecane in the polymer formulation. *Significant at 95% confidence level, **significant at 99% confidence level.

Variables	DF	SS	MS	F-Value	P
% Kraton	2	0.26236	0.13118	0.26	0.771
% dodecane	1	0.05837	0.05837	1.84	0.183
% divinylbenzene	2	0.37841	0.18920	1.30	0.285
% total diluent	1	0.02101	0.02101	2.67	0.111
Interactions					
%K x %dod	2	0.14097	0.07048	0.53	0.591
%K x %dvh	4	0.02631	0.00658	2.37	0.071
% K x %td	2	0.04532	0.02266	5.95 *	0.006
%dod x %dvh	2	0.02805	0.01403	0.08	0.927
%dod x %td	1	0.00017	0.00017	1.32	0.259
%dvh x %td	2	0.01833	0.00916	1.71	0.195
% K x %dod x %dvh	4	0.14100	0.03525	2.27	0.080
%K x %dod x %td	2	0.00417	0.00208	6.69 *	0.003
%K x %dvh x %td	4	0.12673	0.03168	1.05	0.394
%dod x %dvh x %td	2	0.12777	0.06388	1.29	0.753
all	4	0.01988	0.00497	0.50	0.738
Error	36	0.75115	0.02087		
Total	71	2.14999			

Complete results of ANOVA performed on swelling times of the beads in acid, neglecting all data that included 66% dodecane in the polymer formulation.
 *Significant at 95% confidence level, **significant at the 99% confidence level.

APPENDIX C

Effects	DF	Sum of Squares	Mean Squares	F-Value
% Kraton G1652	1	0.041675	0.041675	16.1**
% Dodecane	1	0.000427	0.000427	0.165
% Divinylbenzene	2	0.089700	0.044850	17.4**
% Total Diluent	1	0.044556	0.044557	17.3**

Complete results of the ANOVA performed on the penetration moduli of all beads excluding those with 2% Kraton G1652 and 66% dodecane. The interactions were used as an estimate of the random error of the system. ** Significant at 99% confidence level. The complete

REFERENCES

1. Arnold, M. A., Ostler, T. J., *Anal. Chem.* **1986**, *58*, 1137-1140.
2. Peterson, J. I., Goldstein, S. R., Fitzgerald, R. V., Buckhold, D. K., *Anal. Chem.* **1980**, *52*, 864-869.
3. Saari, L. A., Seitz, W. R., *Anal. Chem.* **1982**, *54*, 823-824.
4. Kawahara, F. K., Fiutem, R. A., Silvus, H. S., Newman, F. M., Frazar, J. H., *Anal. Chim. Acta* **1983**, *151*, 315-327.
5. Peterson, J. I., Fitzgerald, R. V., Buckhold, D. K., *Anal. Chem.* **1984**, *56*, 62-67.
6. Wolfbeis, O. S., Posch, H. E., *Anal. Chim. Acta* **1986**, *185*, 321-327.
7. Zhang, Z., Seitz, W. R., *Anal. Chem.* **1986**, *58*, 220-222.
8. Lee, E. D., Werner, T. C., Seitz, W. R., *Anal. Chem.* **1987**, *59*, 279-283.
9. Zhujun, Z., Seitz, W. R., *Anal. Chim. Acta* **1984**, *160*, 305-309.
10. Wolfbeis, O. S., *Anal. Chem.* **1986**, *58*, 2874-2876.
11. Zhujun, Z., Mullin, J. L., Seitz, W. R., *Anal. Chim. Acta* **1986**, *184*, 251-258.
12. Bright, F. V., Poirier, G. E., Hieftje, G. M., *Talanta* **1988**, *35*, 113-118.
13. Miller, H. H., Hirschfield, T. B., *SPIE Fiber Optic and Laser Sensors IV* **1986**, *718*, 39-45.
14. Ballantine, D. S., Wohltjen, H., *Anal. Chem.* **1986**, *58*, 2883-2885.
15. Wolfbies, O. S., *Fiber Optic Chemical Sensors and Biosensors, Volume I*. Boca Raton: CRC Press, Inc., 1991.
16. Wolfbeis, O. S., *Fiber Optic Chemical Sensors and Biosensors, Volume II*. Boca Raton: CRC Press, Inc., 1991.
17. McCurley, M. F., Seitz, W. R., *Anal. Chim. Acta* **1991**, *249*, 373-380.
18. Bai, M., Seitz, W. R., *Talanta* **1994**, *41*, 993-999.
19. Flory, P. J., *Principles of Polymer Chemistry*. Ithaca: Cornell University Press, 1953; Chapter XIII.
20. McCurley, M. F., Seitz, W. R., *Anal. Chim. Acta* **1991**, *249*, 373-380.
21. Straub, Amy, Ph.D. Dissertation, The University of New Hampshire, 1992, pg. 29.
22. Cook, R. O., Hamm, C. W., *Applied Optics* **1979**, *18*, 3230-3241.
23. Bai, Mingqi, Ph.D. Dissertation, The University of New Hampshire, 1992, pg. 12.
24. McCurley, M. F., Seitz, W. R., *Anal. Chim. Acta* **1991**, *249*, 373-380.
25. Straub, Amy, Ph.D. Dissertation, The University of New Hampshire, 1992, pg. 101.

26. Bai, Mingqi, Ph. D. Dissertation, The University of New Hampshire, 1992, pg. 100.
27. Bai, Mingqi, Ph. D. Dissertation, The University of New Hampshire, 1992, pg. 116.
28. Billmeyer, F.W., *Textbook of Polymer Science, 3rd Ed.* New York: John Wiley & Sons, Inc., 1984.
29. Akelah, A., Moet, A., *Functionalized Polymers and Their Applications.* New York: Chapman and Hall, 1990.
30. Itsuno, S., Uchidoshi, K., Ito, K., *J. Am. Chem. Soc.*, 1990, 112, 8187-8188.
31. Dow Chemical Company, *VBC Vinylbenzyl Chloride.* Midland (Michigan, USA), 1988 (504-0026-88R). Trade Brochure.
32. Millar, J.R., Smith, D.G., Marr, W.E., Kressman, T.R.E., *J. Chem. Soc.* 1963, 218-225.
33. Millar, J.R., Smith, D.G., Kressman, T.R.E., *J. Chem. Soc.* 1965, 304-310.
34. Sederel, W.L., De Jong, G. J., *J. Appl. Poly. Sci.* 1973, 17, 2835-2846.
35. Moore, J.C., *J. Poly. Sci: Part A* 1964, 2, 835-843.
36. *Chemical & Engineering News*, August 31, 1992, pg. 34.
37. Amos, J.L., *Polymer Engineering and Science* 1974, 14, 1-12.
38. Durst, R.R., Griffith, R.M., Urbanic, A.J., Van Essen, W.J., *Adv. Chem. Ser.* 1976, 154 (Toughness & Brittleness of Plastics), 239-246.
39. Sardelis, K., Michels, H. J., Allen, G, *Polymer* 1987, 28, 244-250.
40. Shell Chemical Company, *Kraton Polymers for Modification of Thermoplastics.* 1990 (SC: 165-88). Trade Brochure.
41. Chlanda, F. P., Cooke, R. S., *U.S. Patent 4,738,764*, 1988; Allied Corporation.
42. Bandrup, J., Immergut, E. H., *Polymer Handbook, Third Edition* New York: John Wiley & Sons, Inc., 1989.
43. Pan, S., Conway, V.L., Shakhsher, Z., Emerson, S., Bai, M., Seitz, W.R., Legg, K. D., *Anal. Chim. Acta* 1993, 279, 195-202.
44. Billmeyer, F.W., *Textbook of Polymer Science, 3rd Ed.* New York: John Wiley & Sons, Inc., 1984.
45. Alkonis, J.J., MacKnight, W.J., *Introduction to Polymer Viscoelasticity (2nd Ed.)*. New York: John Wiley and Sons, 1983; Chapter 1.
46. Billmeyer, F.W., *Textbook of Polymer Science, 3rd Ed.* New York: John Wiley & Sons, Inc., 1984.
47. Alkonis, J.J., MacKnight, W.J., *Introduction to Polymer Viscoelasticity (2nd Ed.)*. New York: John Wiley and Sons, 1983; Chapter 3.
48. Sherrington, D.C., *Preparation, Functionalization, and Characteristics of Polymer Supports* 1980, John Wiley & Sons.
49. Hodge, P., Sherrington, D. C., *Polymer Reactions in Organic Synthesis* 1980, John Wiley & Sons.

50. Sherrington, D.C., *Preparation, Functionalization, and Characteristics of Polymer Supports* 1980, John Wiley & Sons.
51. Flory, P.J., *Principles of Polymer Chemistry*. Ithaca: Cornell University Press, 1953; Chapter XIII-3b.
52. Flory, P.J., *Principles of Polymer Chemistry*. Ithaca: Cornell University Press, 1953; Chapter XIII-3c.
53. Hassen, Kenneth D., Master's Dissertation, The University of New Hampshire, 1993, pg. 22.
54. Hassen, Kenneth D., Master's Dissertation, The University of New Hampshire, 1993, pg. 42.
55. Sardelis, K., Michels, H.J., Allen, G., *Polymer* 1987, 28, 244-250.
56. Miller, J. N., Miller, J. C., *Statistics for Analytical Chemistry, 2nd Ed.* New York: John Wiley and Sons, 1988, Ch 7.
57. Millar, J.R., Smith, D.G., Kressman, T.R.E., *J. Chem. Soc.* 1965, 304-310.
58. Millar, J.R., Smith, D.G., Marr, W.E., Kressman, T.R.E., *J. Chem. Soc.* 1963, 218-225.
59. Peska, J., Stamberg, J., Hradil, J., Ilavsky, M., *Journal of Chromatography* 1976, 125, 455-469.
60. Wiczorek, P. P., Ilavsky, M., Kolarz, B. N., Dusek, K., *Journal of Applied Polymer Science* 1982, 27, 277-288.
61. Wiczorek, P. P., Ilavsky, M., Kolarz, B. N., Dusek, K., *Journal of Applied Polymer Science* 1982, 27, 277-288.
62. Alkonis, J.J., MacKnight, W.J., *Introduction to Polymer Viscoelasticity (2nd Ed.)*. New York: John Wiley and Sons, 1983; Chapter 2.